PATHOLOGICAL ROLE OF ACROLEIN IN NEUROTRAUMA AND NEURODEGENERATION

by

Jonathan An Tang

A Dissertation

Submitted to the Faculty of Purdue University

In Partial Fulfillment of the Requirements for the degree of

Doctor of Philosophy

Weldon School of Biomedical Engineering

West Lafayette, Indiana

August 2021

THE PURDUE UNIVERSITY GRADUATE SCHOOL
STATEMENT OF COMMITTEE APPROVAL

Dr. Riyi Shi, Chair

Weldon School of Biomedical Engineering

Dr. Kevin Hannon

Department of Basic Medical Sciences

Dr. Zhongming Liu

Department of Biomedical Engineering, University of Michigan

Dr. Joseph Rispoli

Weldon School of Biomedical Engineering

Approved by:

Dr. Andrew O. Brightman

Dr. Harm HogenEsch

To my family for their unwavering support

ACKNOWLEDGMENTS

First and foremost, I would like to thank my advisor, Dr. Riyi Shi, for his guidance and support throughout my career. My experience in the Laboratory of Translational Neuroscience as an undergraduate student was highly influential in my decision to pursue graduate study. His passion for science and organization of the laboratory as a team provided support through even the most difficult times. Next, I would like to thank my committee: Drs. Kevin Hannon, Zhongming Liu, and Joseph Rispoli, for their direction following my preliminary proposal.

I would also like to thank Shi Lab members, past and present, who I have worked with over the years. I would especially like to thank Drs. Gary Leung, Melissa Tully, and Jonghyuck Park, who mentored me as an undergraduate and laid the groundwork for much of my work in multiple sclerosis. To those who I interacted with as a graduate student: Nick, Ran, Sasha, Glen, Jessica, Bre, Marcela, Seth, Joe, Ed, Brock, Sunny, Siyuan, Anna, Jennifer, and Daisy. Thank you for being there to bounce ideas off and to just talk about any problems in the lab or in life. I consider myself fortunate to have count you all as friends and teammates throughout these years of organized chaos.

To Drs. Joseph Rispoli and Nicole Vike with whom I collaborated directly, I thank you for sticking with me while troubleshooting scan conditions and arranging the relaxometry studies with the NMR facility. Finally, I would like to thank Sandy and Tammy in the BME office for their support in navigating the procedural and professional aspects of graduate school.

TABLE OF CONTENTS

LIST OF FIGURES

ABSTRACT

Oxidative stress has been implicated in the pathology of neurotrauma and neurodegeneration. However, direct antioxidant treatments have largely failed in clinical trials. Reactive unsaturated aldehyde byproducts of oxidative stress, such as acrolein, are potentially critical in mediating oxidative damage due to greater persistence in the body and while retaining significant reactivity with nucleophilic macromolecules. This study further characterizes the role of acrolein in the pathogenesis of neurotrauma and neurodegeneration. We observed elevated levels of acrolein metabolites in neuronal tissue and in systemic biofluids in animal models of multiple sclerosis, Parkinson's disease, spinal cord injury, and traumatic brain injury. These findings were partially corroborated with a pilot clinical study in which acrolein metabolites were elevated in the urine and serum of multiple sclerosis patients. Indeed, *in vitro* incubation of α-synuclein, a major component of Lewy bodies, with acrolein revealed that acrolein covalently modifies α-synuclein in a manner that induces formation of oligomers. Furthermore, carbonyl scavenging treatments, such as hydralazine, were found to protect dopaminergic nerve terminals in a model of Parkinson's disease, and to alleviate mechanical hyperalgesia in animal models of multiple sclerosis and spinal cord injury. Pharmacokinetic analysis of two hydrazine-based scavengers indicated a short half-life and suggests that efficacy of scavenging can be improved with alternative drugs or extended-release formulations. ALDH2 was investigated as an endogenous method of acrolein detoxification. Motor symptom severity and acrolein metabolite levels were significantly improved in EAE mice treated with Alda-1, an ALDH2 agonist, and significantly worse in ALDH2*2 knock-in mice compared to wild-type EAE mice. Furthermore, myeloperoxidase was found to correlate with acrolein modified proteins in spinal cord white matter. Taken together, acrolein appears to be a key pathological convergence point in the pathogenesis of neurotrauma and neurodegenerative disease. Accordingly, anti-acrolein treatment may be an effective treatment strategy for multiple pathological conditions in the nervous system.

1. INTRODUCTION

1.1 Oxidative stress and reactive aldehydes in neuropathology

Oxidative stress, or excess accumulation of reactive oxygen species (ROS), has been implicated in a variety of neurological conditions trauma such as Parkinson's disease (PD) [1], multiple sclerosis (MS) [2, 3], and neurotrauma [4, 5]. Following initial pathological or traumatic insult, recruitment of immune cells and activation of microglia may cause localized oxidative stress [6, 7] and result in the production of additional reactive aldehyde byproducts [8]. These primary and secondary products of oxidative stress propagate damage through lipid peroxidation in the lipid rich neuronal environment[9] and oxidative damage to proteins [10], ultimately resulting in cellular dysfunction or death.

Although less reactive than free radicals such as superoxide, unsaturated aldehydes, such as acrolein, 4-hydroxynonenal, and malondialdehyde, remain capable of furthering oxidative stress via lipid peroxidation and of adducting to nucleophilic amino acid residues [8, 10-14]. Furthermore, these products possess a half-life on the order of days, allowing them to potentially diffuse from the production site and propagate a long-term cycle of oxidative stress [10]. Due to the greater persistence of reactive aldehydes, it has been suggested that targeting these compounds may have greater therapeutic success than directly scavenging free radicals directly [11, 12, 15, 16].

Acrolein, the simplest and most abundant of the α,β-unsaturated aldehydes, is of particular interest as it reacts with glutathione, a major endogenous antioxidant, up to 150 times faster than 4-hydroxnonenal [13] and is produced in concentrations nearly 100 times that of 4-hydroxynonenal [8]. It is an electrophile and Michael acceptor which readily forms covalent adducts with cysteine, lysine, histidine, and deoxyguanosine [13, 17]. *Ex* vivo acrolein exposure has been shown to damage myelin with paranodal splitting and retraction from the node of Ranvier [18]. Acrolein injection to the spinal cord *in vivo* has also been shown to cause functional deficits in the absence of other trauma or chemical insult [19]. At this time, endogenous acrolein can be estimated via immunoblotting against adducted lysine residues [10] or by estimating end metabolites in systemic biofluids [20].

Acrolein can be derived from both endogenous and exogenous sources. Endogenously, acrolein can be produced through lipid peroxidation, breakdown of polyamines or chlorination of L-threonine [8, 21]. The body can be exposed to exogenous acrolein produced through, combustion, overheating of cooking oils, or pyrolytic breakdown of glycerol [8]. Of note, cigarette smoke contains between 40 and 70 μg per cigarette [22] which may contribute in part to associations of smoking with disease.

The primary metabolic pathway of acrolein is detoxification by glutathione [13] and subsequent urinary excretion as 3-hydroxypropylmercapturic acid [20, 23] (3-HPMA). Additionally, acrolein can be acted upon by aldehyde dehydrogenase 2 [24] (ALDH2), a mitochondrial enzyme which performs the rate-limiting step in alcohol metabolism, to form acrylic acid. Notably, approximately 40% of the East Asian population possesses a nearly nonfunctional mutant form of ALDH2 [25] which has been linked to Alzheimer's disease [26].

Although hydralazine and phenelzine have been evaluated as acrolein scavengers in a variety of animal models [27-29], specific aspects of pharmacology may limit clinical application. As such, alternative strategies including enhancement of endogenous antioxidant and carbonyl processing or design of novel compounds with minimized off-target effects may prove essential in advancing acrolein scavenging as a therapeutic strategy.

1.2 Multiple sclerosis

Multiple sclerosis (MS) is an inflammatory demyelinating disease of the brain and spinal cord which affects approximately 2.5 million individuals worldwide [30]. Patients experience a variety of motor, sensory, and cognitive deficits throughout disease progression [30-32]; however, the etiology of MS is not fully understood, and therapeutic strategies focus primarily on immunomodulation or symptomatic relief [32]. Although the mechanism which initiates the disease is not known, demyelination, inflammation, oxidative stress, and axonal degeneration are considered to be key pathologies in disease progression [3, 32-39]. Growing evidence has identified reactive oxygen species and their secondary byproducts as potential mediators MS pathology [3, 40-43]; however, ROS scavenging therapies have shown limited effect in alleviating symptoms or slowing disease progression [6, 44-46].

Given that acrolein is a byproduct of oxidative stress and is capable of directly attacking the myelin sheath, it remains likely that acrolein contributes in the molecular pathology of MS. Acrolein metabolites have been demonstrated to be elevated in both experimental autoimmune encephalomyelitis (EAE) mice, and in MS patients [40, 47, 48]. Furthermore, treatment with hydralazine, a hydrazine based carbonyl scavenger, alleviated peak motor symptom severity, reduced demyelination, and delayed disease progression in EAE mice [27]. There is limited evidence that acrolein may contribute in part to increased MS risk in tobacco smokers [49, 50] given detectable increases in metabolites when exposed gaseous acrolein at similar concentrations; however, a direct causal link cannot be inferred due to the multitude of components in tobacco smoke [22].

Neuropathic pain is also a common symptom in multiple sclerosis with between 50 and 80 percent of patients experiencing some level of pain [51, 52]. Approximately one third of these patients consider it to be their most concerning symptom. Unfortunately, first-line medications for neuropathic pain such as tricyclic antidepressants and gabapentin only achieve partial relief in 40-60% of patients [51]. Although the mechanisms of this pain are not well understood, animal studies have implicated oxidative stress as a factor in animal models [53]. Furthermore, pain related signaling is capable of inducing relapse in EAE mice, further exacerbating disease progression [54].

1.3 Traumatic brain injury

According to the CDC definition, traumatic brain injury (TBI) is an alteration of normal neurological function resulting from external forces such as a blow to the head [55, 56]. It is estimated that approximately 1.7 million individuals in the civilian population of the United States are affected by TBIs each year [55, 57-59] and that approximately 3.17 million individuals continue to experience long term neurobehavioral symptoms such as headaches and dizziness [60]. TBI can be further classified as mild, moderate, or severe TBI based on clinical criteria including duration of loss of consciousness, duration of post-traumatic anterograde amnesia [61, 62], and in some cases Glasgow Coma Scale (GCS) [63, 64]. TBI has been associated with a variety of neurobehavioral sequelae including depression [65, 66] and post-traumatic epilepsy [67, 68] in

addition to degenerative pathologies such as chronic traumatic encephalopathy[69, 70] and Parkinson's disease [71].

TBI is most often associated with a physical blow to the head resulting from traumatic events such as falls [57], motor vehicle collisions [58], or sports related injuries [69]. The rapid acceleration-deceleration of the head following impact is thought damage the brain via impact with the cranial wall in spite of the normal cushioning afforded by cerebrospinal fluid [72]. This contact may occur ipsilateral to the blow, contralateral to the blow, and is also described in literature as coup and contre-coup, respectively [73]. In severe cases, intracranial hemorrhage, cerebral edema, or penetrating injury may occur [61]

In the days, weeks, and months following the primary physical injury, nervous tissue can continue to experience secondary injury due to neurochemical changes in both neurons and glia [68, 70, 74-76]. In particular, disruption of the axolemma or changes in the levels of neurotransmitters and excitatory amino acids results in increased generation of free radicals and reactive oxygen species (ROS) including peroxides and the superoxide anion [4, 77, 78]. Free radicals and ROS are generated constantly by the mitochondria [79], and in a healthy physiological state are often utilized by the immune system for their bactericidal and antiviral activity [80]. However, under pathological conditions, such as those resulting from TBI, oxidative stress can overwhelm the endogenous antioxidant systems [75] and cause further neuronal damage via lipid peroxidation [16] and protein modification [81].

Acrolein metabolites have been shown to be elevated in both traumatic brain injury [82] and suggested to contribute to elevated risk of neurodegeneration through covalent modification of proteins such as α-synuclein [14, 29, 83, 84] due to regions of nucleophilic rich residues that play key roles in fibril formation [85-87]. In particular, incubation of α-synuclein has been shown to induce oligomerization *in vitro*, and immunoprecipitation of whole brain lysates from TBI demonstrated interaction between acrolein and α-synuclein [83].

1.4 Spinal cord injury

Traumatic brain injuries and spinal cord injuries (SCI) are frequently associated with events such as falls [57], motor vehicle collisions [58], or sports related injuries [69]. Injury can be broadly categorized as the primary physical insult and secondary biochemical damage. The

direct force of primary injury can result in membrane disruption, localized metabolite imbalance, or vascular injury [88]. Secondary injury can occur in the days, weeks, and months following physical injury due to neurochemical changes in both neurons and glia [68, 70, 74, 75, 89, 90]. Changes in the levels of neurotransmitters such as glutamate can cause increased generation of free radicals and ROS such as peroxides and superoxides [4, 77, 78]. Immune cell infiltration can further contribute to the localized oxidative environment and result in continuation of oxidative stress[89] and generation of reactive aldehyde byproducts [15, 91-93].

Acrolein has also been implicated in spinal cord injury with elevated metabolites present in rat spinal cord and biofluids following contusion injury [5, 93, 94]. Treatment with acrolein scavengers has been shown to reduce presence of acrolein metabolites and improve motor recovery after injury [28, 91, 92]. Furthermore, acrolein has been implicated in post-SCI neuropathic pain via activation and upregulation of the receptor-channel TRPA1 [28, 95-98]. Although the mechanism resulting in genetic upregulation is not well understood, acrolein mediated TRPA1 activation is thought to occur through covalent adduction to cysteine residues [97, 99]. TRPA1 is also knowns to respond to other aldehyde species including formalin [97-99]

1.5 Summary

In summary, oxidative stress is thought to be a key pathology in neurotrauma, neuroinflammation, and neurodegeneration. However, direct antioxidant therapies which aim to scavenge reactive aldehydes have generally failed up on reaching clinical trials. We have previously identified acrolein, a reactive α,β-unsaturated aldehyde, as both a product and initiator of lipid peroxidation and oxidative stress with a half-life significantly longer than free radical species.

In this dissertation, we aim to further elucidate the role of acrolein in animal models of MS, PD, TBI, and SCI by examining the effects of acrolein scavengers on both biochemical and behavioral changes associated with these injuries and diseases. Additionally, we aim to produce evidence that acrolein alone is sufficient to induce degenerative processes. Finally, we will evaluate the roles of ALDH2 as an endogenous scavenger by utilizing ALDH2*2 knock in mice and treating Alda-1, an ALDH2 agonist. In doing so, we hope to provide new insight into the role of oxidative stress and carbonyl load in neurotrauma and neurodegeneration.

2. ROLE OF ACROLEIN AND MEMBRANE PERMEABILITY IN THE PATHOPHYSIOLOGY OF MULTIPLE SCLEROSIS

2.1 Introduction

Multiple sclerosis is an inflammatory demyelinating disease of the central nervous system which affects approximately 2.5 million individuals worldwide [30]. Patients experience a variety of motor, sensory, and cognitive deficits throughout disease progression [31, 32]; however, the etiology of MS is not fully understood, and therapeutic strategies focus primarily on immunomodulation and symptomatic relief [32]. Although the initiating process is not fully understood, demyelination, inflammation, oxidative stress, and axonal degeneration are considered to be critical processes in MS pathophysiology [32-35]. Growing evidence has identified reactive oxygen species and their reactive byproducts as potential mediators of MS pathology [3, 40]; however, direct ROS scavenging has shown limited effect in alleviating symptoms or slowing disease progression in clinical studies[6, 44, 45].

Acrolein, the simplest and most reactive of the α,β-unsaturated aldehydes, is a product of oxidative stress and lipid peroxidation [8, 13]. It is a potent electrophile which can further react with proteins, lipids, and deoxyguanosine, resulting in generation of additional reactive species [13]. As a result, acrolein may act as both a product and initiator of lipid peroxidation which can perpetuate oxidative and inflammatory insult.

Ex vivo studies have confirmed that acrolein alone is capable of degrading the myelin sheath, suggesting that it may contribute to the molecular pathology of MS [100]. This is supported by elevation of acrolein modified proteins in spinal cord lysates of EAE mice [27]. Furthermore, treatment with hydralazine, a hydrazine-based carbonyl scavenger, alleviated motor symptom severity, reduced demyelination, and delayed disease progression in EAE mice [27].

The purpose of this study is to further elucidate the role of acrolein MS pathology through a pilot clinical study to confirm presence of acrolein metabolites in the biofluid of MS patients. The efficacy of hydralazine in reducing levels of acrolein was also confirmed in EAE mice by measurement of both systemic metabolites and tissue lysates. Finally, polyethylene glycol (PEG) was examined to explore the role of axon permeability in EAE.

2.2 Methods

2.2.1 Animals

Female C57BL/6 mice (8 weeks old) were purchased from Harlan Laboratories (Indianapolis, IN, USA) and were allowed to acclimate to laboratory housing for two weeks prior to experimentation. All live animal procedures were performed under protocols approved by the Purdue Animal Care and Use Committee.

2.2.2 EAE model induction

Ten-week-old mice were injected subcutaneously with 0.1 mL MOG_{35-55}/CFA emulsion (EK-0115, Hooke Laboratories, Lawrence, MA, USA) over the rostral and caudal ends of the spinal column. 0.1 mL of deconjugated pertussis toxin (EK-0115, Hooke Laboratories) was administered intraperitoneally on the day of MOG application and again 22-26 hours later. Motor function was scored daily using an established 5-point system to assess degree of paralysis. Scores were assigned in the following manner: 0-No deficit, 2-hind limb paresis or ataxia without leg dragging, 3-hind limb paresis with one or both hind limbs dragging, 4-Complete hind limb paralysis, 5-Moribund. Humane endpoints requiring euthanasia prior to experimental timepoints included loss of over 20% body weight and attaining a motor function score of 5.

2.2.3 Dot immunoblotting

Animals were anesthetized with a mixture of ketamine (90 mg/kg) and xylazine (10 mg/kg) via intraperitoneal injection. Mice were then perfused transcardially with cold oxygenated Krebs solution prior to harvesting spinal cords. Tissues were incubated in 1% Triton and Protease Inhibitor Cocktails (P8340, Sigma-Aldrich, St. Louis, MO, USA), homogenized, and incubated on ice for at least 1 hour. Samples were then centrifuged at 13,500 g at 4°C for 30 minutes.

A BCA assays was performed to ensure equal loading of samples. Samples were transferred to a nitrocellulose membrane using a Bio-Dot SF (Bio-Rad, Hercules, CA, USA). The membrane was blocked for 1h in a blocking buffer consisting of 0.2% Casein and 0.1% Tween 20 in phosphate buffered saline. The membrane was then transferred to a solution of polyclonal rabbit anti-acrolein antibody (Novus Biologicals) at a 1:1000 dilution in 2% goat serum and incubated at 4°C for 18

hours. The membrane was then washed with blocking buffer and incubated in a 1;10,000 dilution of alkaline phosphatase conjugated goat anti-rabbit antibody (Vectastain ABC-AmP Kit, Vector Laboratories). Next, the membrane was washed again in blocking buffer followed by 0.1% Tween 20 in Tris-buffered saline. Finally, the membrane was exposed to substrate for the ABC-AMP kit and visualized by chemiluminescence. Band density was quantified using ImageJ.

2.2.4 Animal urine collection

Mice were housed in metabolic cages for 12-24 hours with *ad libitum* access to normal diet and water. Samples of approximately 0.5 mL were obtained between days 21 and 23 post induction which corresponds with peak behavioral deficits. Samples were then transferred to 1 mL centrifuge tubes and frozen at -80°C.

2.2.5 Hydralazine and polyethylene glycol treatment

Hydralazine hydrochloride (Sigma) was dissolved in phosphate buffered saline, sterilized through a 0.45 μm filter, and stored at 4°C. Hydralazine was given daily at a dose of 1 mg/kg via intraperitoneal injection starting from the day of induction and continuing until the end of the study at 22 days post-induction.

Similarly, 30% polyethylene glycol (295906, Sigma Aldrich) in phosphate buffered saline was filter sterilized. A 0.1 mL volume of PEG solution was given daily for the duration of the study. Animals not receiving PEG or hydralazine were given an equivalent volume of saline.

2.2.6 Horseradish peroxidase exclusion assay

Animals were anesthetized with ketamine (90 mg/kg) and xylazine (10 mg/kg) and perfused transcardially with cold oxygenated Krebs solution. Spinal cords were excised and placed in cold oxygenated Krebs solution with 0.015% horseradish peroxidase (HRP) for 2 hours prior to fixation in 2.5% glutaraldehyde in phosphate buffered saline for 4 hours. A vibratome (Electron Microscopy Sciences, Hatfield, PA, USA) was used to cut 30 μm axial sections. Spinal cord sections were developed in a diaminobenzidine solution to visualize HRP uptake. Brightfield images were analyzed by counting stained axons and expressed as axons/mm2. Tissue was

collected pre-induction (control) and at 8 days (pre-symptom) and 4 weeks post-induction (peak symptom).

2.2.7 Human subject enrollment

All human specimens were collected at the Indiana University Multiple Sclerosis Center, Indianapolis, IN, USA. Subject selection criteria consisted of an MS diagnosis and that the patient is not receiving corticosteroids at the time of sample collection. This study was carried out in accordance with a protocol approved by the Indiana University Human Subjects Institutional Review Board. All patients provided written informed consent using a consent form approved by the Institutional Review Board.

2.2.8 Human biofluid collection

Venous blood samples were obtained by standard technique and placed in a BD Vacutainer® Plus Venus Blood Collection Tube with Clot Activator. Samples were incubated at room temperature for 15 minutes to facilitate clotting prior to centrifugation at 2800 rpm for 15 minutes. Serum was then transferred to a labeled cryovial and stored at -80°C until analysis.

Subjects were provided a specimen cup without preservative for urine collection. Urine samples were then pipetted into cryovials and stored at -80°C until analysis.

2.2.9 3-HPMA quantification

3-Hydroxypropyl mercapturic acid (3-HPMA) was quantified in urine and serum according to Eckert et al [20]. In brief, Isolute ENV+ (Biotage, Charlotte, NC) were pre-conditioned with 1 mL of methanol followed by 1 mL water, and 1 mL 0.1% formic acid. 500 µL of biofluid sample was combined with 200 ng deuterated 3-HPMA (Toronto Research Chemicals Inc., New York, Ontario), 500 µL of 50 MM ammonium formate, and 10 µL of formic acid prior to loading onto the pretreated cartridges. Cartridges were then washed with 1 mL 0.1% formic acid followed by 1 mL 10% methanol/90% 0.1% formic acid. Cartridges were dried with nitrogen gas and eluted with three volumes of 600 µL methanol plus 2% formic acid. The eluates were combined and dried in a rotary evaporation device. Each sample was reconstituted in 0.1% formic acid before analysis.

Quantification was performed Agilent 1200 Rapid Resolution liquid chromatography system coupled to an Agilent 6460 series QQQ mass spectrometer and a Waters Atlantis T3 2.1mm x 150mm, 3 μm column. Buffers utilized include water + 0.1% formic acid and acetonitrile + 0.1% formic acid.

2.2.10 Creatinine assay and BSA assay

Creatinine concentration was determined using a urinary creatine assay kit (Cayman Chemical Company, Item no. 500701). Urine samples were diluted 12x and 14x prior to measurement. Alkaline picrate solution was prepared according to the assay manual. Diluted samples and creatinine standards were loaded into a 96 well plate and incubated in alkaline picrate solution for 20 minutes at room temperature. Absorbance at 490-500nm was determined using a spectrophotometer. After initial reading, 5 μL of acid solution was added to each sample and incubated at room temperature for an additional 20 minutes. A spectrophotometer was used to take an additional reading, and the difference between these two measurements were used for analysis.

Serum protein concentrations were quantified using the Bicinchoninic Acid protein assay kit (Pierce, Rockford, IL, USA). Serum samples were diluted 100-fold and loaded in triplicate into a 96 well plate along with BSA standards. BCA reagent was added to all wells and allowed to incubate at 37°C for 30 minutes prior to measuring absorbance at 560-570 nm on a spectrophotometer.

2.2.11 Statistical analysis

Students t-test was used to compare acrolein measurements between control and EAE or MS groups. For comparisons involving three or more groups, ANOVA with *post-hoc* Newman-Keul test was used to compare data (α=0.05). Linear correlation is expressed by Pearson correlation coefficient (r), and other data is expressed as mean ± standard error of the mean.

2.3 Results

2.3.1 Acrolein metabolites are elevated in EAE mice

Systemic acrolein levels in EAE mice were measured via quantification of urinary 3-HPMA levels days 7-9 post induction and at peak deficits from days 21-23 post induction (Figure 2.1). 3-HPMA was elevated in EAE mice (27.3 ± 4.2 μg/mg creatinine) compared to control mice (30.5 ± 3.6 μg/mg creatinine, $p<0.05$) during the asymptomatic time point. Similarly, at peak deficits, EAE mice continued to exhibit elevated systemic acrolein metabolites (30.5 ± 3.6 μg/mg creatinine) relative to health controls (19.5 ± 1.0 μg/mg creatinine, $p<0.05$) (Figure 2.2). This finding was confirmed with dot immunoblotting of spinal cords collected at day 28 post induction (Figure 2.3). We found that acrolein-lysine adducts in spinal cord lysates of EAE mice were increased (19.1 ± 1.8 au) relative to controls (12.5 ± 0.7 au, $p<0.01$). Linear regression demonstrates a significant positive relationship between urinary 3-HPMA and acrolein-lysine adducts in tissue (Figure 2.4) with a Pearson correlation coefficient of 0.87 ($p<0.005$).

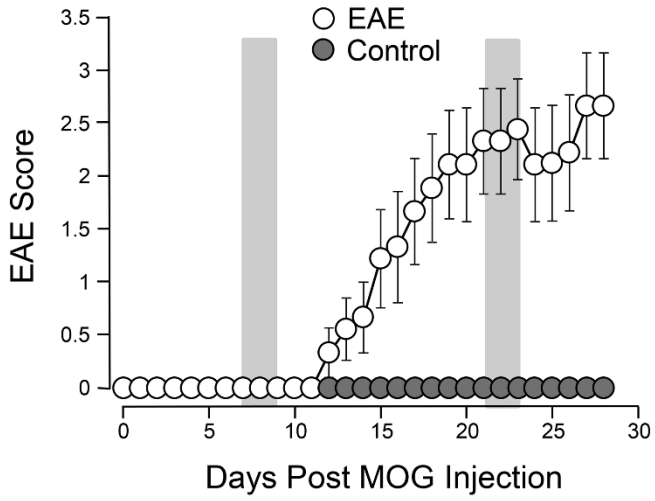

Figure 2.1 Experimental timeline starting from day of EAE induction. Urine was collected during days 7-9 post-induction and days 21-23 post induction.

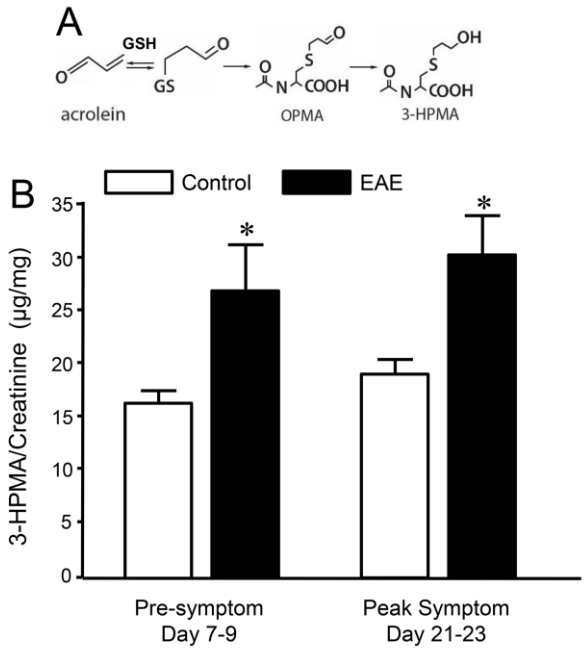

Figure 2.2 Systemic acrolein metabolites are elevated in EAE mice. Urinary 3-HPMA was elevated both prior to the emergence of motor symptoms and at the time of typical peak symptoms. (*p<0.05 compared to control, N=9)

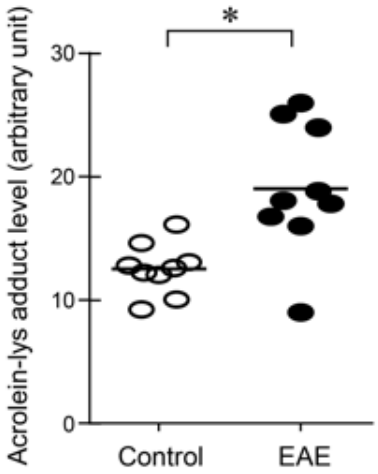

Figure 2.3 Acrolein metabolites are elevated in the spinal cords of EAE mice. Immunoblotting of spinal cord lysates revealed an increase in acrolein-lysine adducts in EAE mice. (*p<0.05 compared to control, N=9)

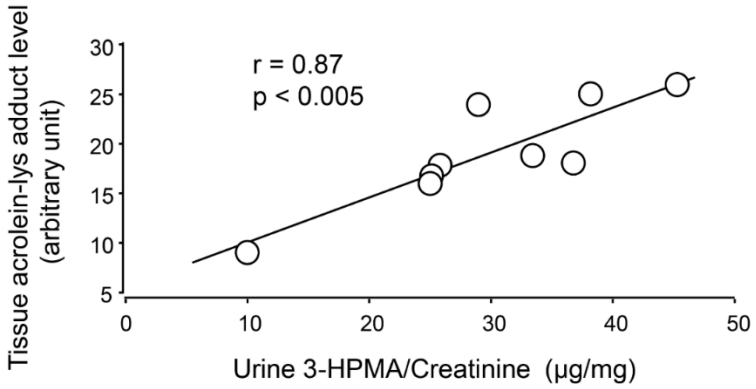

Figure 2.4 Correlation of local and systemic acrolein metabolites. Urinary 3-HPMA was plotted against spinal cord acrolein-lysine adducts. Regression analysis revealed a Pearson correlation coefficient of 0.87 ($p<0.005$).

2.3.2 Hydralazine treatment reduces local and systemic acrolein metabolites

Urine was collected from hydralazine treated mice at days 21-23 post induction, and spinal cords were harvested at day 28 post induction. Urinary 3-HPMA in hydralazine treated mice (9.25 ± 1.54 µg/mg creatinine) was significantly lower than untreated EAE mice (29.9 ± 3.6 µg/mg creatinine, $p<0.01$). Similarly, levels of acrolein-lysine adducts in spinal cord lysates of hydralazine treated EAE mice (14.2 ± 1.1 au) was significantly lower than untreated EAE mice (19.1 ± 1.8 au, $p<0.05$) (Figure 2.5).

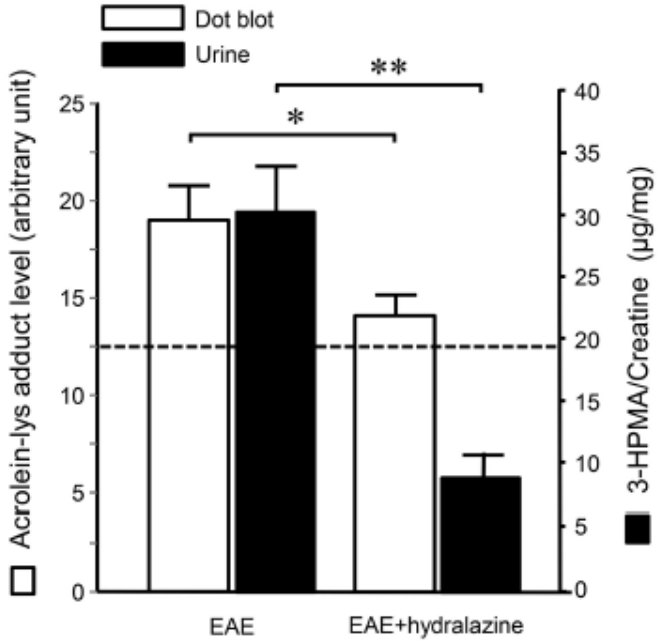

Figure 2.5 Hydralazine treatment reduces local and systemic acrolein metabolites in EAE mice. Hydralazine treated EAE mice exhibited lower levels of urinary 3-HPMA and tissue level acrolein-lysine compared to untreated EAE mice (*$p<0.05$, **$p<0.01$)

2.3.3 Axon permeability in EAE mice is reduced by polyethylene glycol

Membrane permeability in EAE mice was examined using an established HRP-exclusion assay. Tissue of control mice, EAE mice prior to symptom onset, and EAE mice at peak motor deficit was examined for membrane permeability. Average HRP labeling in these groups was 811 ± 130, 3293 ± 500, and 6147 ± 655 axons/mm^2, respectively (Figure 2.6). EAE mice at peak motor deficits exhibited significantly higher levels of HRP labeled axons compared to healthy controls ($p<0.01$). Notably, pre-symptomatic EAE mice also showed significantly higher membrane permeability than controls ($p<0.05$).

Daily treatment with PEG resulted in improved axonal integrity (1581 ± 247 axons/mm^2) compared to EAE mice at peak deficit (6147 ± 655 axons/mm^2, $p<0.01$). Furthermore, PEG treatment significantly reduced peak symptom severity from 3.33 ± 0.3 in untreated EAE mice to 1.92 ± 0.4 in PEG treated EAE mice ($p<0.05$) (Figure 2.7). In addition, the time to reach peak symptom severity was delayed from 18.7 ± 0.8 days in untreated mice to 23.1 days in PEG treated animals ($p<0.05$)

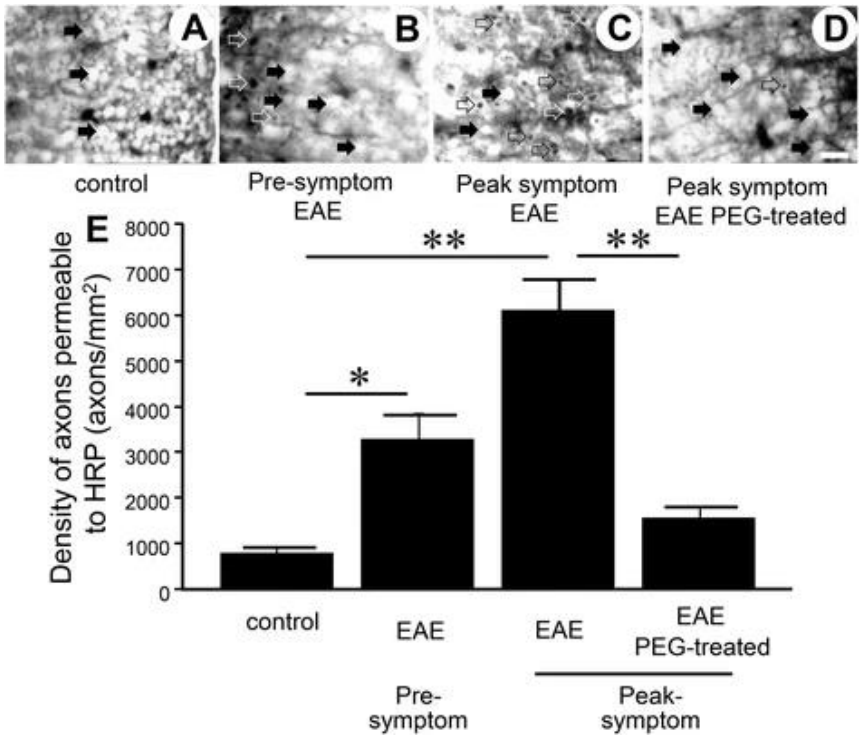

Figure 2.6 Horseradish peroxidase exclusion test for membrane permeability. Spinal cords were collected from control mice and EAE mice at 8 days post-induction (pre-symptom) and 28 days post-induction (peak-symptom). A-D) Images of HRP labeled spinal cord segments with open arrows indicating areas of HRP penetration while closed arrows indicate areas of HRP exclusion. E) Quantification of HRP labeled axon density. EAE mice exhibited higher levels of HRP uptake at both pre-symptom and peak symptom time points. PEG treatment significantly decreased HRP labeling compared to untreated animals. *$p<0.05$, **$p<0.01$

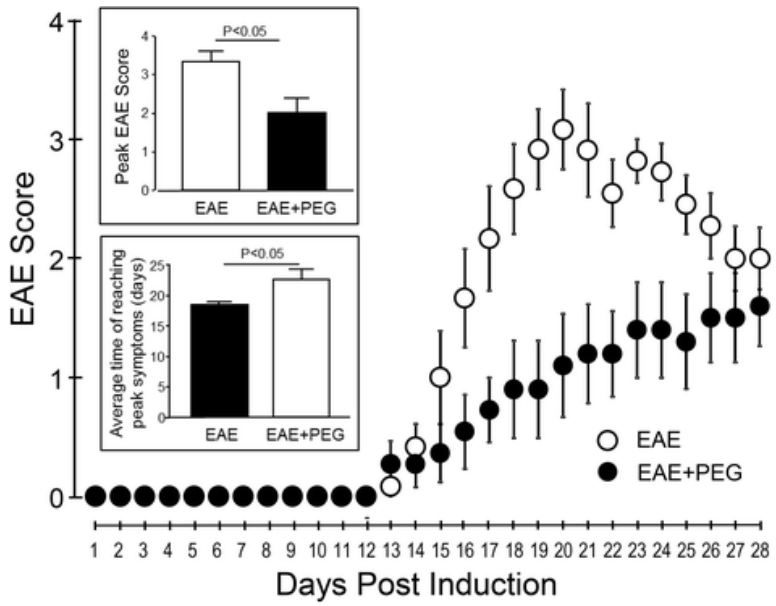

Figure 2.7 PEG alleviated motor deficits in EAE mice. Scatter plot depicts the mean motor function score for each group throughout the study duration. Peak symptom severity was significantly decreased in PEG treated animals compared to EAE ($p<0.05$). Time to reach peak symptoms was significantly greater in PEG treated animals compared to EAE ($p<0.05$). Animals which did not reach a score of 2 or greater were recorded as 28 days to reach peak symptoms.

2.3.4 Acrolein metabolites are elevated in the biofluids of MS patients

Urine and serum samples were collected from MS patients (n=40) and healthy controls (n=23). Among the MS patients, 31 were diagnosed with relapsing-remitting MS, 8 were diagnosed as secondary progressive MS, and 1 as primary progressive MS. Of these, two were in relapse at the time of specimen collection.

Acrolein content in urine and serum samples was estimated through assessment of 3-HPMA via LC/MS/MS (Figure 2.8). Mean urinary 3-HPMA in MS patients (1.094 ± 0.212 μg/mg creatinine) was significantly elevated compared to healthy controls (0.570 ± 0.082 μg/mg creatinine, $p<0.05$). Similarly, serum levels of 3-HPMA were increased in MS patients (0.065 ± 0.009 μg/g protein) compared to the control group (0.036 ± 0.004 μg/g protein). Linear regression revealed as significant positive relationship between urine and serum levels of 3HPMA with a Pearson correlation coefficient of 0.75 ($p<0.0001$) (Figure 2.9).

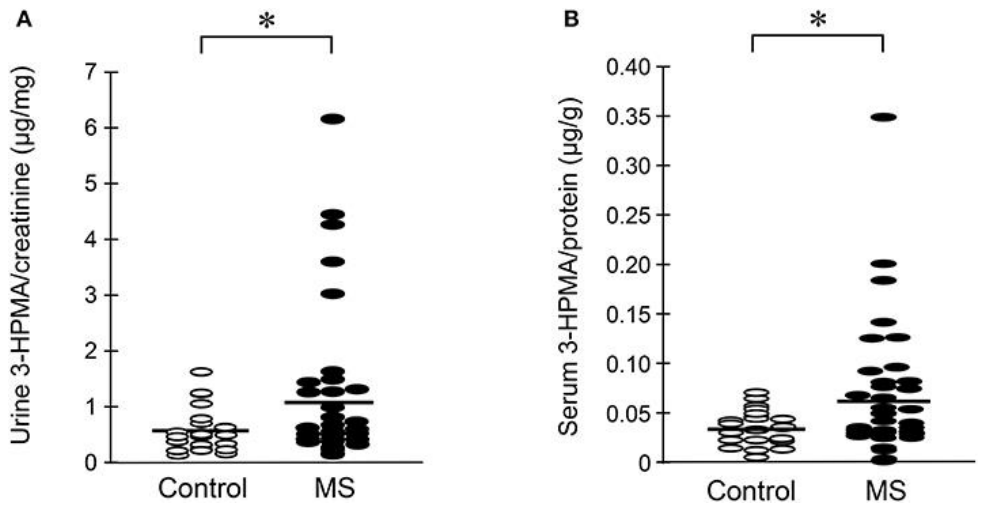

Figure 2.8 Measurement of urine and serum 3-HPMA in MS patients and healthy controls. Mean urine (A) and serum (B) 3-HPMA was elevated in MS patients relative to controls. Scatter plots display overall distribution of samples with solid line indicating mean. Notably, many MS patients exhibited 3-HPMA levels similar to that of healthy controls. *p<0.05

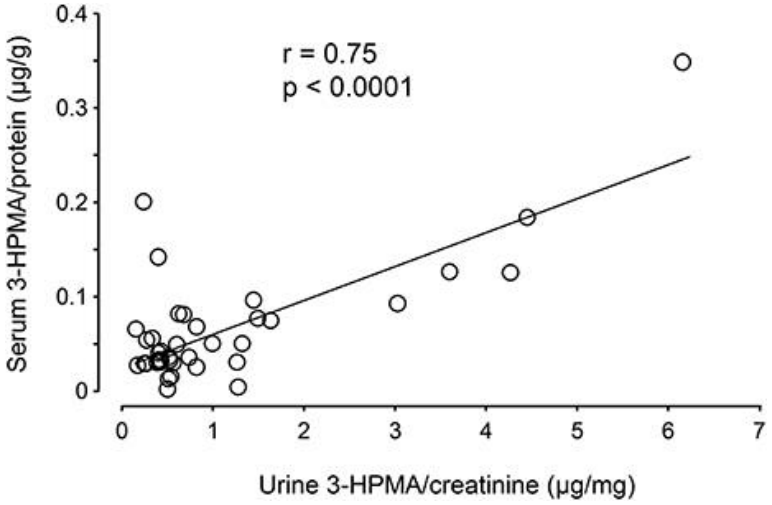

Figure 2.9 Linear regression of urine and serum 3-HPMA. Regression analysis of urine and serum 3-HPMA reveals a significant positive relationship with a Pearson correlation coefficient of 0.75 (p<0.0001)

2.4 Discussion

In this study, we have demonstrated elevation of 3-HPMA, a systemic acrolein metabolite, in EAE mice at asymptomatic and peak stages of disease using a non-invasive method. The levels of this metabolite have been correlated with tissue level acrolein adducts and shown to be

responsive to hydralazine. Furthermore, we have observed that 3-HPMA is significantly elevated in both the urine and serum of MS patients when compared to healthy controls. To the best of our knowledge, this is the first clinical evidence that MS patients exhibit elevated systemic acrolein metabolites.

Given the established reactivity of acrolein and its elevation in both EAE mice and human MS patients, we suggest that acrolein is likely to play a critical role in instigating neuronal tissue damage in MS. Considering that acrolein scavenging treatment has been shown to reduce levels of acrolein and to be neuroprotective in EAE mice, we postulate that acrolein could be a viable therapeutic target for intervention and monitoring.

Of interest, we found that urinary 3-HPMA was elevated in EAE mice prior to the emergency of obvious motor deficits. Similarly, we observed increased axonal membrane permeability at similar time point. This may represent increased inflammatory activity which has not yet reached the point of causing observable motor symptoms. Consistent with this postulation, it has been shown that membrane damage and allodynia, both of which can be associated with inflammation, are detectable prior to the emergency of motor deficits in EAE mice. As such, 3-HPMA measurement could serve as a diagnostic or monitoring tool to identify or predict the emergence of symptoms or to evaluate the effect of treatment. However, considering the differences between inducible animal models and human disease, translation of this technique must be done with caution.

The non-invasive measurement of 3-HPMA could enable longitudinal *in vivo* studies of acrolein in EAE mice to better understand the dynamics of inflammation in disease and evaluate acrolein scavenging treatments. In addition, the non-invasive or minimally invasive nature of the techniques allows detection of acrolein in human patients. In this study, 3-HPMA was quantified in both urine and serum to ensure reliability, and both measurements demonstrated significant elevation in MS patients and were well correlated. One limitation in this pilot study is the low number of total participants and an uneven distribution in patient subgroups. A more comprehensive longitudinal study could provide insights into how 3-HPMA levels may correlate to factors including presence of active lesions, symptomatic presentation, and disease classification.

In addition to providing insights into disease development, acrolein measurement could serve as a criterion for patient selection and dose optimization. For example, while we found a significant elevation in mean 3-HPMA levels of MS patients, examination of the scatter plot

demonstrated that some MS patients exhibited 3-HPMA levels in line with the control group. In theory, the patients exhibiting more marked elevations in acrolein metabolites may be more responsive to acrolein scavengers than those with similar levels to controls.

Although we have detected elevated acrolein in both animal and human subjects, there are key differences in our findings. First, urinary 3-HPMA in EAE mice was 1.56 times that of control while spinal cord lysates showed 1.53 times that of controls, suggesting a fairly proportional elevation in CNS tissue and systemic circulation. This differs from previous findings in SCI which show 4.5 times greater levels of acrolein in tissue, but only a 1.8 fold increase in urinary 3-HPMA [93]. This may simply reflect the focal nature of contusive SCI when compared to a diffusive inflammatory disease like MS. As such, while the exact relationship between urinary 3-HPMA and acrolein in the tissue of interest is likely to vary based on the characteristics of injury or disease.

In summary, we have observed elevated 3-HPMA levels in MS patients using a non-invasive method. This further supports the previously proposed role of acrolein in MS. In addition, the non-invasive nature of the technique presents possibilities in diagnosis and management of MS by determining the effect of treatment on acrolein metabolites as a marker for active inflammation.

3. ANTI-ACROLEIN-MEDIATED NEUROPROTECTION AND FUNCTIONAL BENEFITS IN EAE MICE

3.1 Introduction

Our laboratory has previously implicated acrolein, a pro-inflammatory and pro-oxidative toxin in the pathology of the animal model experimental autoimmune encephalomyelitis (EAE) [27]. The relative stability of secondary reactive aldehyde species compared to reactive oxygen species may provide greater efficacy in scavenging treatments when compared to standard antioxidant approaches with more transient targets. In prior *ex vivo* and *in vivo* studies, we have demonstrated that acrolein and its metabolites are elevated both locally and systemically [27, 47], that acrolein can directly damage myelin and the axonal membrane [18], and that scavenging of free acrolein using hydrazine pharmaceuticals such as hydralazine improves behavioral and pathological outcomes in EAE mice [27]. A pilot clinical study has also shown increases in acrolein metabolites in the biofluids of human MS patients [47].

Acrolein can be produced or metabolized by a variety of endogenous enzymes. The interaction of these enzymes and local levels of acrolein may provide novel methods for reducing acrolein. Here we examine levels of myeloperoxidase (MPO) in response to acrolein scavenging treatment in EAE mice and the effect of modulating aldehyde dehydrogenase 2 (ALDH2) function on the severity of EAE and on endogenous acrolein levels. Myeloperoxidase, which is secreted by inflammatory cells, is known to convert L-threonine into acrolein via formation of a monochloramine intermediate and is elevated in MS plaques [101-104]. Aldehyde dehydrogenase 2 is a mitochondrial enzyme which detoxifies aldehydes by oxidation into carboxylic acids. Activation of ALDH2 has previously been shown to alleviate motor function decline in EAE mice and to suppress reactive aldehydes [24].

We have previously reported primarily on the motor deficits observed in EAE; however, in many cases including the studied EAE model, mechanical hypersensitivity can precede the onset of clear motor impairment. Acrolein has been shown to activate TRPA1, a nociceptive receptor-channel found in sensory ganglia [105-110], by reacting with nucleophilic residues such as lysine and cysteine [97-99]. Expression of TRPA1 has also been demonstrated to increase in animal models of spinal cord contusion, a condition which also exhibits significant inflammation and

oxidative stress [111]. Furthermore, treatment with acrolein scavengers such as hydralazine has significantly alleviated mechanical hypersensitivity within rats with spinal cord contusion while also reducing the presence of acrolein-lysine adducts [28, 95, 96, 111]. Direct microinjection of acrolein to the spinal cord has also been shown to induce similar sensory disruptions to contusion injuries [93], further supporting the role of acrolein in this type of pathology. Recent work has confirmed that TRPA1 expression is also elevated in the C57BL6 progressive EAE model [112] and that TRPA1 antagonists reduce mechanical allodynia in progressive and relapsing-remitting EAE [113]. As such, it is possible that acrolein can induce TRPA1 mediated hyperreflexia and hyperalgesia through increased expression and activation of TRPA1. Given that inflammation and oxidative stress are also key components of EAE and MS pathology, we propose that hyperreflexia in EAE mice may be at least partially mediated by similar mechanisms.

The current study aims to further investigate the role of acrolein in the pathology of EAE. Our previous work in EAE mice has utilized only hydralazine as a potential scavenger, leaving open the question of whether the observed effect can be primarily attributed to hydrazine-based carbonyl scavenging rather than to separate structure specific interaction. In this study, we examined the efficacy of alternative acrolein scavenging, the effect of acrolein on EAE-induced mechanical hypersensitivity, and the effect of ALDH2 activity on the pathological progression of EAE.

3.2 Methods

3.2.1 Animals

C57BL/6 mice (8 weeks old) were purchased from Envigo (Indianapolis, IN) and allowed to acclimate to laboratory housing facilities for a minimum of one week prior to experimentation. All live animal procedures were performed under protocols approved by the Purdue Animal Care and Use Committee.

ALDH2*2 knock-in mice were obtained from Stanford University [114] and maintained in a breeding colony in laboratory animal housing facilities. Transgenic mice were transferred from the breeding colony to experimental laboratory housing a minimum of one week prior to experimentation and wild type mice were ordered to match age to within one week.

3.2.2 EAE induction and motor function scoring

Mice between 9 and 12 weeks of age were injected subcutaneously with 0.1 mL MOG_{35-55}/CFA emulsion (EK-2110, Hooke Laboratories) over rostral and caudal ends of the spinal column. 100 ng of deconjugated pertussis toxin was administered intraperitoneally 60-90 minutes following injection of emulsion and again between 22 and 24 hours later. Motor function was scored daily using an established 5-point system to assess degree of paralysis. Scores were assigned in the following manner: 0-No deficit, 2-hind limb paresis or ataxia without leg dragging, 3-hind limb paresis with one or both hind limbs dragging, 4-Complete hind limb paralysis, 5-Moribund. Humane endpoints requiring euthanasia prior to experimental timepoints included loss of over 20% body weight and attaining a motor function score of 5.

3.2.3 Acrolein scavenging treatments

All drugs were dissolved in phosphate buffered saline and sterilized with a 0.45 μm filter prior to storage at 4 C. Hydralazine hydrochloride (Millipore Sigma, St. Louis, MO) was administered at a dose of 1 mg/kg daily via intraperitoneal injection starting from either the day of induction or upon reaching a motor score of 1 and continuing through the duration of the study. Phenelzine (Millipore Sigma) and dimercaprol (Alfa Aesar, Ward Hill, MA) were administered in separate cohorts at 1 mg/kg daily to further elucidate the role of acrolein scavenging in alleviating EAE related pathology. Experimental groups not receiving pharmaceutical intervention received 0.1 mL phosphate buffered saline.

3.2.4 Alda-1 treatment

Alda-1 (Cayman Chemical, Ann Arbor, MI) was dissolved in vehicle consisting of 50% PEG-400 in DMSO. Treatment animals were given 50 mg/kg by intraperitoneal injection daily while animals in other groups received an equivalent volume of vehicle.

3.2.5 Assessment of mechanical hyperreflexia

Mechanical hyperreflexia was evaluated using calibrated von Frey filaments to quantify paw withdrawal thresholds in response to known mechanical stimulus. Animals were placed on an

elevated metal mesh platform, covered by a transparent plastic container, and allowed to acclimate for a minimum of 10 minutes prior to assessment. Calibrated von Frey filaments (NC12775-99, North Coast Medical, Morgan Hill, CA) were applied to the plantar aspect of the hind paw with adequate bending force for between 3 and 5 seconds. As with our previous studies, the up-down method was utilized to determine 50% withdrawal thresholds with brisk movement of the affected limb being defined as a positive reaction. The average result of the two limbs was recorded for each animal. These assessments took place prior to induction as well as days 5 and 10 post induction to reduce false negatives resulting from hind limb motor inhibition.

3.2.6 Immunohistochemistry

Fixed spinal cords were cryoprotected by incubating for 48 hours in 30% sucrose solution at 4 C. 1 cm segments were cut from the thoracic spinal cord, embedded in PolyFreeze (Polysciences, Warrington, PA), and frozen in a slurry of dry ice and 2-propanol. 25 μM sections were cut using a cryostat microtome (HM 525 NX, Thermo Scientific) and stored in 0.1% sodium azide in phosphate buffered saline. Prior to staining, sections were rinsed with phosphate buffered saline for 5 minutes remove any remaining embedding compound followed by a 30-minute incubation in 3% hydrogen to quench endogenous peroxidase activity. Sections were permeabilized in 3% Triton-X in phosphate buffered saline and blocked with 5% normal donkey serum in 0.3% Triton-X for two hours. After washing three times with PBS, sections were incubated in a mouse anti-acrolein (SMC-505, Stressmarq Biosciences, Victoria, Canada) or anti-myeloperoxidase antibody (GTX54393, GeneTex, Irvine, CA) at 4 C for 24. Sections were then washed four times with PBS and incubated in biotinylated goat anti-mouse IgG for 2 hours at room temperature. Slides were then washed three times with 0.1% Triton-X in PBS prior to incubation in avidin-biotin complex according to the manufacturer's instructions (#32020, Thermo Scientific). After an additional three washes in 0.1% Triton-X, sections were developed with a Pierce DAB substrate kit (Thermo Scientific, Catalog No 34002) for five minutes and rinsed in distilled water. Sections were dehydrated with increasing concentrations of ethanol prior to mounting on positively charged slides (Tissue Tack, Polysciences, Warrington, PA) and applying coverslips with Permount. DAB stain intensity was determined with ImageJ according to Furhich et al [115].

3.2.7 Statistical analysis

All data are presented in the format of mean ± standard error of the mean (SEM). One way ANOVA with Tukey's test *post-hoc* or Student's t-test were used for statistical assessment (α=0.05).

3.3 Results

3.3.1 Acrolein scavengers phenelzine and hydralazine improve motor symptom progression in EAE mice

EAE mice were treated with phenelzine, a hydrazine based acrolein scavenger, and motor symptoms were scored using an established 5-point scale (Figure 3.1). Phenelzine treated animals exhibited a delayed onset of symptoms, defined as the day post-induction of reaching a score of 1.0, with the average day of onset shifting from 13.14 ± 1.03 days post induction in untreated mice (n=6) to 23.5 ± 2.92 days post induction in treated mice (n=7, $p<0.01$). Furthermore, peak symptom severity was reduced from 3.43 ± 0.43 in untreated animals to 1.33 ± 0.67 in those receiving phenelzine ($p<0.05$)

Delaying acrolein scavenging treatment until the onset of motor symptoms also conveyed significant reduction in motor symptom severity (Figure 3.2). Treated animals showed significantly less severe motor scores starting on the fourth day of hydralazine treatment. Furthermore, peak symptom severity was improved from 3.54 ± 0.24 in untreated EAE mice (n=13) to 2.38 ± 0.32 in hydralazine treated mice (n=8).

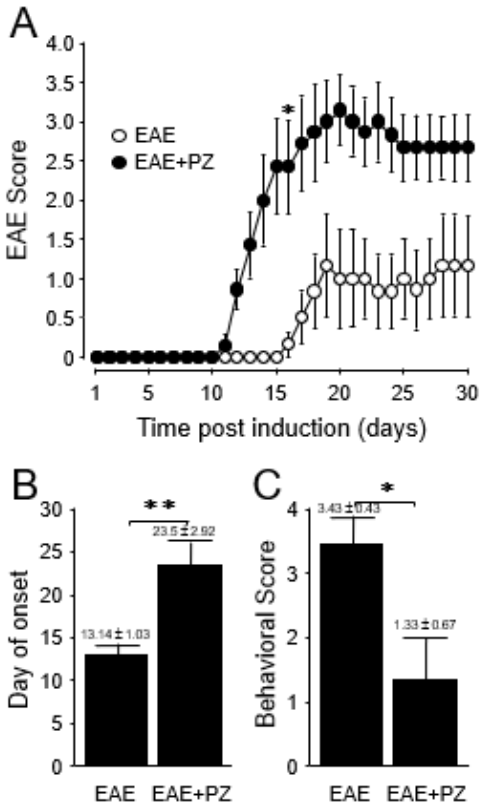

Figure 3.1 EAE motor symptom scores of EAE mice with and without phenelzine treatment. A) Symptom scores over time for untreated and phenelzine treated EAE mice. Phenelzine treatment significantly reduced the severity of symptoms after day 16 ($p<0.01$) with both later apparent onset and lower peak severity. B) Phenelzine treatment delayed the average day of onset, defined as the day on which motor score reached 1.0, from 13.14 ± 1.03 days post induction to 23.5 ± 2.92 days post induction ($p<0.01$). C) Phenelzine treatment reduced peak severity of motor impairment from 3.43 ± 0.43 to 1.33 ±0.67.

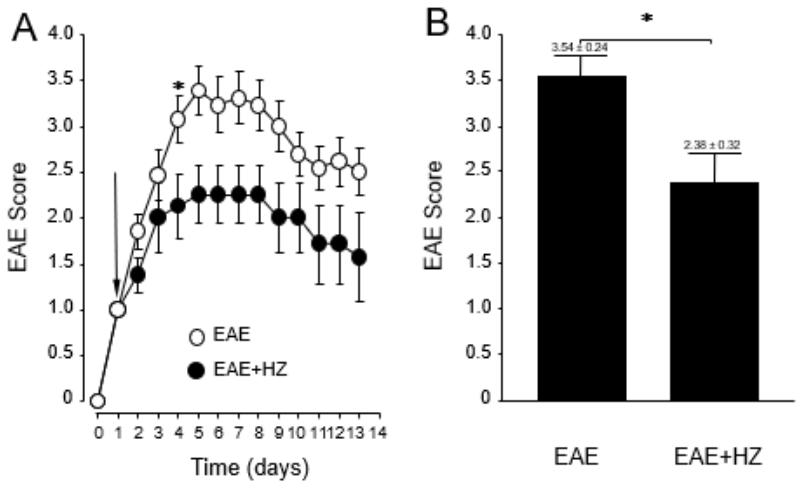

Figure 3.2 Effect of delayed application of acrolein scavenging therapy. A) Delaying hydralazine treatment to the appearance of motor symptoms reduced disease severity starting on the fourth day of treatment ($p<0.05$) and continued through the end of the study. B) Delayed treatment reduced peak motor symptom scores from 3.54 ± to 0.24 to 2.38 ± 0.32 ($p<0.05$)

3.3.2 Acrolein scavengers alleviate mechanical hyperreflexia in EAE mice

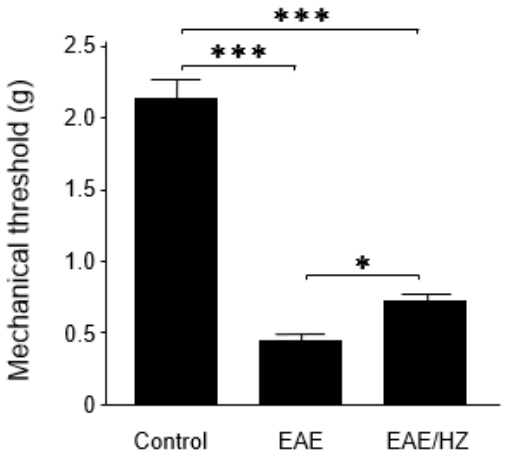

Figure 3.3 Effect of hydralazine treatment on mechanical hyperreflexia on day 10 post-induction. EAE mice exhibited significantly lower hind paw withdrawal thresholds at 0.45 ± 0.05 grams compared to healthy controls which showed an average withdrawal threshold of 2.11 ± 0.15 ($p<0.001$). Hydralazine treatment partially alleviated this to 0.76 ± 0.09 grams which is improved compared to untreated EAE mice ($p<0.05$), but still exhibited higher sensitivity than the control group ($p<0.001$).

Calibrated von Frey filaments were used to obtain 50% withdrawal thresholds according to established methodology. EAE mice exhibited significantly lower mechanical response thresholds at 0.45 ± 0.05 g compared to healthy control animals at 2.11 ± 0.15 g (Figure 3.3, $p<0.001$). Hydralazine treatment significantly improved mechanical thresholds when compared to EAE mice (0.76 ± 0.09, $p<0.05$), but this remained significantly lower than the control group ($p<0.001$).

Similar results were obtained when using dimercaprol, a thiol-based acrolein scavenger (Figure 3.4). EAE mice again showed significantly lower mechanical withdrawal thresholds at 0.37 ± 0.06 g compared to controls at 2.10 ± 0.17 g ($p<0.0001$). Similarly, treatment with dimercaprol provided partial relief to 1.00 ± 0.26 g ($p<0.05$), but this again remained significantly lower than control animals ($p<0.01$).

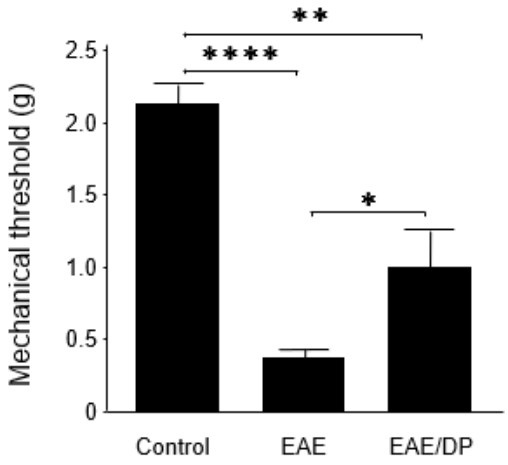

Figure 3.4 Effect of dimercaprol treatment on hind paw withdrawal thresholds on day 10 post-induction. EAE mice were significantly more sensitive to mechanical stimulus than controls with an average hind paw withdrawal threshold of 0.37 ± 0.06 grams compared to 2.10 ± 0.17 ($p<0.0001$). Dimercaprol, a thiol-based carbonyl scavenger, alleviated sensitivity in EAE mice to 1.00 ± 0.26 grams ($p<0.05$) but did not fully return to the level of healthy controls ($p<0.01$).

3.3.3 Hydralazine reduces endogenous acrolein adducts and myeloperoxidase

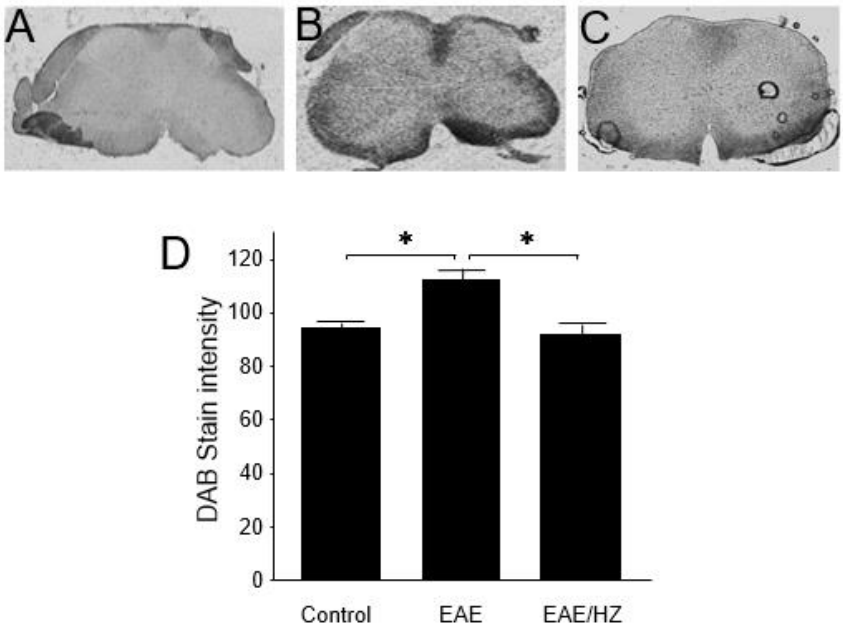

Figure 3.5 Imaging of FDP-Lysine in spinal cords of EAE mice. FDP-Lysine was significantly elevated in the spinal cords of EAE mice compared to controls on day 10 post-induction ($p<0.05$). Hydralazine treatment reduced the presence of FDP-Lysine compared to untreated mice ($p<0.05$).

Immunostaining revealed elevated levels of acrolein-modified lysine residues in the dorsal spinal cord of EAE mice compared to controls (Figure 3.5, $p<0.05$). Tissue from hydralazine treated EAE mice displayed significantly lower levels of acrolein adducts compared to untreated EAE ($p<0.05$) and were not significantly different than controls ($p>0.05$). Similarly, EAE mice exhibited higher levels of myeloperoxidase in the dorsal spinal cord compared to controls (Figure 3.6$p<0.05$), and this was reduced with hydralazine treatment ($p<0.05$).

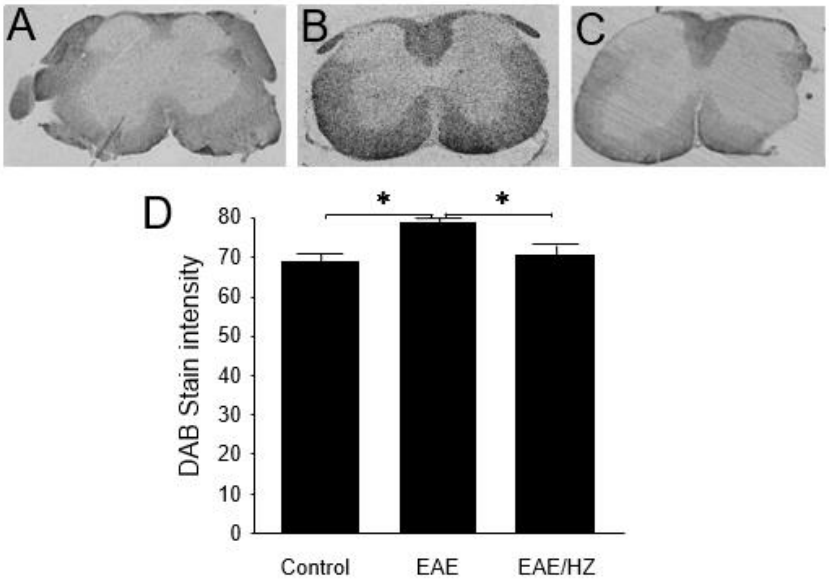

Figure 3.6 Imaging of myeloperoxidase in spinal cords of hydralazine treated EAE mice. MPO was significantly elevated in the dorsal spinal cord of EAE mice compared to controls on day 10 post-induction ($p<0.05$). Hydralazine treatment reduced the presence of MPO compared to untreated mice ($p<0.05$). No significant differences were observed between hydralazine treated mice and control animals.

3.3.4 Modulation of ALDH2 activity impacts white matter acrolein levels

Treatment with the ALDH2 agonist Alda-1 reduced levels of acrolein-lysine adducts in the spinal cord white matter of EAE mice (Figure 3.7, $p<0.05$). In contrast, ALDH2*2 mutant mice exhibited significantly elevated levels of acrolein adducts compared to wild type EAE mice ($p<0.05$). Similarly, MPO levels were suppressed with Alda-1 treatment and elevated in ALDH2*2 mice when compared to wild type EAE (Figure 3.8, $p<0.05$). Linear regression of MPO and acrolein levels demonstrated fair correlation between MPO and acrolein (Figure 3.9, $r=0.7419$, $p<0.05$).

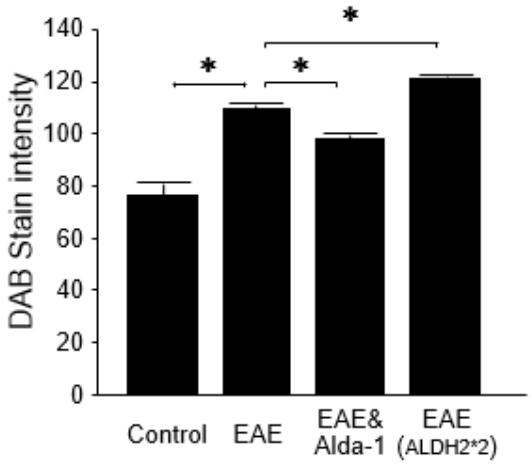

Figure 3.7 Immunostaining of FDP-Lysine in the spinal cords of ALDH2*2 and Alda-1 treated EAE mice. FDP-Lysine was significantly elevated in spinal cord white matter of EAE mice compared to control ($p<0.05$). ALDH2*2 mutant EAE mice exhibited increased FDP-lysine when compared to wild type EAE mice ($p<0.05$). Alda-1 treatment in wild type EAE mice suppressed levels of FDP-Lysine compared to untreated mice ($p<0.05$). No significant differences were observed between controls and Alda-1 treated mice.

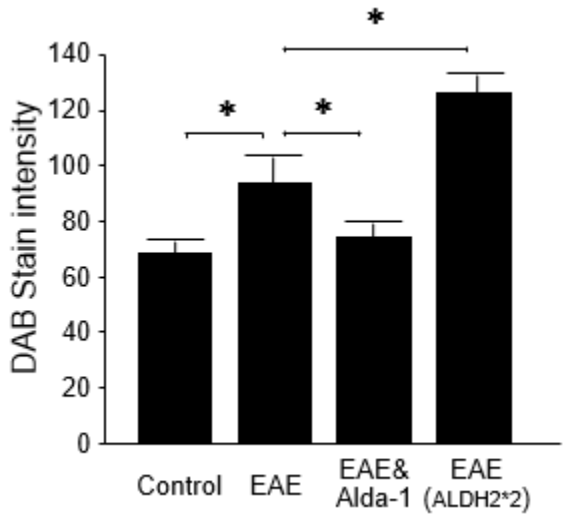

Figure 3.8 Immunostaining of myeloperoxidase in the spinal cords of ALDH2*2 and Alda-1 treated EAE mice. FDP-Lysine was significantly elevated in spinal cord white matter of EAE mice compared to control ($p<0.05$). ALDH2*2 mutant EAE mice exhibited increased MPO when compared to wild type EAE mice ($p<0.05$). Alda-1 treatment in wild type EAE mice suppressed levels of MPO compared to untreated mice ($p<0.05$). No significant differences were observed between controls and Alda-1 treated mice.

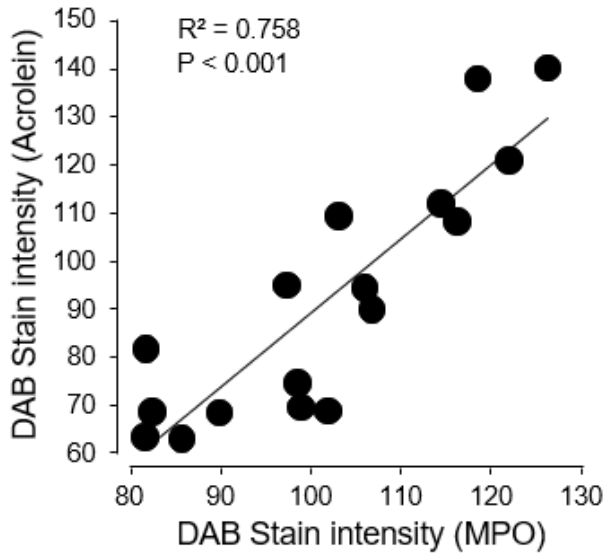

Figure 3.9 Correlation of FDP-lysine with myeloperoxidase. Linear regression of observed staining intensity shown in Figure 8 and Figure 9 demonstrated fair correlation between levels of acrolein and myeloperoxidase ($r=0.7419$, $p<0.05$).

3.3.5 Modulation of ALDH2 activity improves sensory and motor deficits in EAE mice

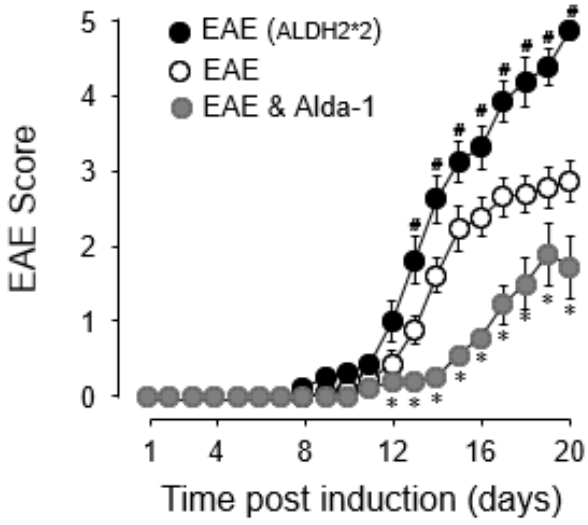

Figure 3.10 Motor scoring of ALDH2*2 and Alda-1 treated EAE mice. Alda-1 alleviated motor deficits in EAE mice on multiple days starting from day 12 post-induction (* $p<0.05$ compared to EAE). Conversely, ALDH2*2 mice exhibited significantly more severe motor deficits when compared to wild-type EAE mice starting from day 13 post-induction (# $p<0.05$ compared to EAE).

Treatment with Alda-1 significantly reduced the severity of motor symptoms starting from day 12 post-induction when compared to EAE (Figure 3.9, $p<0.05$). Conversely, ALDH2*2 mice, exhibited significantly more severe motor symptoms than wild type EAE mice ($p<0.05$). Notably, four ALDH2*2 animals reached humane timepoint for motor symptoms severity between days 18 and 20. EAE mice exhibited significantly lower hind paw mechanical withdrawal thresholds on day 10 post-induction compared to control (Figure 3.11, $p<0.05$). This increased sensitivity was partially alleviated in Alda-1 treated EAE mice ($p<0.05$), however, ALDH2*2 mutant mice could not be distinguished from control ($p>0.05$).

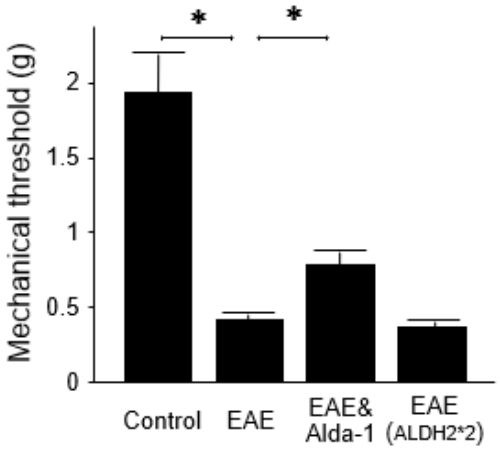

Figure 3.11 Mechanical withdrawal thresholds at day 10 post-induction. EAE mice had significantly lower 50% hind paw withdrawal thresholds compared to controls ($p<0.05$). This hypersensitivity was significantly alleviated in Alda-1 treated animals ($p<0.05$)

3.4 Discussion

Although the precise etiology of multiple sclerosis is unknown, demyelination, inflammation, oxidative stress, and axonal degeneration are considered key components of its pathophysiology [32, 116, 117]. Our previous work as identified acrolein as potential mediator in propagating oxidative damage in experimental autoimmune encephalomyelitis [27]. In this study, we expand upon this by evaluating alternative acrolein scavenging therapies and by examining whether these can alleviate EAE induced nociceptive behaviors. We found that motor symptoms were alleviated with alternative carbonyl scavengers and by a delayed treatment regimen. Furthermore, we observed that acrolein scavenging treatments alleviated mechanical hyperreflexia and reduced

oxidative and inflammatory markers in the dorsal spinal cord of EAE mice. Finally, we explored how modulation of endogenous enzymes affect EAE progression.

Acrolein and other reactive carbonyl species have been extensively examined as secondary mediators of oxidative stress due to high reactivity with proteins, lipids, and DNA. It has been proposed that acrolein contributes to EAE and MS pathology through multiple mechanisms including direct damage to myelin and axonal membranes. Furthermore, acrolein can induce mitochondrial dysfunction resulting in further oxidative stress. As such, acrolein scavenging treatments may provide neuroprotection in MS by reducing damage to lipid rich myelin and axonal membranes.

Currently, hydrazine compounds such as hydralazine, are among the most well studied acrolein scavengers. In this study, we examined phenelzine as an alternative scavenger to confirm whether the effect of hydralazine is due to hydrazine functionality or due to a mechanism specific to the phthalazine scaffold. Given that phenelzine provided similar reduction of motor deficits when compared to hydralazine, it is likely that the effects of hydrazine and phenelzine are due to the hydrazine group which readily forms a Schiff base with reactive carbonyls such as acrolein. Furthermore, hydralazine treatment was delayed to the onset of motor symptoms to present a more realistic treatment regimen. This delayed treatment showed significant improvement after four days and significantly reduced the peak severity of motor symptoms. This suggests that production of acrolein occurs throughout disease progression and can be mitigated through pharmaceutical scavengers.

Neuropathic pain is a common symptom in patients with multiple sclerosis with between 50 and 80 percent of patients experiencing some degree of pain. This is thought to result from demyelination and neuroinflammation typical of the disease. Thus far, efforts to treat neuropathic pain have limited success with frontline therapies providing relief in only 40 to 60 percent of cases. Recent work in both a relapsing-remitting and chronic variant of EAE has also demonstrated that reactive carbonyls contribute to nociceptive behavior via the receptor channel TRPA1 and that TRPA1 antagonists can reduce mechanical allodynia in EAE mice. Here, we found that acrolein scavenging treatments alleviated EAE related nociceptive behaviors and reduced the presence of myeloperoxidase and acrolein adducts in the dorsal spinal tracts of EAE mice. In addition, our quantification of TRPA1 mRNA concurs with previous findings which found elevated TRPA1 transcripts in MOG induced progressive EAE. However, this was not significantly reduced with

hydralazine treatment. As such, it is likely that hydralazine and dimercaprol reduce nociceptive behaviors primarily by scavenging acrolein, thereby reducing the presence of TRPA1 agonists.

Previous work in EAE has demonstrated that increasing the activity of ALDH2 with Alda-1 treatment improves functional outcomes and decreases presence of aldehyde metabolites. In this study, we found concurring evidence that Alda-1 reduces the presence of acrolein metabolites and of myeloperoxidase. Furthermore, mice with the deficient ALDH2*2 mutation exhibited more severe clinical progression and elevated acrolein metabolites and myeloperoxidase in white matter. Together, these suggest that ALDH2 may be a viable therapeutic target to enable nonstoichiometric detoxification of reactive aldehydes such as acrolein.

The observed correlation of white mater myeloperoxidase and acrolein presents an opportunity for longitudinal assessment of inflammation and oxidative stress. Present methods of estimating the relative levels of reactive aldehydes are limited by either invasiveness or lack of specificity to the region of interest. However, it is possible to examine myeloperoxidase via magnetic resonance imaging through a targeted gadolinium contrast agent. This would enable longitudinal examination of inflammation and oxidative stress in EAE and provide insight into therapeutic efficacy at different stages of the disease.

The efficacy of multiple acrolein scavengers in alleviating both motor and sensory symptoms suggests a broad involvement of acrolein in the pathology of MS. This is further supported by histological examination which found elevated quantities of acrolein metabolites and myeloperoxidase in EAE mice that were alleviated with hydralazine. Although previous studies focused primarily on the use of hydralazine and phenelzine, we found that dimercaprol and Alda-1 were also effective in alleviating EAE symptoms. Conversely, deficiency in ALDH2 exacerbated progression of EAE and increased oxidative and inflammatory metabolites in white matter, suggesting that ALDH2 may be a viable enzymatic target for improving aldehyde clearance. Future work may focus on development of alternative acrolein scavenging strategies with reduced off target effects which could restrict application based on patient condition.

4. NEUROPROTECTION IN VITRO AND IN ANIMAL MODELS OF PARKINSON'S DISEASE BY MULTIPLE ACROLEIN SCAVENGERS

4.1 Introduction

Parkinson's Disease is a neurodegenerative disease clinically characterized by a severe movement disorder [118]. PD results from the death of dopaminergic neurons in the substantia nigra which project into the striatum, which is critical for motor function. Although the initiating factors are not known, oxidative stress has been proposed as a key contributor to dopaminergic cell death in PD [1, 14, 119-121]. However, drugs which attempt to directly scavenge free radicals and reactive oxygen species have been ineffective in delaying or alleviating motor deficits in PD.

Acrolein possesses a significantly longer half-life than reactive oxygen species, and it has been proposed to contribute to secondary neurotrauma of the brain and spinal cord [5, 82, 91, 95]. Its reactivity with nucleophilic amino acid residues such as lysine, histidine and cysteine [13] is of particular interest in PD as α-synuclein, the primary component of Lewy bodies in PD, is relatively lysine rich with many of these present in the α-helical structure which interacts with the membrane under normal conditions [84-87, 122]. We postulate that acrolein modified lysine may be more prone to aggregation and thereby contribute to neurodegeneration in PD.

The aim of the present study is the examine the role of acrolein in dopaminergic cell death. To accomplish this, cellular and animal models were utilized to elucidate the role of acrolein in dopaminergic cell death. Furthermore, multiple acrolein scavenging compounds were tested to examine the potential neuroprotective effects of this therapeutic strategy in PD.

4.2 Methods

4.2.1 MES23.5 cell culture

MES23.5 is a mouse-rat hybrid dopaminergic cell line. Cells were propagated in Sato's N1 medium as described by Crawford et al [123]. One group of MES23.5 cells was incubated with 400 μM 6-OHDA for 2 hours. A second group was treated with 500 μM hydralazine 15 minutes following 6-OHDA exposure. Cell viability was determine using either MTT assay or Trypan Blue.

4.2.2 Trypan blue assay

A 0.5 mL cell suspension (1 x 10^6 cells/mL in HBSS) was thoroughly mixed with an equal volume of 0.4% trypan blue at room temperature. 10 μL of this mixture was transferred to each side of a hemocytometer. The total number of viable cells was counted using a light microscope with viability of cells expressed as the percentage of viable cells out of the total cell count. Viability percentage was calculated as the average of duplicates from each side of the hemocytometer with four replicates.

4.2.3 MTT assay

Cells were seeded in 12 well plays at 1 x 10^6 cells/mL in HBSS. [4,5-Dimethylthiazol-2-yl]-2,5-diphenyl tetrazolium bromide (MTT) was reconstituted in phosphate buffered saline and added to each well prior to the end of the experiment. An equal volume dimethyl sulfoxide was then added to each well to dissolve any remaining formazan crystals, and the resulting absorbance at 500 nm was measured with a spectrophotometer (Spectra), and background absorbance at 660 nm was subtracted from the obtained values. Values are expressed as a percentage of the control sample.

4.2.4 Animal surgeries and treatments

Male Sprague-Dawley rats weighing 250-300 g were ordered from Harlan Laboratories (Indianapolis, IN) and housed in a temperature-controlled environment (25°C) with a 12-hour day and night cycle and *ad libitum* access to standard diet and water. All animal experiments were performed in compliance with a protocol approved by the Purdue Animal Care and Use Committee.

Rats were divided into five groups: controls (no surgery), sham injury, 6-OHDA, 6-OHDA with treatment, and acrolein. Animals that underwent surgery were anesthetized with a mixture of ketamine (100 mg/kg) and xylazine (10 mg/kg) and secured in a Kopf stereotaxic frame. A midsagittal incision was made to expose the skull, and a dental drill was used to drill a hole and expose the dura mater.

Animals receiving 6-OHDA received a unilateral injection to the right side of the brain in the medial forebrain bundle (8 μg/2μL) at the following coordinates from bregma AP: -4.0, ML: 1.5, and DV: -8.5. A Hamilton syringe was used to infuse at 1 μL/minute and the needle was withdrawn after 5 minutes. Acrolein administration was performed under similar procedures with

acrolein at 500 μM/2 μL in saline with 0.01% ascorbic acid. Sham operated animals were injected with equivalent volumes of saline under the same procedures. Following injection, the incision was closed with stainless steel wound clips.

Hydralazine was dissolved in phosphate buffered saline and administered daily via intraperitoneal injection (5 mg/kg). Similarly, animals which received dimercaprol treatment were given 5 mg/kg in phosphate buffered saline.

4.2.5 Rotarod

A rotarod test, in which animals must maintain balance on a rotating drum, was used to assess motor coordination. The test was performed as described by Jones and Roberts [124]. In brief, animals were first allowed to remain on a stationary drum for 10 s. The speed was then increased by 5 rpm per 10s until reaching a speed of 30 rpm. The test ends if the rat falls completely off the drum or grips the device and spins twice without walking on the rungs.

4.2.6 Von Frey test

Hind paw withdrawal threshold was tested as an indicator of mechanical hyperreflexia. The test was performed weekly on days 8, 16, 22, 29, and 35 after 6-OHDA injection. Rats were placed on an elevated metal mesh and covered with a transparent plastic container and allowed to acclimate for 10 minutes prior to testing. Subsequently, a series a calibrated Von Frey filaments (NC12775-99, North Coast Medical) was applied perpendicular to the plantar aspect of the hind limb with sufficient bending force for 3-5 seconds. Rapid withdrawal of the hind limb with or without licking and biting was recorded as a positive response. The up-down method was utilized to determine a 50% withdrawal threshold [125, 126] and the average score of the hind limbs was calculated per animal.

4.2.7 Western blotting

After the conclusion of behavioral testing, animals were anesthetized with ketamine and xylazine and perfused transcardially with cold oxygenated Krebs solution. Brais were collected and homogenized in 3% Triton with protease inhibitor cocktail. The lysate was stored on ice for 1 hour and centrifuged at 14,000g for 30 minutes. Supernatants were collected and stored at -80°C.

Protein was mixed with loading dye, added to a 7.5% acrylamide gel, and electrophoresed at 200 V for 50 min. Protein was transferred to a nitrocellulose membrane by electroblotting at 100 V for 3 hours. The membrane was blocked for 1 hour with blocking buffer (0.2% casein and 0.1% Tween 20 in PBS) prior to incubation with either polyclonal rabbit anti-acrolein (Abcam, #37110) or mouse anti-αSyn (BD Transduction, #610786) at a 1:1000 dilution in blocking buffer with 2% goat serum (Novus Biologicals) for 18 hours at 4°C. The membrane was washed with blocking buffer and transferred to a solution of alkaline phosphatase-conjugated goat Anti-rabbit IgG (1:10,000). After washing with blocking buffer followed by 0.1% Tween 20 in Tris-buffered saline, the membrane was exposed to Rad Immuno-Star Substrate (Bio-Rad), and visualized by chemiluminescence. Band densities were evaluated using Image J.

4.2.8 Immunohistochemistry

Animals were deeply anesthetized with ketamine and xylazine and perfused transcardially with Krebs solution followed by 4% paraformaldehyde in PBS. Brains were removed and postfixed in 4% paraformaldehyde for 3 days, prior to cryoprotection in 30% sucrose. Fixed brains were frozen in OCT compound and 15µm coronal sections were cut using a cryostat microtome. Striatal sections were washed in phosphate buffered saline and placed in 3% H_2O_2 to quench endogenous peroxidase activity. Sections were washed 3 times in PBS prior to blocking with 5% goat serum for 30 minutes at room temperature and reacted with mouse anti-TH antibody at a 1:1000 dilution (Biolegend Sandiego, CA) overnight at 4°C. After washing, sections were incubated with anti-mouse IgG for 2 hours at room temperature and processed using an ABC staining kit (Vector, PK-4000). After rinsing three times in PBS, sections were incubated in peroxidase substrate until the desired staining intensity was obtained.

4.2.9 Statistical analysis

Statistical analysis was carried out using one-way ANOVA with either Tukey or Newman-Keuls *post hoc* test. Student's t-test was used when only comparing two groups. $p<0.05$ was considered to be statistically significant, and results were expressed as mean ± SEM.

4.3 Results

4.3.1 6-OHDA mediated dopaminergic cell death

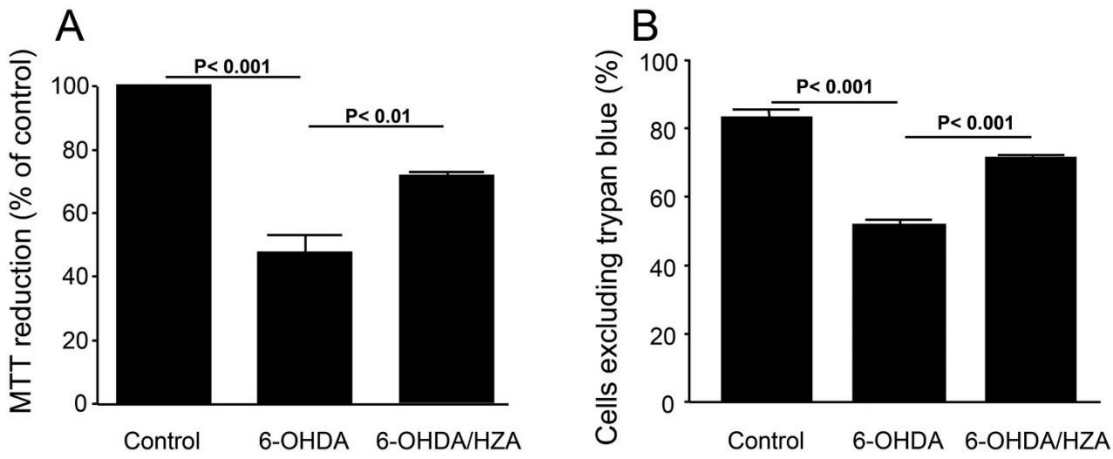

Figure 4.1 Mitigation of 6-OHDA induced dopaminergic cell death by hydralazine. A) Cell viability in MTT assay was determined by absorption at 550 nm and expressed as a percent of control. B) Cell viability in trypan blue assay is expressed as percentage of cells excluding trypan blue dye. 6-OHDA reduced cell viability compared to control in both trypan blue and MTT assays ($p<0.001$). Delayed hydralazine infusion improved cell viability in both MTT ($p<0.01$) and trypan blue ($p<0.001$) assays compared to 6-OHDA alone.

Exposure to 6-OHDA significantly reduced MES23.5 cell survival (48 ± 6%) compared to controls ($p<0.001$) (Figure 4.1). Hydralazine treatment improved cell viability compared to 6-OHDA alone (71 ± 1%, $p<0.01$). Similar results were obtained through trypan blue exclusion (Figure 4.1B). 6-OHDA reduced cell viability from 83 ± 3% in control to 52 ± 2% in 6-OHDA exposed cells ($p<0.001$). This reduction was partially reversed with hydralazine treatment (71 ± 1%, $p<0.001$).

4.3.2 Brain acrolein levels are increased in 6-OHDA and acrolein injected rats

Acrolein-lysine adducts were elevated in brain tissue lysates obtained 14 days after injection. IN 6-OHDA injected animals, these adducts were detected particularly at approximately 75 kDa compared to sham operated animals (Figure 4.2). This was partially mimicked in acrolein injected animals. Analysis of band density demonstrated a significant difference between the 6-OHDA and sham group ($p<0.05$), and between the acrolein group compared to either the 6-OHDA

group ($p<0.05$) or sham group ($p<0.05$). Furthermore, urinary 3-HPMA was also increased compared to the sham group at two weeks post injection ($p<0.05$).

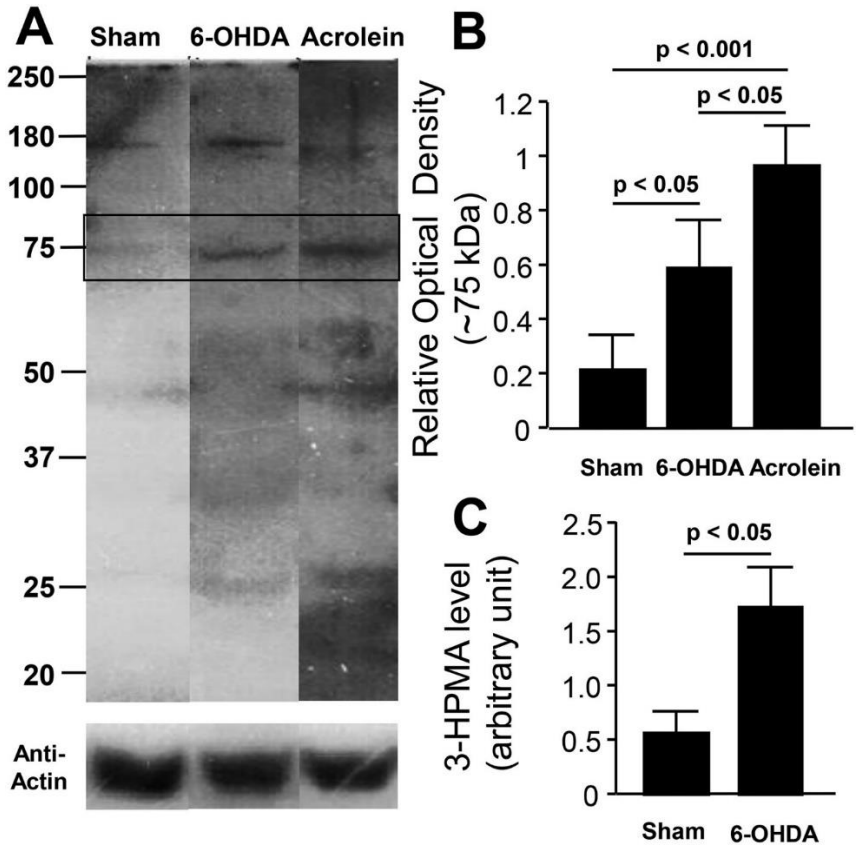

Figure 4.2 Elevation of local and systemic acrolein metabolites following injection of 6-OHDA or acrolein. A) Immunoblots of whole brain lysates collected 14 days post injection. Immunoreactivity occurred in a variety of bands but was particularly notable at approximately 75 kDa. B) Analysis of band density at 75 kDa. Band densities were significantly greater in 6-OHDA ($p<0.05$) and acrolein ($p<0.001$) injected animals compared to control and acrolein injection compared to 6-OHDA ($p<0.05$). C) Urinary 3-HPMA quantification. 6-OHDA injected animals exhibited significantly higher levels of systemic acrolein metabolites at 2 weeks post-surgery compared to sham ($p<0.05$)

4.3.3 Acrolein scavengers alleviate 6-OHDA induced motor deficits in rotarod activity

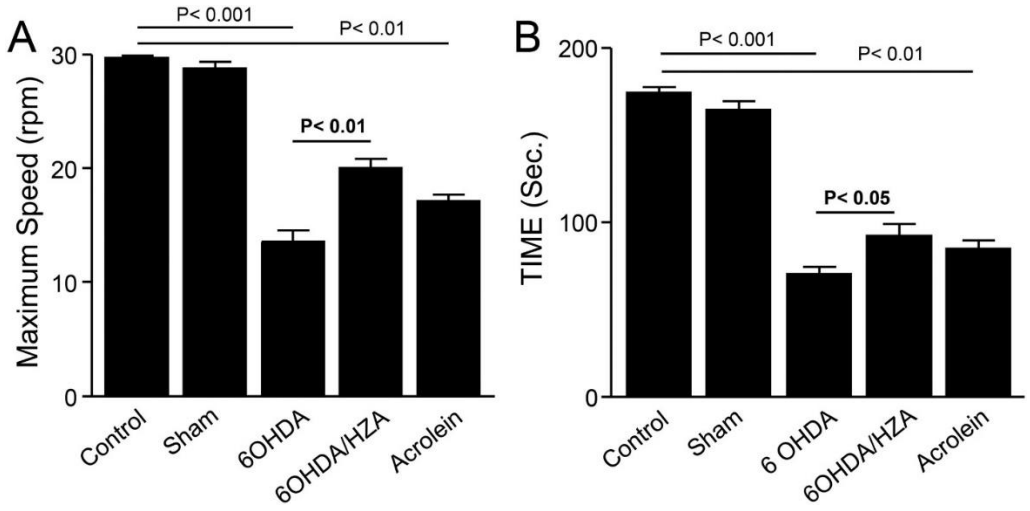

Figure 4.3 Rotarod test of 6-OHDA and acrolein injected rats with or without hydralazine treatment. A) 6-OHDA and acrolein injected animals reached significantly lower top speeds ($p<0.001$ and $p<0.01$, respectively) compared to control. Hydralazine treatment attenuated 6-OHDA induced reduction of top speed ($p<0.01$). B) 6-OHDA and acrolein-injected animals maintained lower time on the rotarod compared to sham ($p<0.001$ and $p<0.01$, respectively). This decrease was partially restored in hydralazine treated 6-OHDA rats ($p<0.05$).

6-OHDA injection reduced the maximal speed that could be sustained on a rotarod (Figure 4.3A). The maximum speed attained by control and sham treated animals was 29.7 and 28.9 rpm, respectively. 6-OHDA and acrolein injection reduced maximum speeds to 13.6 ± 3.0 ($p<0.001$) and 17.2 ± 1.4 ($p<0.01$), respectively. Hydralazine treated 6-OHDA rats showed a maximum speed of 20.1 ± 2.1 rpm which is significantly higher than untreated 6-OHDA ($p<0.01$).

Similar results were obtained when instead examining the maximum time that could be attained on a 30 rpm rotarod (Figure 4.3B). Specifically, control and sham animals showed maximum times of 174.9 ± 8.3 and 165 ± 13.4 s, respectively. 6-OHDA and acrolein injected animals exhibited significantly reduced times of 70.9 ± 10.7 ($p<0.001$), and 85.4 ± 12.5 s ($p<0.05$), respectively. Hydralazine significantly improved performance to 93.1 ± 17.9 s when compared to 6-OHDA alone ($p<0.05$).

Dimercaprol, an alternative acrolein scavenger, demonstrated similar efficacy in improving motor performance in the rotarod test (Figure 4.4). When testing weekly after injection, maximum time on the rotarod in dimercaprol treated animals was improved in weeks 4 and 5 post injection

(318 ± 23.5 s and 300 ± 40.1 s, respectively) compared to 6-OHDA alone (174 ± 65.0 and 167 ± 24.3 s, $p<0.01$). Similarly, maximum speeds in dimercaprol treated animals reached higher maximum speeds at weeks 4 and 5 post injection compared to 6-OHDA alone ($p<0.01$).

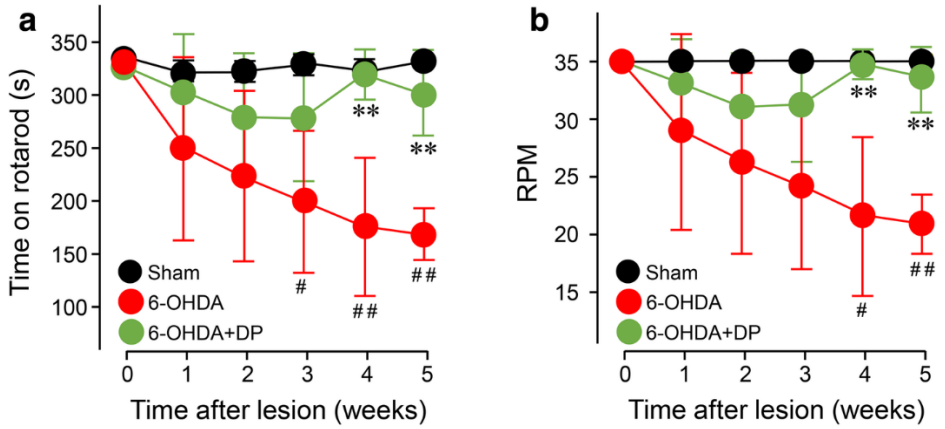

Figure 4.4 Rotarod test of 6-OHDA injected rats with or without dimercaprol treatment. A) Maximum time on rotarod was significantly reduced in 6-OHDA injected animals compared to sham starting on week 3 post-injection. Dimercaprol attenuated 6-OHDA induced deficits starting from week 4. B) Maximum attainable speed was also decreased in 6-OHDA injected animals and restored with dimercaprol treatment starting on 4 weeks post-injection ** $p<0.01$ compared to 6-OHDA; #$p<0.05$, ##$p<0.01$ compared to sham (N=5)

4.3.4 Dimercaprol alleviates hyperreflexia in 6-OHDA rats

Because acrolein has been linked to neuropathic pain in rodents, hind paw withdrawal thresholds were obtained by the up-down method (Figure 4.5). 6-OHDA injected animals exhibited significantly lower hind paw withdrawal thresholds (5 ± 2.9 g) compared to sham (15 ±0.9g, $p<0.01$) starting from week 2 and persisting through week 5 ($p<0.01$). Dimercaprol treatment significantly attenuated the effect of 6-OHDA on hind paw mechanical withdrawal thresholds starting from week 3 post injection ($p<0.05$).

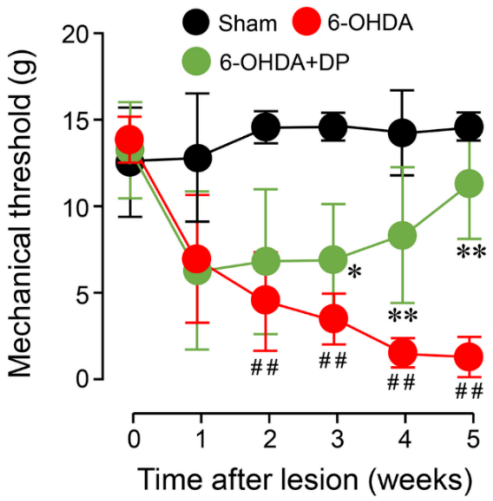

Figure 4.5 6-OHDA induced hyperreflexia alleviated by dimercaprol. 6-OHDA injected animals exhibited significantly lower hind paw withdrawal thresholds compared to control starting on week 2 post-injection. This hyperreflexia was attenuated by dimercaprol treatment starting on week 3 post-injection. ##p<0.01 compared to sham; *p<0.05, **p<0.01 compared to 6-OHDA.

4.3.5 Hydralazine mitigates 6-OHDA induced dopaminergic cell loss

Immunostaining for tyrosine hydroxylase revealed a 92.75% decrease in tyrosine hydroxylase immunolabeling in the striatum of 6-OHDA lesioned rats when compared to control rats (Figure 4.6). This loss in tyrosine hydroxylase positive dopaminergic terminals was mitigated by hydralazine treatment ($p<0.05$). This suggests that hydralazine provides a neuroprotective effect against the pathological processes induced by 6-OHDA.

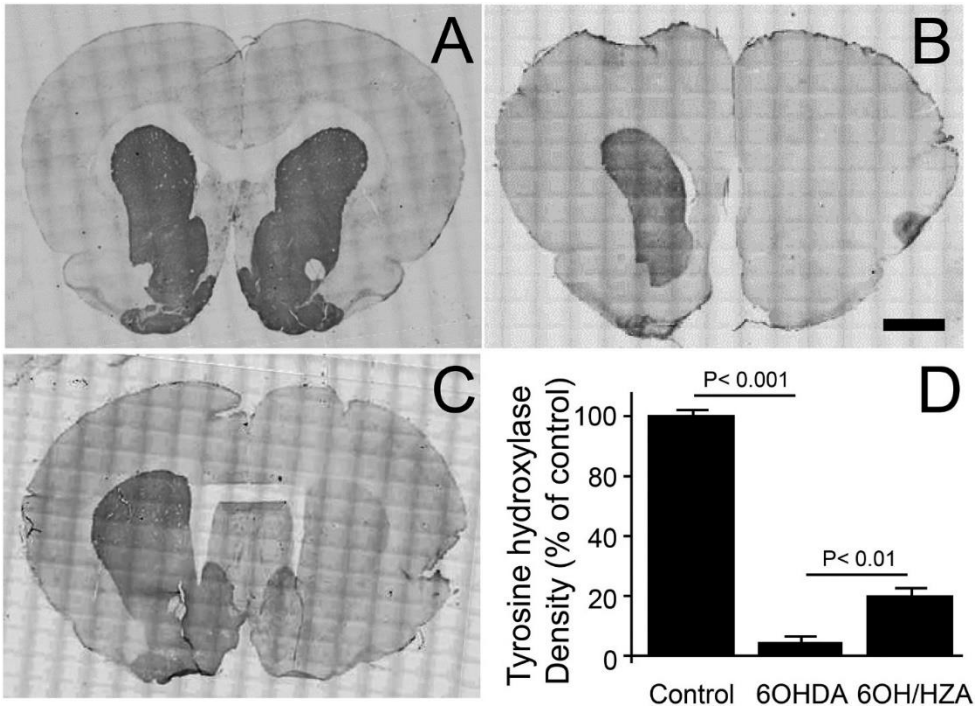

Figure 4.6 Tyrosine hydroxylase staining following injection of 6-OHDA. Representative images of axial brain sections in control (A), 6-OHDA injected (B), and hydralazine treated 6-OHDA rats (C). Analysis of band densities revealed a significant decrease in tyrosine hydroxylase in the striatum of 6-OHDA injected rats ($p<0.001$) which was significantly mitigated by hydralazine treatment ($p<0.01$).

4.4 Discussion

In this study we have conducted *in vitro* and *in vivo* studies with behavioral examination to gather evidence regarding the role of acrolein in pathology of 6-OHDA induced Parkinsonism in the rat. We have found that the levels of acrolein-lysine adducts are significantly elevated in the rat midbrain two weeks following injection with 6-OHDA and that injection of acrolein produces not only similar increases in acrolein metabolites, but also similar motor deficits. We have found that acrolein scavenging treatment with hydralazine mitigates dopaminergic cell death in 6-OHDA injected rats. This is further supported by cell culture experiments which demonstrated 6-OHDA induced cell death and its mitigation with hydralazine treatment. Similar improvements in cell viability were observed with dimercaprol, an alternative thiol based acrolein scavenger. Taken together, these suggest that acrolein is a critical factor in mediating cytotoxicity within these cellular and animal models.

Immunoblotting revealed a marked elevation in acrolein adducted protein particularly at 75 kDa, while previous work in SCI demonstrated elevation among a greater variety of molecular weights. This may be due in part due to the differences between contusive injury and the 6-OHDA and acrolein injection models. While microinjection still produces a somewhat focal injury, it is likely less immediately severe when compared to direct contusive trauma. As such, it is possible that the less severe injury produces lower global acrolein adduction while concentrating on a subgroup of proteins which are not easily cleared such as α-synuclein. Even if the effect of acrolein is mostly confined to α-synuclein, this could still allow acrolein to play a critical role in PD pathology.

Examination of mechanical hyperreflexia revealed a marked decrease in withdrawal thresholds in 6-OHDA injected rats compared to sham surgery. Similar to our previous studies in spinal cord injury and EAE, we find that acrolein scavenging treatment with dimercaprol significantly alleviates the observed hypersensitivity. This is consistent with the notion of inflammation and oxidative stress contributing to neuropathic pain. Previous work in SCI suggests that the effect of acrolein may be partially mediated by TRPA1 which is known to respond to a variety of reactive compounds including acrolein and formalin.

In conclusion, we have presented *in vitro* and *in vivo* evidence that acrolein may mediate pathology in PD. In addition, we have demonstrated the efficacy of two acrolein scavengers in alleviating behavioral and molecular changes induced in the 6-OHDA model of PD. Given the potential of acrolein to pathologically modify α-synuclein, acrolein reducing therapeutic strategies may provide a viable option in modifying PD progression.

5. CONTRIBUTION OF ACROLEIN IN POST-TRAUMATIC BRAIN INJURY PARKINSON'S PATHOLOGY

5.1 Introduction

Traumatic brain injury (TBI) has been suggested as a risk factor for Parkinson's disease (PD) [71]. Athletes and veterans who are at risk for TBI, are at higher risk of developing PD compared to the general population [127-129]. The majority of combat related TBI results from explosive blasts, most of which are mild in severity [88, 130-133]. These injuries may go undiagnosed or unreported creating a risk of repeated injury [131]. Despite clinical evidence associating TBI with PD, the mechanisms by which TBI increases risk of PD are not well understood.

During TBI, the brain undergoes rapid primary physical trauma resulting in damage to neurons and microvasculature [88]. This primary insult induces secondary biochemical processes including oxidative stress, lipid peroxidation, and inflammation which may occur on the order of minutes to months after injury [74, 82, 134, 135]. Changes in the levels of neurotransmitters such as glutamate can cause increased generation of free radicals and ROS such as peroxides and superoxide s[68, 75, 136]. Immune cell infiltration can further contribute to the localized oxidative environment and result in continuation of oxidative stress and generation of reactive aldehyde byproducts [15].

It has been demonstrated that the processes of TBI secondary injury overlap with degenerative processes in PD [137, 138]. α-Synuclein, the primary inclusion in PD Lewy bodies, is thought to play a role in PD pathogenesis [122, 139]. The lysine rich regions of α-synuclein have been suggested to be critical in inducing aggregation and subsequent dopaminergic cell death [85, 86]. Acrolein, an α,β-unsaturated aldehyde which is known to be elevated after TBI, is capable of adducting to nucleophilic residues such as lysine and could be a potential link between the common pathological features of TBI and PD [14, 84].

In this study, we further examine common processes of PD and post TBI pathological processes. Specifically, we examine the α-synuclein aggregation and lipid peroxidation in the striatum and substantia nigra after injury. Furthermore, we show that acrolein is sufficient to

directly modify α-synuclein and induce aberrant expression both *in vitro* and *in vivo*. Finally, we present initial work in detection of acrolein through nuclear resonance spectroscopy.

5.2 Methods

5.2.1 Mild blast traumatic brain injury model

All live animal procedures were conducted under protocols approved by the Purdue Animal Care and Use Committee. Mild blast TBI (bTBI) was performed as previously described by Walls et al [82]. In brief, 300g male Sprague-Dawley rats were anesthetized with a mixture of ketamine (80 mg/kg) and xylazine (20 mg/kg). After verifying the absence of toe withdrawal reflex, animals were secured 50 mm from the end of an open-ended shock tube, and a shield was placed over the body to reduce systemic confounders. A blast was generated by building up pressure in in a reservoir until it exceeds the burst strength of the membrane. The blast wave was directed downward with a peak overpressure of 150 kPa. Sham animals were similarly anesthetized and placed in the same room as the blast apparatus, but outside the range of the blast wave.

5.2.2 3-HPMA quantification

Urine samples were collected in standard metabolic cages prior to b-TBI and 1-, 2-, 5-, and 7-days post-injury. Quantification of urinary 3-HPMA was conducted as described in 2.2.9

5.2.3 Western blot

Rats were sacrificed for Western blot analysis at day 2 or 7 post injury. Animals were deeply anesthetized with ketamine and xylazine and transcardially perfused with Krebs solution. Whole brains were removed, frozen on dry ice, and stored at -80°C. Tissue from the striatal regions and substantia nigral region were dissected using Paxinos and Watson as a reference [140]. Tissue was sonicated in 1 x RIPA buffer (Sigma, #R0278) with protease inhibitor cocktail (Sigma, P8340). Lysates were centrifuged at 15,000 g for 40 minutes at 4°C and supernatants were retained for Western blot. Protein concentrations were measured using a bicinchoninic acid assay (Pierce, Rockford, IL, USA) kit and a Spectramax (Molecular Devices, Sunnyvale, CA). Sixty micrograms of protein were with 20% SDS, β-mercaptoethanol, and 2x Laemmli buffer were loaded into 15%

Tris-HCl gels and electrophoresed at 80V for 2-3 hours. Proteins were transferred to nitrocellulose by electroblotting at 70V at 4°C for 1-2 hours in Tris-Glycine buffer with 20% methanol (Bio-Rad). The membrane was blocked in 1x casein (vector, #SP-5020) at room temperature for 1 hour and immunolabeled with one of the following antibodies overnight at 4°C: anti-ACR (Abcam, #37110); anti-α-synuclein (BD Transduction, #610786); and anti-actin (Sigma, #A2066). The membranes were further incubated in biotinylated anti-mouse or anti-rabbit secondary antibody (Vector, #BA-200, #BA-1000) at room temperature for 1 hour. DuoLux substrate (Vector, #SK-6605) was used for chemiluminescent detection, and images were analyzed in AlphaView (Protein Simple, San Jose, CA, USA).

5.2.4 Detection of acrolein modification by α-synuclein

Purified wild-type α-synuclein was obtained from Dr. Jean-Christophe Rochet (Purdue University) and incubated in the presence of 0.125, 0.25, 0.5, 1, 5, or 10 mM of acrolein at 37°C for 20 hours. Then an equal volume of loading buffer was added to the reaction mixture prior to heating at 95°C for 5 minutes. The samples were then loaded in a 15% SDS-PAGE gel and blotted to a nitrocellulose membrane as described above. A sample of α-synuclein alone was used as a control.

5.2.5 Immunoprecipitation

Whole brain lysates from sham and 2-days and 7-days post-injury rats were immunoprecipitated using a Pierce Classic IP Kit (ThermoFisher, #26146). IN brief, 2 mg/mL protein lysate was cleared using the control agarose resin. The lysate was incubated overnight at 4°C with 5 µL of either anti α-synuclein or anti acrolein primary antibody. 20 µL Pierce A/G agarose was added to capture the formed immune complex and incubated overnight at 4°C. The complex was eluted with 2x non-reducing lane marker sample buffer and DTT. Collection tubes were incubated at 100°C for 5 minutes, and eluates were loaded onto a 15% SDS-PAGE gel for immunoblotting with α-synuclein and acrolein antibodies.

5.2.6 T_1 and T_2 Relaxometry of acrolein

Neat acrolein (Sigma Aldrich, 4S8501) was diluted to 90 mM in D_2O. Relaxometry was conducted with a Bruker ARX 300 NMR system. T1 relaxometry was performed with an eight-point inversion recovery system with inversion times of 0.01, 2.5, 5, 8 ,12, 18, 30, and 50 s. T_2 relaxometry utilized the Carr-Purcell-Meiboom-Gill sequence with PROJECT suppression of J modulation. Again, eight measurements were required with delay times of 0.08054, 0.8054, 2.416, 4.832, 8.054, 16.108, 24.162, and 32.216 s. Both experiments were performed in triplicate and MestReNova was used to calculate T_1 and T_2 relaxation times.

5.2.7 Magnetic resonance spectroscopy

A whole brain phantom was prepared using values indicated on the BrainO phantom (GE Medical Systems). 1M acrolein was added to a 40 mL phantom for an end acrolein concentration of 10 mM. Spectroscopy was performed with a Bruker Biospec 70/30 USR using a Point RESolved Spectroscopy sequence. B_0 mapping and shimming procedures were performed prior to spectral acquisition. Pulse sequence parameters were TE=16.5 ms, TR= 6000 ms, averages=256, flip angle=90°/180°/180°, bandwidth=5.4/2.4/2.4 kHz with a total scan time of 25:36 min. Spectra were analyzed in MestReNova.

5.2.8 Statistical analysis

All data are presented as mean ± standard error of the mean. One way ANOVA with Tukey or Fisher *post hoc* and Student's t-test were u sed for statistical analysis as appropriate. $p<0.05$ was considered to be statistically significant.

5.3 Results

5.3.1 Elevation of 3-HPMA after mild bTBI

Urinary 3-HPA was significantly increased in injured rats at 1-day (1.93 ± 0.46 μg/mg), 2-days (2.37 ± 0.40 μg/mg), 5-days (1.78 ± 0.15 μg/mg), and 7-days (2.35 ± 0.44 μg/mg) post-injury compared to pre-injury baseline measurements (1.13 ± 0.22 μg/mg, $p<0.01$) (Figure 5.1).

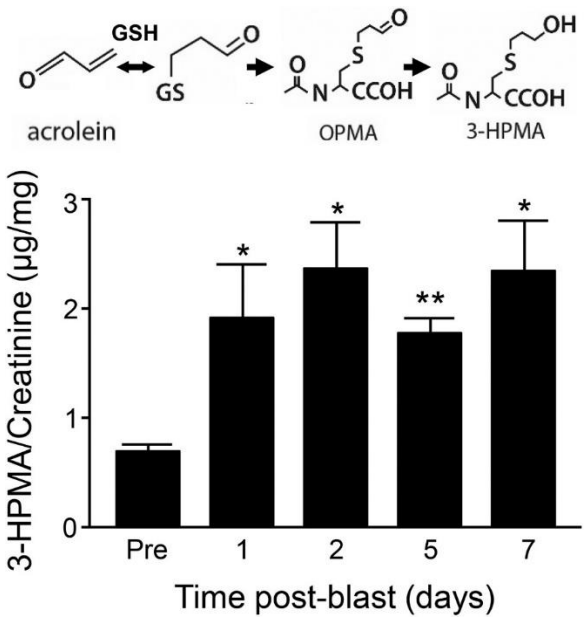

Figure 5.1 Elevation of urinary 3-HPMA after mild bTBI. Above: Schematic of 3-HPMA production from acrolein and glutathione. Below: Urinary 3-HPMA normalized to creatinine. Repeated measures ANOVA indicates a significant day effect ($F(4,2) = 5.20$, $p = 0.005$). Pairwise comparison to baseline measurements demonstrate a significant increase in urinary 3-HPMA through at least day 7 post-injury. *p<0.05, **p<0.01

5.3.2 Elevation of acrolein-lysine adducts in the whole brain, striatum, and substantia nigra

Acrolein levels after bTBI were measured in the whole brain, anterior and posterior striatum, and substantia nigra (Figure 5.2). Acrolein adducts were significantly elevated in whole brain lysates at 2 days (22.96 ± 4.97%) and 7-day (22.53% ± 8.01) post injury compared to controls (100 ± 4.28% p<0.05). Similarly, acrolein-lysine adducts were increased in the anterior striatum at 2 days (93.18 ± 24.68%) and 7 days (60.89 ± 10.41%) post injury when compared to control (100 ± 17.37; p<0.01 for 2 days, p<0.05 for 7 days post injury). Lysates from the posterior striatum also showed elevated levels of acrolein adducts at 2 days (98.44 ± 24.84%) and 7 days (72.80 ± 20.49%) post injury compared to control (100 ± 12.62%; p<0.01 for 2 days, p<0.05 for 7 days). Acrolein was also significantly elevated in the substantia nigra at 2 days (81.66 ± 23.64%) and 7 days (117.57 ± 29.07%) post-injury compared to control (100 ± 19.8%; p<0.05 for 2 days, p<0.01 for 7 days).

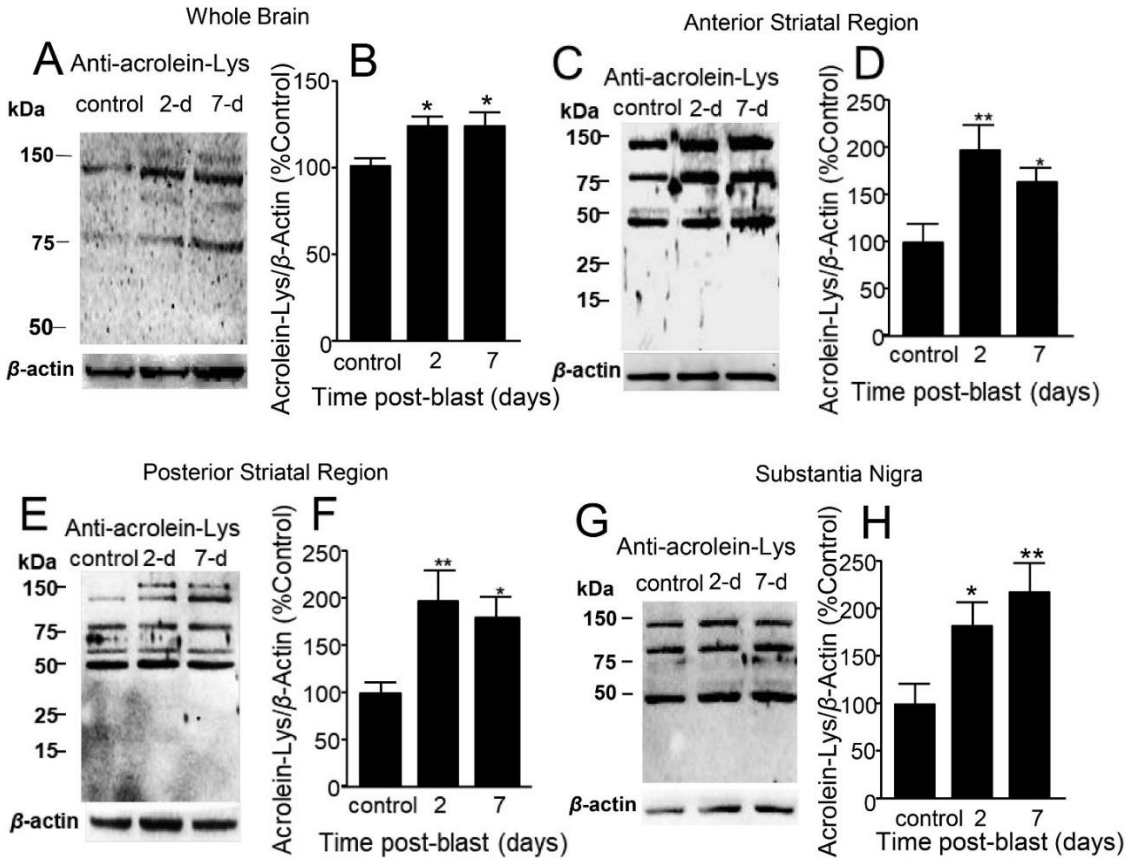

Figure 5.2 Elevation of acrolein-lysine adducts in whole brain, stratal, and nigral lysates. Western blot images of acrolein adducted lysine in the whole brain (A), anterior striatum (C), posterior striatum (E), and substantia nigra (G). All bands were analyzed for quantification. Acrolein-lysine adducts were increased at days 2 and 7 post-injury in bTBI rats compared to control (B,D,F,H). *$p<0.05$, **$p<0.01$.

5.3.3 Aberrant expression of α-synuclein after mild bTBI

α-Synuclein, the primary protein in PD Lewy bodies, is typically found as a 14 kDa monomer. Western blotting of striatal and substantia nigral lysates revealed two bands of α-synuclein protein at 19 kDa, the predicted size given by the antibody manufacturer, and at 25 kDa (Figure 5.3). The heavier 25 kDa protein was significantly elevated in anterior striatal lysates at days 2 (149.50 ± 17.04) and 7 (163.07 ± 18.28%) post-injury compared to control (100±5.47, $p<0.05$). Similarly, the 25 kDa species was increased in the posterior striatum at days 2 (211.36 ± 37.08%) and 7 (184.87 ± 10.64) post injury compared to control (100 ± 8.89, $p<0.05$). However, α-synuclein protein levels at 19 kDa also decrease significantly in both the anterior and posterior striatum ($p<0.05$ or $p<0.01$). In addition, the ratio of 25 kDa to 19 kDa α-synuclein was

significantly elevated at days 2 and 7 post injury in both the anterior and posterior striatum compared to control (p,0.05 or p<0.01).

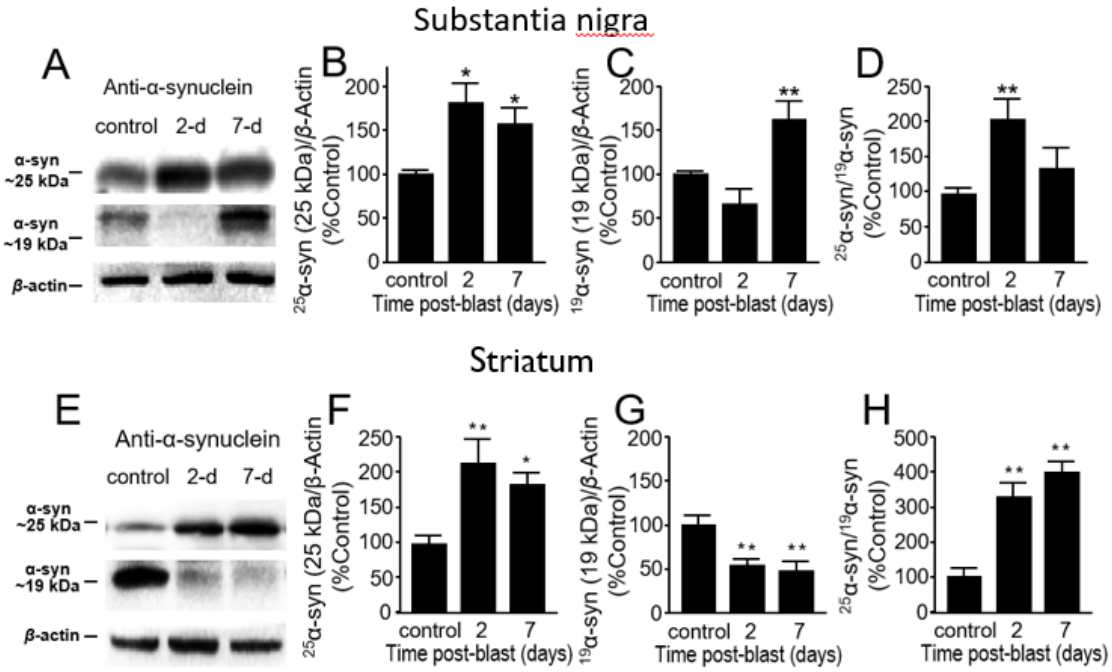

Figure 5.3 Aberrant form of α-synuclein in the substantia nigra and striatum after mild bTBI. Western blot images of substantia nigra (A) and posterior striatum (E) are shown with α-synuclein bands at approximately 19 and 25 kDa. The higher molecular weight 25 kDa form was elevated at both 2- and 7-days post-blast in the nigral (B) and striatal (F) preparations. However, while the 19kDa monomeric form was increased at 7 days post-blast in the substantia nigra (C), it was suppressed at both days 2 and 7 in the striatum (G). The ratio of 25 kDa to 19 kDa α-synuclein was significantly elevated on day 2 in the substantia nigra and on days 2 and 7 in the striatum (D,H). *p<0.05, p<0.01 compared to control.

5.3.4 Acrolein induces α-synuclein oligomerization *in vitro*

Purified α-synuclein was treated with acrolein for 2 hours. All samples were run in triplicates and detected by Western blot (Figure 5.4). Quantification of band densities indicated that α-synuclein at 15 kDa remained relatively constant up to acrolein concentrations of 500 μM.; however, this band began to fade at concentrations above 1 mM. Analysis of the 37 kDa band revealed a broader band with increasing acrolein concentrations starting at 125 μM, although this too fades at higher than 1 mM acrolein.

Blotting for acrolein-lysine adducts demonstrates that the band of acrolein modified α-synuclein broadens with increasing concentrations before fading at 10 mM. Acrolein adducted protein is also observed at higher molecular weights starting at 250 μM acrolein before fading at 1 mM. Together, these suggest that α-synuclein oligomerization is dose-dependent with respect to acrolein up to a point at which immunolabeling diminishes. This may suggest that the protein degrades at higher concentration or is so extensively immunolabeled that antibody binding sites are either inaccessible or disrupted.

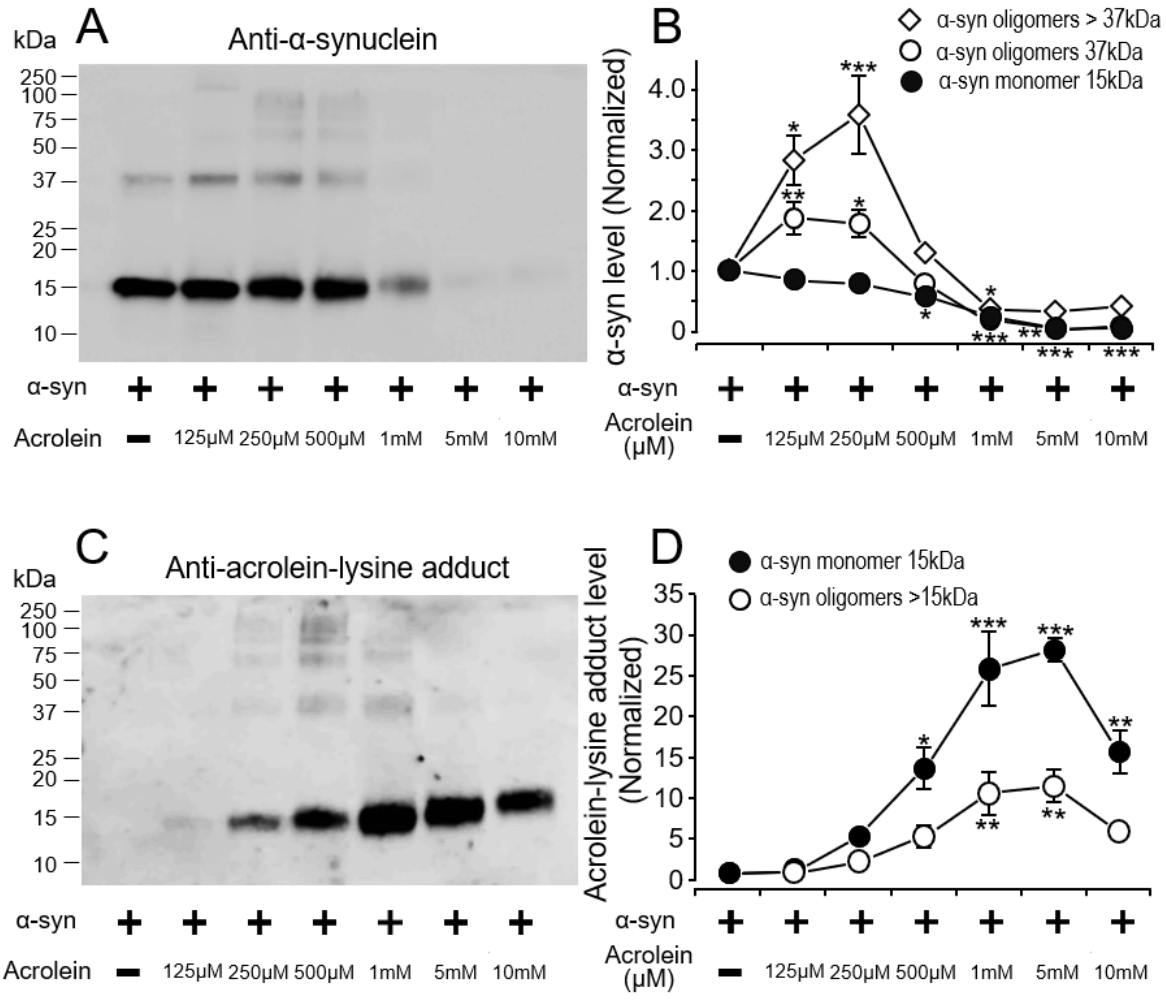

Figure 5.4 Acrolein induced α-synuclein oligomerization. Purified α-synuclein was incubated in the presence of acrolein and analyzed by Western blot (A, C). Quantification of α-synuclein immunolabeling (B) revealed a significant increase in α-synuclein oligomers when incubated in125 μM and 250 μM acrolein and a significant decrease in both monomers and oligomers at 500 μM or greater concentrations of acrolein. Analysis of acrolein-lysine immunolabeling (D) demonstrated a significant increase in acrolein adducted α-synuclein monomers at concentrations

at or above 500 μM and a significant increase in acrolein adducted α-synuclein oligomers at 1 mM and 5 mM. *p<0.05, **p<0.01, ***p<0.001 when compared to α-synuclein alone.

5.3.5 Interaction of acrolein and α-synuclein *in vivo*

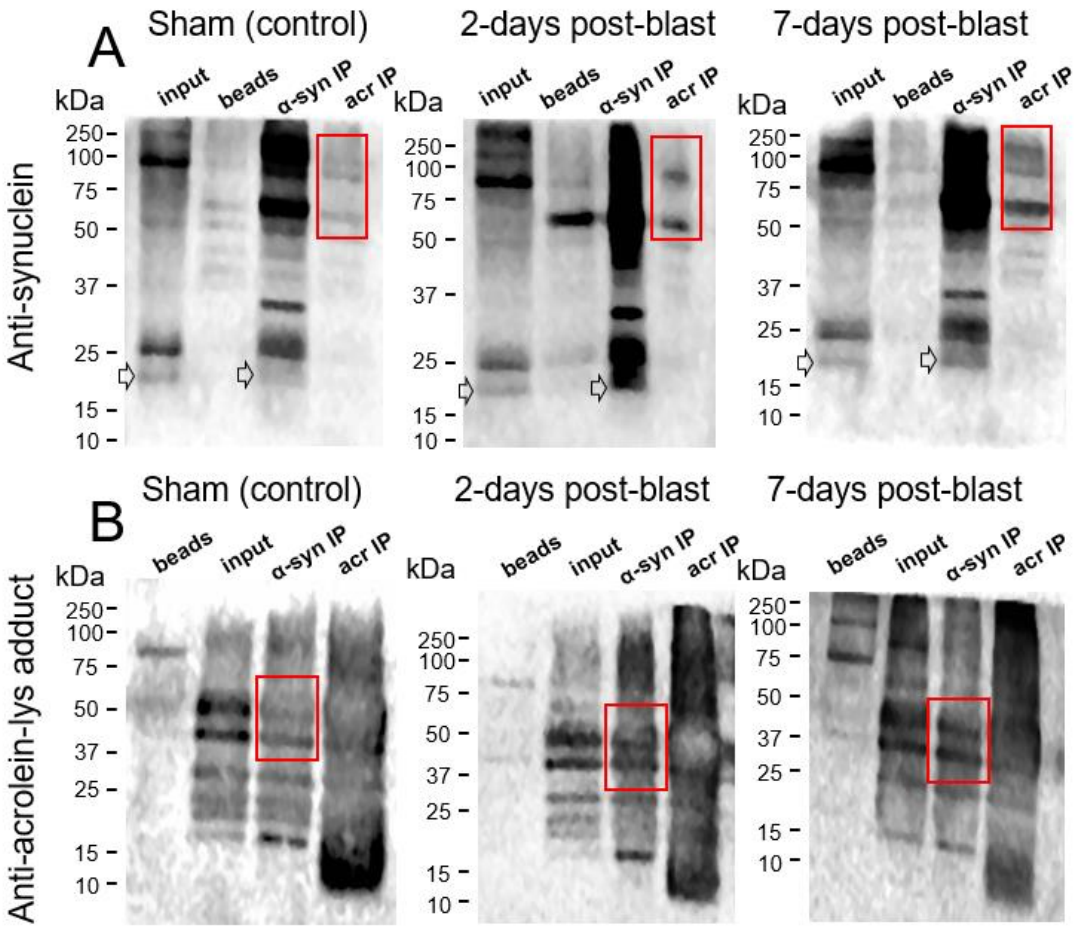

Figure 5.5 *In vivo* modification of α-synuclein by acrolein after bTBI. Whole brain lysates were obtained from controls and injured rats at 2 days and 7 days post-injury. Lysates were immunoprecipitated with α-synuclein or anti-acrolein antibodies and analyzed by Western blot against α-synuclein (A) or anti-acrolein (B). Red boxes denote bands of interest which contain acrolein modified α-synuclein while arrows indicate monomeric α-synuclein.

Interaction of acrolein and α-syn *in vivo* was confirmed by co-immunoprecipitation in whole brain lysates on days 2 and 7 post blast TBI. Distinct bands of anti-synuclein labeling were identified in the acrolein immunoprecipitate which appear to intensify on days 2 and 7 post-injury

(Figure 5.5A). Similarly, bands of anti-acrolein labeling were identified in the α-synuclein immunoprecipitate (Figure 5.5B).

5.3.6 Detection of acrolein through magnetic resonance spectroscopy

Currently, endogenous acrolein can be estimated by immunoblotting for modified proteins or by measurement of metabolites in systemic biofluids. Unfortunately, immunoblotting is highly invasive and does not typically allow for longitudinal study, while systemic measurements lack regional specificity. Here we describe preliminary work to investigate magnetic resonance spectroscopy as a method for quantifying local concentrations of acrolein. Initial spectroscopy of 10 mM acrolein in a standard brain phantom showed acrolein related signals which were distinct from background metabolites at 6.3 ppm, 6.6 ppm, and 9.3 ppm (Figure 5.6).

Although acrolein related signals were easily separated from homeostatic metabolites, our current methodology is limited to detection in the millimolar range while our previous *in vivo* work has shown that micromolar concentrations can induce significant physiological alterations. Relaxometry was performed to provide guidance in pulse sequence development. T_1 of the 9.3 ppm proton peak was determined to be 13.31 s, and the 6.3 and 6.6 ppm was 11.19 s (Figure 5.7). T2 of the downfield signal was 11.17 s while the 6.3 and 6.6 ppm group had T2 of 9.26 s (Figure 5.8). Adjusting repetition time for the long T1 lengthened scan times to nearly 25 minutes for a single voxel. At this time further work is required to create an applicable protocol with the correct balance of scan time and signal to noise ratio.

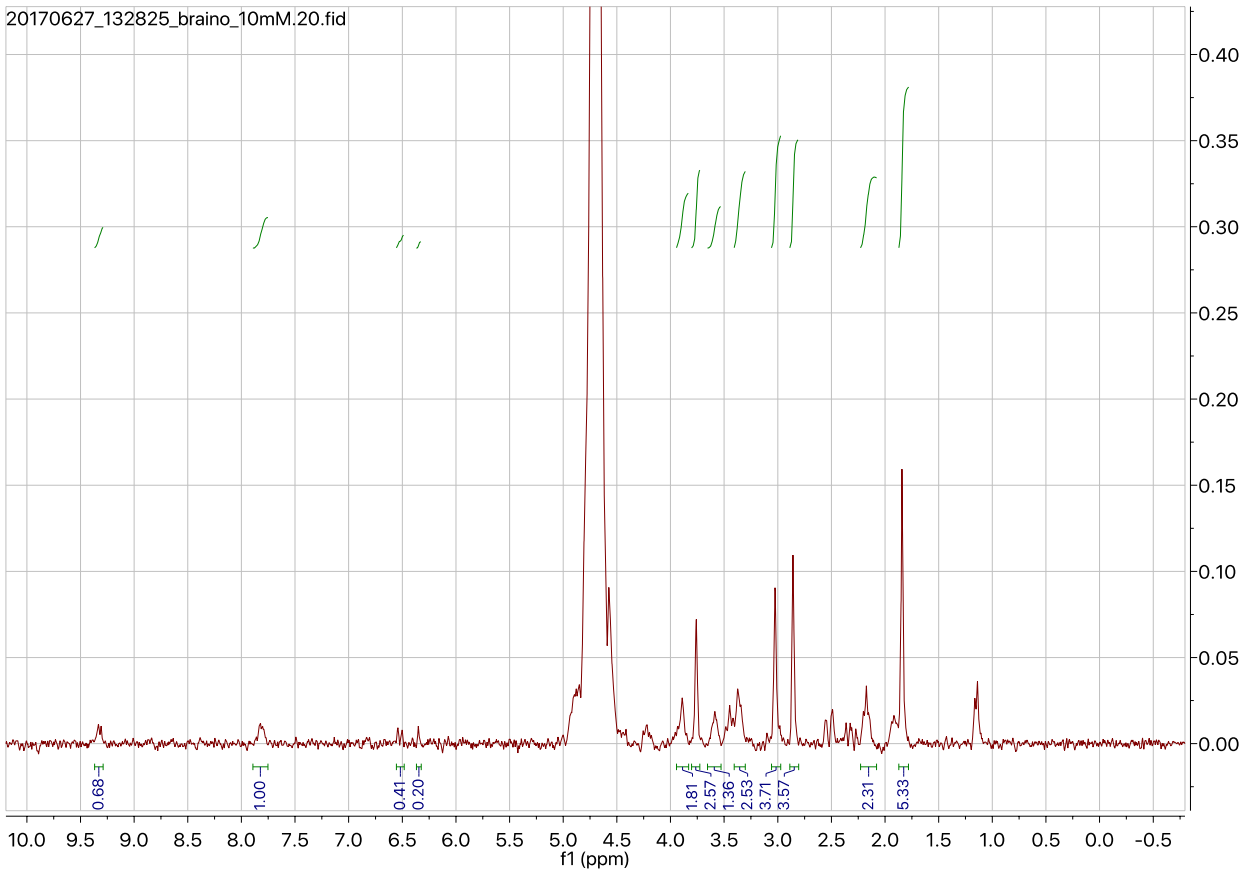

Figure 5.6 ^{1}H spectrum of 10 mM acrolein in whole brain phantom. Acrolein related signals from 6.3-6.6 ppm and 9.25-9.4 ppm are spectroscopically distinct from components of the brain phantom.

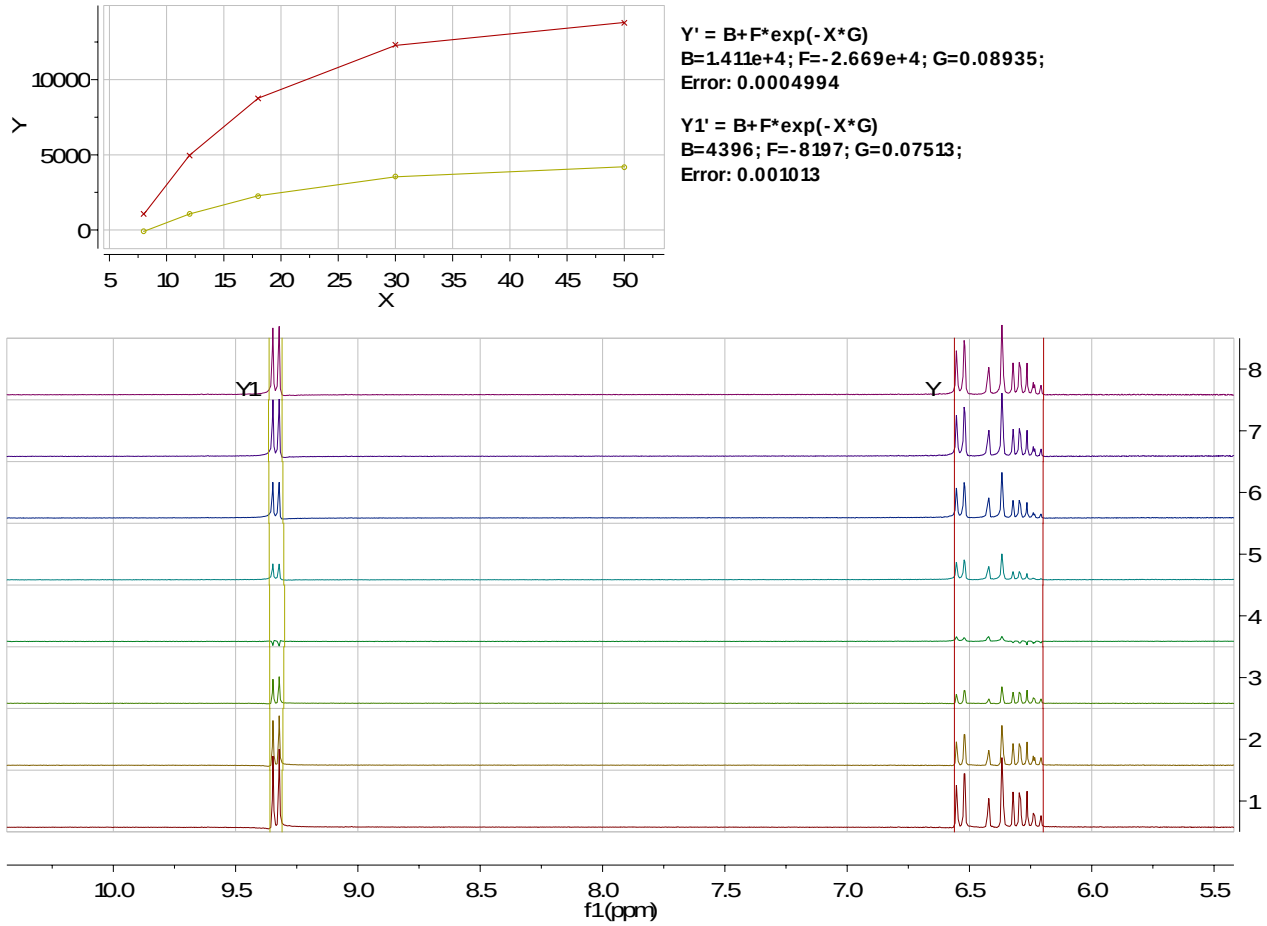

Figure 5.7 T_1 relaxometry for selected acrolein peaks between 6.3 ppm and at 9.3 ppm. T_1 was calculated for each peak by fitting exponential decay with $T_1 = 1/R$. Measured T1 was 13.31 seconds at 9.3 ppm and 11.19 seconds between 6.3 and 6.6 ppm

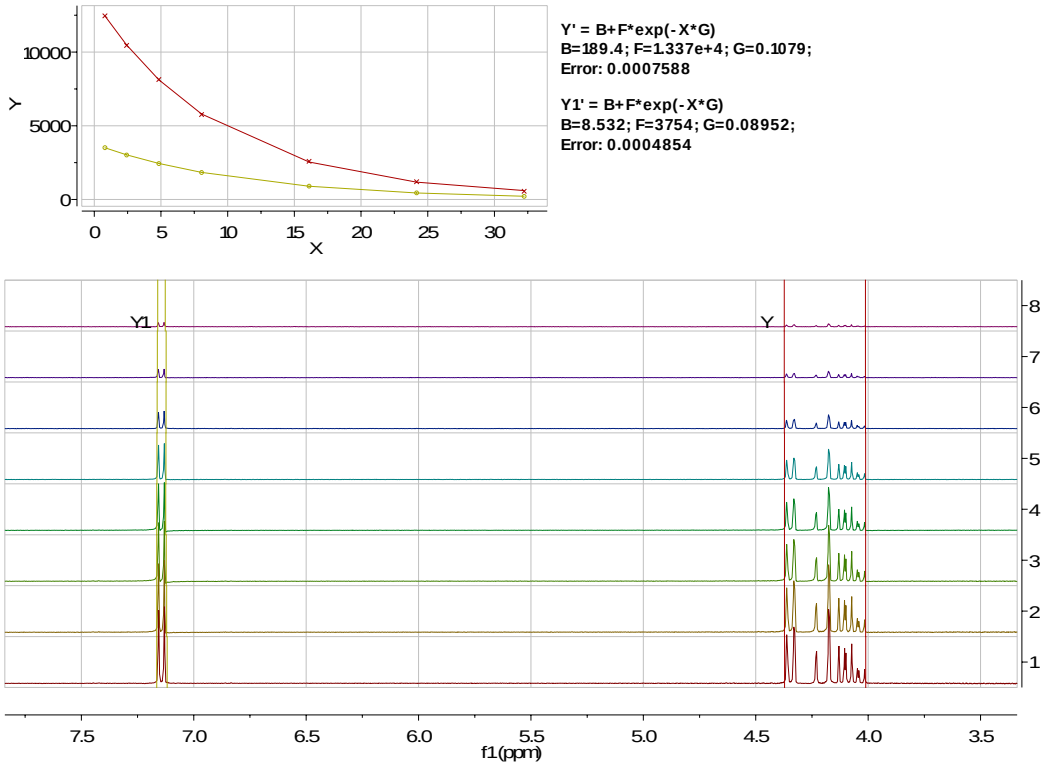

Figure 5.8 T_2 relaxometry of acrolein. T_2 was calculated using an exponential fit with $T_2 = 1/R$. Calculated T2 was 11.17 seconds at 9.3 ppm and 9.26 s between 6.3 and 6.6 ppm.

5.4 Conclusion

In this study, we report direct evidence that acrolein modifies α-synuclein both *in vitro* and *in vivo*. As such, we postulate that post-traumatic oxidative stress and lipid peroxidation products may be key factors in initiating and perpetuating neurodegenerative processes which may increase susceptibility to or accelerate onset of PD in TBI patients. Specifically, we have observed elevated acrolein metabolites both systemically and locally the substantia nigra and striatum of rats after bTBI at days 2 and 7 post-injury. These results expand up on our previous work in bTBI and the 6-OHDA rat model of PD.

Due to the lipid rich environment of the central nervous system, a large portion of oxidative stress manifests as lipid peroxidation which can produce a variety of reactive aldehydes including 4-hydroxynonenal, malondialdehyde, and acrolein. Of these, acrolein is the most reactive and most abundant while being persisting in the body for longer than reactive oxygen species. Acrolein has also been implicated in the pathophysiology of PD, Alzheimer's, MS, and SCI. As a potent

electrophile, it binds to nucleophilic residues such as lysine. α-Synuclein, the primary component of Lewy bodies in PD is relatively rich in lysine compared to other pre-synaptic proteins and may be significantly disrupted by acrolein adduction.

We identified two species of α-synuclein in the brain of bTBI rats at 19 kDa and 25 kDa. In the striatal and nigral regions at days 2 and 7 after mTBI, expression of the 25 kDa relative to the monomeric 19 kDa is increased. In the substantia nigra, we found a decrease in 19 kDa α-synuclein two days post injury, but a significant increase at seven days post injury. We postulate that the 19 kDa form is the normal state of the protein and that the 25 kDa form possesses a post translational modification. This species may merit further study as its nature is currently unclear. We speculate that adduction of acrolein to lysine residues may disrupt the structure of α-synuclein and induce post translational modification and subsequent oligomerization.

Given the importance of acrolein to post-TBI pathophysiology, we examine the use of nuclear magnetic resonance spectroscopy for localized *in vivo* detection of acrolein. At this time, our methods for measuring acrolein *in vivo* are limited to measurement of systemic metabolites which may not be specific to the region or organ of interest. We present initial relaxometry and spectroscopic data to show that acrolein produces signals that are distinct from homeostatic metabolites; however, our current technique is limited to millimolar concentrations and present poor line widths. At this time, further refinement in scan protocols is needed to balance scan time and signal to noise ratios. Alternative methods of evaluating oxidative stress such as contrast imaging may also provide insight into the role of oxidative stress in bTBI secondary injury.

6. ALLEVIATION OF SCI-INDUCED SENSORY DEFICITS BY PHENELZINE

6.1 Introduction

Similar to TBI, injury in SCI can be divided into the primary physical insult, which acutely disrupts neurons and microvasculature, and secondary biochemical injury which may occur in the minutes to months following SCI [89]. Among these secondary processes, oxidative stress is thought to play a pivotal role in perpetuating a deleterious environment with recruitment of inflammatory immune cells and generation of reactive aldehyde products [4, 141].

We have previously determined that acrolein is elevated in the spinal cords of injured rats [5, 142]. Furthermore, acrolein has been suggested to contribute to SCI related neuropathic pain [28, 111]. It has been proposed that acrolein contributes to neuropathic pain through activation of the receptor channel transient receptor potential ankyrin 1 (TRPA1) [97]. TRPA1 is a nociceptive cation channel which responds to a variety of noxious stimuli including formalin and acrolein [98]. As a product and catalyst of oxidative stress, acrolein may promote generation of additional reactive species which cause an increase in inflammatory cytokines which may further intensify pain sensation through increases in both receptor and agonist.

Previously, we have shown that acrolein is elevated on similar timescales as the emergence of sensory hypersensitivity after SCI [95, 96]. Furthermore, direct microinjection of acrolein to the spinal cord elicited similar pain related behaviors and increased TRPA1 mRNA transcripts consistent with findings in SCI [93]. Treatment with acrolein scavenging agents such as hydralazine attenuated post-SCI acrolein levels, suppressed TRPA upregulation, and alleviated pain related behavior [28, 91-93]. In combination, it is likely that acrolein is a key mediator in the sensory hypersensitivity which arises following SCI.

In this study, we present additional evidence of the role of acrolein scavenging in alleviating motor and sensory deficits after SCI by evaluating phenelzine as an alternative acrolein scavenger. Although we have observed alleviation of these deficits with hydralazine in previous studies, hydralazine has limited clinical application in traumatic injuries due to its primary on-label activity as a vasodilator. As such, here we examine phenelzine, another hydrazine containing

pharmaceutical, as an alternative to provide additional evidence for the role of acrolein in SCI secondary injury and the potential efficacy of acrolein scavenging treatments.

6.2 Methods

6.2.1 Animals

Male Sprague-Dawley rats weighing 200-250g were obtained from Harlan Laboratories (Indianapolis, IN) and housed in laboratory animal facilities. All live animal procedures were performed under protocols approved by the Purdue Animal Care and Use Committee. Animals were allowed to acclimate to the housing facility for a minimum of 1 week prior to surgery.

6.2.2 Spinal cord contusion injury model

Rats were anesthetized with a mixture of ketamine (80 mg/kg) and xylazine (10mg/kg). After confirming the absence of toe-pinch reflex, a dorsal laminectomy was performed at the T-10 spinal level. A New York University impactor was used to contuse the spinal cord with a 10 g rod dropped from a height of 25mm. Sham operated animals received a dorsal laminectomy without contusion of the spinal cord. Animals were given 3 mL saline subcutaneously and placed on a heating pad to aid in recovery. The bladder of injured animals was expressed twice per day until rats regained control of bladder function.

6.2.3 Acrolein scavenging treatments

Phenelzine sulfate (Sigma) was dissolved in phosphate buffered saline and sterilized with a 0.45 μm filter. Dosages of 5, 15, and 60 mg/kg were selected for this study. In order to determine the efficacy of phenelzine at different stages of injury, phenelzine was administered immediately following injury (acute), beginning 21 days post-injury (delayed), and beginning 2 months post-injury (chronic) for 14 days of treatment in each condition. Hydralazine hydrochloride (Sigma) was similarly dissolved in phosphate buffered saline and filter sterilized. Doses of 5 and 25 mg/kg hydralazine were given via intraperitoneal injection.

6.2.4 Pharmacokinetic assessment

Male Sprague-Dawley rats were anesthetized using isoflurane with pre-operative analgesia administered subcutaneously. Surgical sites were shaved and cleaned with ethanol and betadine. Gastric catheters (BASi Culex rat gastric, Bioanalytical Systems In., West Lafayette, IN, USA) were implanted into the peritoneal cavity and the carotid artery (BASI Culex rat carotid, Bioanalytical Systems, Inc.) into each rat. Catheters were secured to the scapular region. Th animal was tethered in a movement-responsive cage and the carotid artery was connected to a Culex automated pharmacology system which periodically flushes the catheters with heparinized saline to maintain patency. Animals were allowed to acclimate to the cage and recover from surgery for 24 hours prior to initial dosing.

For hydralazine, animals were given 5 mg/kg intraperitoneally and 200 μL blood samples were collected at 15, 30, 45 min, 1, 2, 4-, 6-, 8-, and 24-hours post-injection. For phenelzine, animals were given a 15 mg/kg dose intraperitoneally and blood samples were collected at 15, 45 minutes, 2, 4, 6, 8-, 9-, 16-, and 24-hours post-injection. Blood samples were deposited into heparinized vials and stored at 4°C.

6.2.5 Hydralazine detection

Sample vials were preloaded with 5 μL 3-cyclohexine-1-carboxaldehyde as a derivatization agent and 1 μL (20 ppm) phenelzine as an internal standard. After deposition of blood by the Culex sampler, a 10 μL sample was withdrawn and injected into a 0.8mm i.d. glass capillary for slug flow extraction with 10 μL ethyl acetate. Finally, nanoESI was utilized for direct mass spectrometry using a TSQ spectrometer (Thermo Fisher Scientific). Spray voltage was set at 1500V and energy for collision-induced dissociation was set at 30 eV. Ions of m/z 253 -> 129 and 229 -> 105 were used for quantification of hydralazine and internal standard, respectively.

6.2.6 Phenelzine detection

Sample vials were pre-loaded with 1μL phenelzine-d5 as an internal standard (20 ppm). After blood was deposited from the Culex sampler, samples were processed for mass spectrometry as described for hydralazine analysis with ions of m/z 137->105 and 142->110 quantified for phenelzine and internal standard, respectively.

6.2.7 Von Frey test

Hind paw withdrawal thresholds were obtained as described in 4.2.6. All sensory tests were performed 24 following IP injection to reduce the effect of injection induced stress.

6.2.8 Tissue collection

Animals were deeply anesthetized with ketamine and xylazine and perfused transcardially with oxygenated Kreb's solution. The vertebral column was quickly harvested, and the spinal cord isolated by complete laminectomy. Lumbar dorsal root ganglia (DRGs) were also isolated, and the skin of the hind paw was also acquired for TRPA mRNA measurement.

6.2.9 Immunoblotting

A 1 cm segment of the spinal cord, including the injury epicenter, was incubated in 1% triton with protease inhibitor cocktail (Sigma-Aldrich) and sonicated. Total protein concentration was determined with a bicinchoninic acid assay to ensure equal loading of each sample. 200 μg of each sample was transferred to a nitrocellulose membrane using a Bio-Dot SF Microfiltration Apparatus (Bio-Rad, Hercules, CA, USA). The membrane was then blocked with 0.2% casein and 0.1% Tween-20 in phosphate buffered saline prior to incubation in a mouse monoclonal anti-acrolein antibody (1:1000, Abcam). After washing the membrane with blocking buffer, the membrane was incubated in a 1:10,000 dilution of alkaline phosphatase conjugated goat anti-mouse IgG (Vectastain ABC-AmP Kit, Vector Laboratories). After a final wash with blocking buffer followed by 0.1% Tween 20 in Tris-buffered saline, the membrane was exposed to substrate and visualized by chemiluminescence.

6.2.10 TRPA1 expression analysis

A 1-cm piece of dorsal horn at T-10, paw skin, and L1-L6 DRs were collected for TRPA1 transcript quantification. Samples were sonicated in Trizol (Sigma-Aldrich). RNA was isolated by chloroform extraction and isopropanol precipitation. Isolated RNA was quantified using a NanoDrop 2000c (Thermo Scientific). cDNA was synthesized using an iScript cDNA Synthesis kit according to the manufacturer's instructions (170-8890, Bio-Rad). Primers for TRPA1 were

5’-TCCTATACTGGAAGCAGCGA-3’ and 5’-CTCCTGATTGCCATCGACT-3 [143]. Primers for 18S were 5'-CGGCTACCACATCCAAGGAA-3' and 5'-GCTGGAATTACCGCGGCT-3'. PCR products were detected using an iQ SYBR Green Supermix (170-8880, Bio-Rad) and TRPA1 expression was normalized with 18S for relative quantification.

6.2.11 3-HPMA quantification

3-HPMA was quantified in urine as described in 2.2.9.

6.2.12 Statistical analysis

Student’s t-test was used when only two groups are compared. For comparisons with three or more groups, ANOVA with Tukey’s honest significant difference was used. $p<0.05$ was considered to be statistically significant.

6.3 Results

6.3.1 Phenelzine provides differential relief of mechanical hyperreflexia based on treatment timing

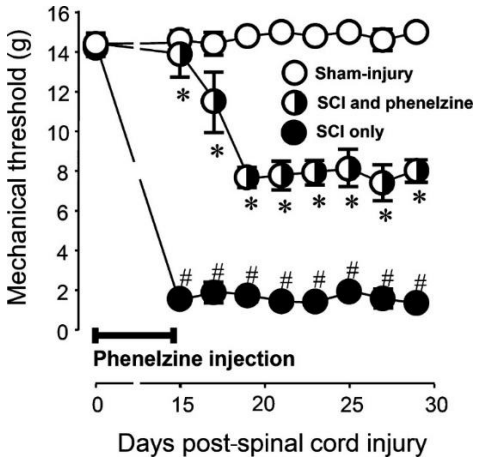

Figure 6.1 Post-SCI hyperreflexia alleviated by phenelzine. SCI animals exhibited significantly lower mechanical withdrawal thresholds than sham surgery. Phenelzine treatment reduced mechanical hyperreflexia compared to SCI only. # $p<0.05$ compared to sham injury, * $p<0.05$ compared to SCI only.

Spinal cord injury rats were treated with phenelzine and assessed for 50% hind paw withdrawal threshold. Rats with spinal cord contusion only displayed higher sensitivity to mechanical stimulus than rats receiving sham surgeries (Figure 6.1, $p<0.05$). Furthermore, treatment with phenelzine, which began immediately after injury and continued for 14 days, significantly attenuated hyperreflexia in injured animals and continued after the discontinuation of therapy ($p<0.05$). Delaying treatment (Figure 6.2A) to day 21 post-injury alleviated hyperreflexia starting on day 22 which persisted until three days after discontinuation of treatment. In chronic treatment, starting on day 67 post-injury (Figure 6.2B), hyperreflexia was significantly attenuated starting on day 72 post-injury and continuing until 3 days after discontinuation of phenelzine. The persistent relief within the acute treatment regimen indicates interruption of a deleterious process resulting in a lower level of sensitivity even after withdrawal of treatment. Because hydralazine, which shares hydrazine functionality, elicited similar relief, while monoamine oxidase (MAO) inhibitors without carbonyl scavenging activity have failed to protect neuronal cells from aldehyde exposure, it is likely that the persistent analgesic effect of phenelzine can be attributed to reduction in acrolein rather than inhibition of MAO. In delayed and chronic treatment, it becomes more difficult to attribute relief solely to the acrolein scavenging activity of phenelzine, as MAO inhibitors are known to reduce hypersensitivity based on their primary pharmacology.

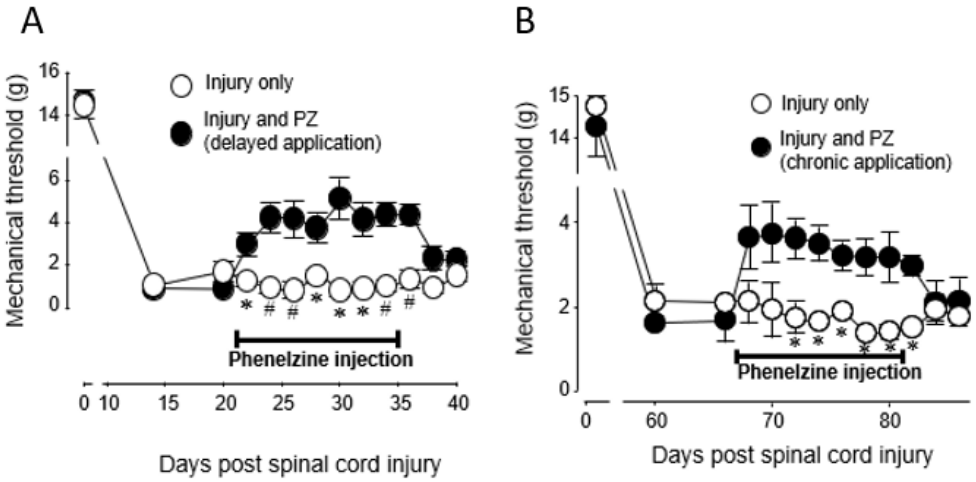

Figure 6.2 Post SCI hyperreflexia attenuated with delayed and chronic phenelzine. A) Delayed phenelzine treatment significantly decreased mechanical hyperreflexia in SCI rats starting 22 days post-injury and continuing to day 36. B) Phenelzine treatment in chronic injury alleviated SCI-induced hyperreflexia starting on day 72 post-injury and continuing until day 82 post-injury. In each condition, relief persisted for 3 days following cessation of treatment. * $p<0.05$, # $p<0.01$ compared to injury only.

6.3.2 Phenelzine suppresses TRPA1 upregulation after SCI

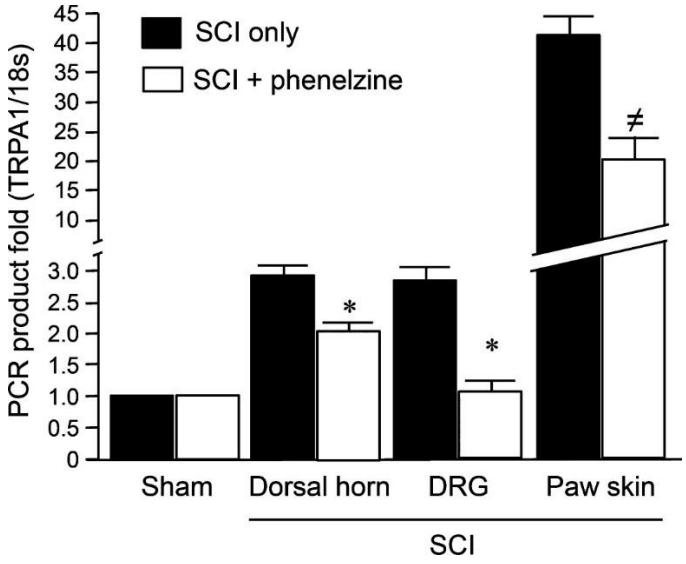

Figure 6.3 TRPA1 mRNA upregulation attenuated by phenelzine. TRPA1 mRNA was significantly increased in the dorsal horn, DRGs ($p<0.05$), and paw skin ($p<0.001$) after SCI. This upregulation was suppressed with phenelzine treatment in all tissue types. *$p<0.05$, ≠ $p<0.005$ compared to SCI only.

TRPA1 mRNA transcripts were quantified in the dorsal horn, DRGs, and paw skin of rats 1 week after SCI (Figure 6.3). We found that phenelzine treatment attenuated TRPA1 transcript levels in each tissue type. Specifically, phenelzine reduced TRPA1 expression from 2.90 ± 0.15 to 2.02 ± 0.22 in the dorsal horn ($p<0.05$), from 2.86 ±0.22 to 1.14 ± 0.11 in DRGs ($p<0.05$), and from 41.43 ± 2.98 to 20.24 ± 3.65 in paw skin ($p<0.005$).

6.3.3 Phenelzine suppresses acrolein metabolites after SCI

Phenelzine was also examined for its ability to reduce local and systemic acrolein metabolites after SCI. Phenelzine (15 mg/kg) and hydralazine (5 mg/kg) treated animals showed significantly lower levels of acrolein adducted lysine residues compared to tissue from untreated SCI rats ($p<0.001$). Furthermore, the level of acrolein adducts was lower in phenelzine treated animals compared to those which received hydralazine ($p<0.05$) (Figure 6.4).

Urinary 3-HPMA was measured to determine whether acrolein scavenging treatments can reduce systemic metabolites (Figure 6.5). Three doses of phenelzine produced a significant and

dose-dependent reduction of urinary 3-HPMA compared to untreated SCI ($p<0.05$). Furthermore, animals treated with 15 mg/kg phenelzine could not be distinguished from control ($p<0.05$), and animals treated with 60 mg/kg exhibited significantly lower levels than controls ($p<0.05$). Similarly, hydralazine at 5 and 25 mg/kg significantly reduced 3-HPMA compared to injury ($p<0.05$) and was similar to phenelzine treatment at 5 and 15 mg/kg.

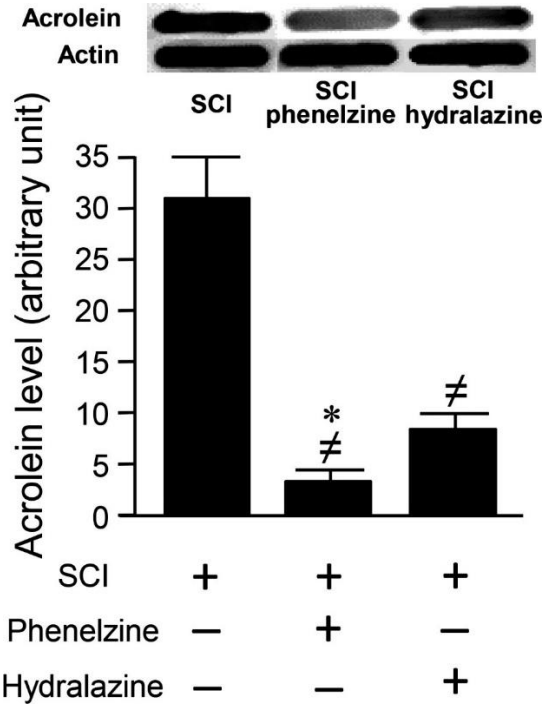

Figure 6.4 Acrolein scavengers suppress acrolein-lysine adducts in the spinal cord after SCI. Phenelzine and hydralazine significantly decreased acrolein-lysine adducts in spinal cord lysates compared to SCI only. Furthermore, acrolein adducts were significantly lower in phenelzine treated animals than in hydralazine treated animals. ≠ $p<0.001$ compared to SCI only, *$p<0.05$ compared to hydralazine treatment.

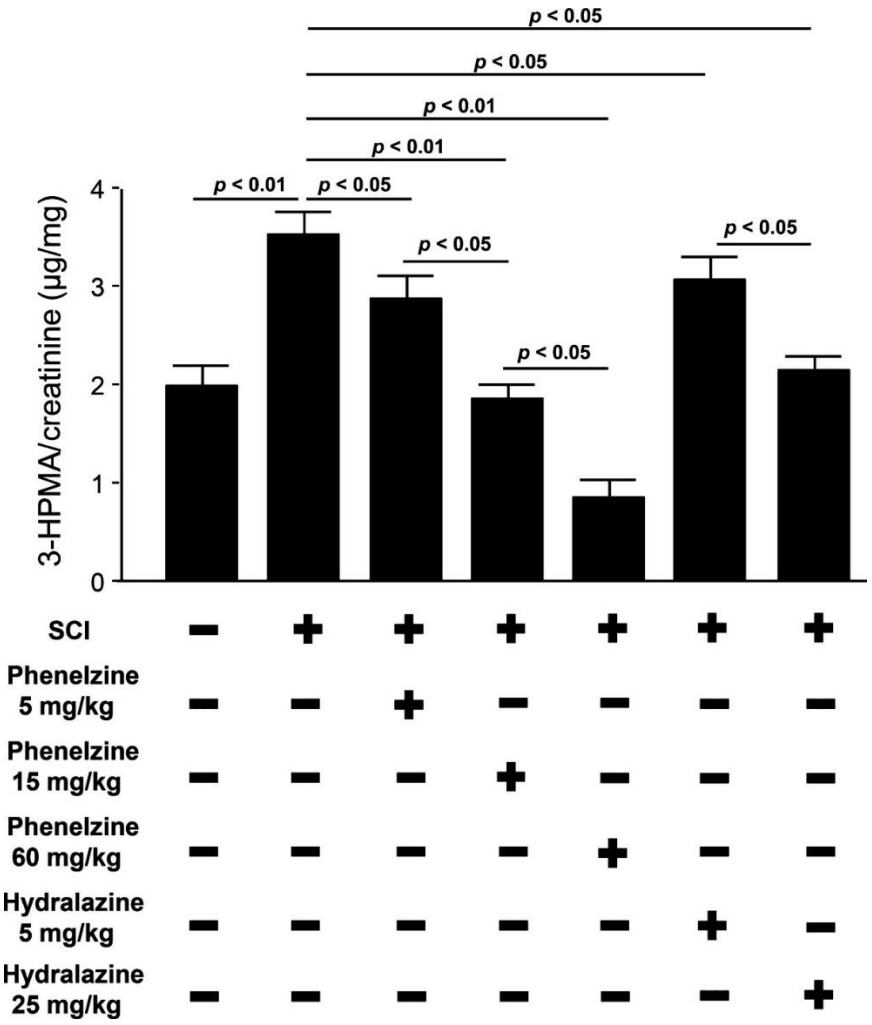

Figure 6.5 Post-SCI 3-HPMA elevation suppressed by acrolein scavengers hydralazine and phenelzine. 3-HPMA was significantly elevated in injured rats compared to sham surgery. Both hydralazine and phenelzine reduced levels of 3-HPMA in a dose-dependent manner.

6.3.4 Apparent pharmacokinetics of hydralazine and phenelzine

Plasma concentrations of hydralazine (Figure 6.6A) and phenelzine (Figure 6.6B) were monitored via mass spectrometry. Apparent plasma half-lives were determined to be 59 minutes for hydralazine and 29 minutes for phenelzine. Although it is not inherently surprising that plasma half-life is decreased compared to established human pharmacology due to higher unit metabolism, it was expected that phenelzine would have a much higher half-life than hydralazine. Upon review, it is likely that this deviation was a result of nonspecific detection of a hydralazine pyruvic acid hydrazone which has a higher plasma half-life than unmodified hydralazine, and the true half-life of free hydralazine can be expected to be lower than observed in this study. Because production

of reactive aldehydes is a continuous process which occurs over the course of days, weeks, or months, it may be more effective to administer hydralazine and phenelzine in multiple doses or in a slow-release manner to improve overall exposure and optimize acrolein scavenging capability.

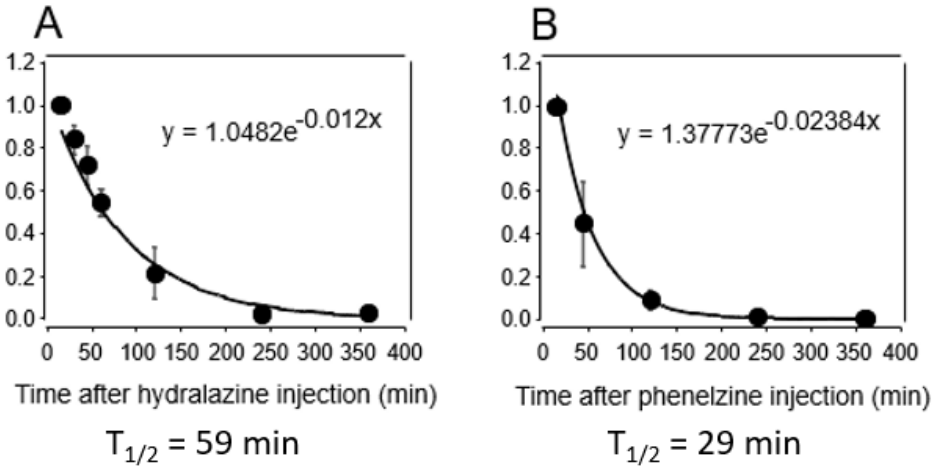

Figure 6.6 Mass spectrometry determination of hydralazine (A) and phenelzine (B) plasma concentrations. Hydralazine or phenelzine was administered by intraperitoneal injection and blood samples were withdrawn regularly over 360 minutes.

6.4 Discussion

In this study, we have shown that phenelzine has the ability to mitigate post-SCI mechanical hyperreflexia and attenuate TRPA1 upregulation. Furthermore, local and systemic acrolein metabolites were suppressed with phenelzine treatment at a similar degree as hydralazine treatment. Given the role of acrolein in perpetuating oxidative stress and its capability to activate TRPA1, we postulate that the analgesic effect of phenelzine and hydralazine derives at least in part if not primarily from trapping of acrolein.

Phenelzine shares a common hydrazine moiety with hydralazine which is capable of scavenging aldehydes such as acrolein by formation of a Schiff base. Although both hydralazine and phenelzine have additional pharmacological effects, we suggest that acrolein scavenging through the shared functional group is more likely to be responsible for the observed neuroprotection than effects unique to each drug. However, the analgesic effect of phenelzine may be confounded in part due to its activity as a monoamine oxidase inhibitor as non-hydrazine monoamine oxidase inhibitors have also been shown to reduce postoperative hypersensitivity in

rodent models. As such, it is likely that the analgesic effect of phenelzine observed in this study may arise from multiple concurrent mechanisms.

Measurement of acrolein metabolites revealed that phenelzine has comparable efficacy to hydralazine when administered at similar dosages. However, each of these compounds has systemic effects which must be considered for *in vivo* study. Because hydralazine is a vasodilator, high does could result in hypotension which may be limiting in traumatic models such as SCI and TBI. Although, we have not observed significant changes in blood pressure at the studied doses, higher doses may induce hypotension and reduce cerebral perfusion pressure. Chronic application of phenelzine can result in hypertensive crisis under certain conditions due to inhibition of hepatic monoamine oxidase. Therefore, pharmaceutical selection should be based on the experimental conditions and monitoring of blood pressure may be necessary when identifying effective doses.

In addition to varied pharmacodynamics, the pharmacokinetics of hydralazine and phenelzine should be considered. Literature reports that the typical plasma half-life of phenelzine is 11.6 hours [144] which is significantly greater than hydralazine's half-life of between 30 to 60 minutes in human subjects [145-148]. In this study, we found conflicting evidence which suggests that the plasma half-life of hydralazine in rats is approximately 60 minutes while the half-life of phenelzine is approximately 30 minutes. There has been some variation in literature regarding the half-life of phenelzine with one study reporting a half-life of 52-191 minutes and another reporting 90-240 minutes [149, 150]. The exact mechanism behind the observed differences remains to be explored, although it is likely that half-life in the rat is suppressed due to higher unit metabolism [151-154]. However, acceptance of this explanation creates additional questions regarding the relatively longer half-life of hydralazine. One potential confounder is the prolonged half-life of the hydralazine pyruvate hydrazone which may remain stable in human plasma for hours after administration [155].

The short half-lives of phenelzine and hydralazine in the rat present a challenge in animal studies since inflammation and oxidative stress may occur on the order of hours to weeks. As such, single daily injections may not be ideal for suppressing overall exposure to acrolein. Therefore, multiple injections or slow-release administration may be needed to optimize the effect of acrolein scavenging with hydralazine and phenelzine.

Interestingly, phenelzine retained its analgesic effects even when treatment was delayed by even weeks or months. Although it remains possible that inhibition of monoamine oxidase

contributes to this effect, we consider it likely that acrolein scavenging is a major factor as acrolein has been shown to be elevated even 2 weeks post injury and may continue at modest levels in chronic injury. Additionally, the upregulation of TPRA1 observed both here and in prior studies suggests that sensory hypersensitivity could arise with normal or even mildly elevated levels of acrolein. Of note, we also found that the analgesic effect of phenelzine persists for an extended period of time with acute application, but not when treatment was delayed or chronic. Given the observed differences, it is possible that acrolein is an important factor not only in initiating hypersensitivity in the acute stage, but also in transitioning to chronic stages of injury. For example, it has been shown that acrolein is elevated two weeks following SCI and that acrolein contributes to TRPA1 upregulation. TRPA1 has also been suggested to be a contributor the transition from acute to chronic inflammatory pain. Furthermore, acrolein scavengers have been shown to attenuate TRPA1 transcript upregulation following SCI. Taken in combination, it is likely that acrolein contributes to the transition from acute to chronic neuropathic pain by inducing TRPA1 upregulation.

7. CONCLUSIONS

7.1 Multiple sclerosis

In the studies described in this chapters 1 and 2, we examined multiple aspects of the pathology and progression of multiple sclerosis. Pathologically, we have produced evidence supporting the roles of oxidative stress and axonal membrane permeability in the progressive loss of function in EAE. We have also further characterized acrolein as a critical factor in mediating oxidative damage MS pathology through measurement of local and systemic metabolites and examining the effect of carbonyl scavenging compounds.

First, we have demonstrated that axonal membrane permeability plays a key role in multiple sclerosis pathology. Treatment with polyethylene glycol reduced HRP uptake in EAE mice and confirmed its action as a membrane sealant in this model. Clinically, PEG treated animals exhibited both lower peak symptom severity and delayed time to peak symptoms.

Next, in preparation for a pilot human clinical study, we confirmed that the systemic acrolein metabolite 3-HPMA is elevated in EAE mice and that this was well correlated with tissue level acrolein-lysine adducts. We then confirmed that both local and systemic metabolites respond to treatment with acrolein scavengers. In a pilot clinical study, we found that 3-HPMA was elevated in both the urine and serum of MS patients and that these values were well correlated. This suggests that acrolein elevation is indeed observed in the human condition and is promising for translation. However, we did observe a number of MS patients exhibiting similar values to control subjects. We speculate that these are primarily patients in remission, although low sample size prevents significant subgroup analyses.

Having shown to our satisfaction the presence of acrolein elevation in the human condition, we returned to examine the role of acrolein more closely in other aspects of MS and EAE. We first confirmed that the neuroprotective effects of hydralazine are more likely to be attributed to the hydrazine moiety rather than the phthalazine scaffold. Next verified that hydralazine continues to produce observable differences in progression of EAE even when delaying treatment to the onset of symptoms.

We then examined the role of acrolein in EAE related neuropathic behaviors. We found that both hydralazine and dimercaprol, a thiol-based carbonyl scavenger, significantly alleviated

mechanical hyperreflexia in EAE. Considering that TRPA1, a nociceptive channel which responds to reactive aldehydes, is upregulated in the myelin oligodendrocyte glycoprotein induced model of progressive EAE, we postulate that may contribute to MS related neuropathic pain via TRPA1.

Finally, we examined the role of ALDH2 and MPO, two endogenous enzymes that interact with acrolein. Current acrolein scavenging strategies have largely been direct stoichiometric scavengers. By modulating ALDH2, we can promote detoxification of acrolein in a nonstoichiometric manner. We found that treatment with Alda-1, an ALDH2 agonist, significantly alleviated both motor deficits and pain-related behaviors in EAE mice. Conversely, ALDH2*2 mice, which have a nonfunctional form of the enzyme, exhibited significantly more severe motor functions suggesting that ALDH2 may be a viable therapeutic target.

We found that MPO, a peroxidase expressed primarily by neutrophil granulocytes, was elevated in the dorsal white matter of EAE mice. In addition, we found that levels of MPO were well correlated with the those of acrolein-lysine adducts. Treatment with hydralazine and Alda-1 reduced the levels of both acrolein-lysine and MPO in the dorsal white matter of EAE mice. Given that MPO can produce acrolein from L-threonine, this suggests that acrolein scavenging reduces carbonyl stress not only by direct removal of local acrolein, but also through subsequent reduction in immune cell recruitment.

7.2 TBI and Parkinson's disease

In chapter 4, we examined the role of acrolein in Parkinson's disease. We confirmed that acrolein scavengers reduce acrolein metabolites, alleviate motor and sensory deficits, and mitigated dopaminergic cell death after microinjection of 6-OHDA. We also confirmed that injection of acrolein alone is sufficient to produce similar behavioral and biochemical changes to 6-OHDA injection.

In chapter 5, we aimed to explore the role of acrolein in post-TBI Parkinsonian pathology. We found that acrolein metabolites were elevated in the whole brain, striatum, and substantia nigra after bTBI. We identified an aberrant 35 kDa form of α-synuclein which was increased in injured rats relative to the unmodified monomeric form. Although the exact nature of this higher molecular weight species is not known, we currently postulate that it is a post-translational modification that may induce oligomerization.

In vitro and *in vivo* experiments confirmed the interaction of acrolein and α-synuclein. Incubation of purified α-synuclein revealed an increase in α-synuclein oligomers in a dose dependent manner. Although α-synuclein immunolabeling was lost at higher concentrations, acrolein-lysine immunolabeling increased through all but the highest concentration of acrolein suggesting either protein breakdown or structural disruption of the recognition site. Immunoprecipitation of whole brain lysates from TBI animals confirmed the interaction of acrolein and α-synuclein *in vivo*.

7.3 Spinal cord injury

In chapter 6, we examined acrolein as a mediator of neuropathic pain in SCI. We utilized phenelzine to confirm that relief previously obtained by hydralazine is likely to be attributed to acrolein scavenging activity. We observed that phenelzine treatment alleviated both symptomatic and biochemical changes. Specifically, we found that phenelzine alleviates pain in SCI rats and that delayed and chronic treatments have more transient effects than acute treatment. This may indicate that acrolein is more active in inducing structural damage and/or biochemical changes in the acute and subacute phases of injury than in chronic injury. This observation could be mediated by chronic upregulation of TRPA1 which could result in increased sensitivity even at relatively normal levels of acrolein. Indeed, we observed that TRPA1 was upregulated in SCI rats and that phenelzine treatment significantly attenuated this effect. Admittedly, phenelzine's activity as a monoamine oxidase inhibitor could serve as a confounding factor in the presented study. However, the doses selected results in relatively low overall exposure due to rapid elimination in the rat.

7.4 Summary

In this dissertation, we have examined the role of acrolein in a variety of traumatic and degenerative conditions of the central nervous system. We have found that systemic and local metabolites are elevated in animal models of MS, PD, TBI, and SCI, that systemic acrolein metabolites are elevated in MS patients, and that acrolein scavenging treatments alleviate sensory and behavioral deficits in EAE and SCI. Furthermore, we find initial evidence that acrolein capable of binding to α-synuclein and inducing oligomerization both *in vitro* and *in vivo*. Together,

these studies provide insight into the role of acrolein in neurotrauma and neurodegeneration and the potential of acrolein scavenging treatment for the alleviation of these conditions.

Within our studies of MS, PD, and SCI, we have found that acrolein contributes to the injurious processes which induce functional loss. In particular, we have seen that application of acrolein scavengers such as hydralazine and phenelzine alleviate motor deficits within our animal models for each of these conditions. Direct microinjection of acrolein into the medial forebrain bundle was also capable of and solely sufficient to induce similar functional and biochemical outcomes as the 6-OHDA rat model of PD. Furthermore, we have observed that deficiency of ALDH2, which is capable of detoxifying acrolein, significantly intensifies the development of motor symptoms in EAE.

Acrolein also appears to contribute to neuropathic pain like behaviors within MS, SCI, and PD. In each model we observed significantly higher sensitivity to mechanical stimulus in disease or injured animals and that acrolein scavengers significantly alleviated these pain related behaviors. We suggest that acrolein contributes to this elevated sensitivity via TRPA1 upregulation. Indeed, TRPA1 has previously been shown to be upregulated in both SCI [111] and the progressive EAE model [112]. Here, we also find initial evidence that acrolein scavenging suppresses injury induced TRPA1 upregulation in dorsal root ganglia, the dorsal spinal cord, and in the skin of the hind paw. Although our study of delayed and chronic phenelzine treatment demonstrated only transient relief after cessation of therapy, it is possible that increased expression of TRPA1 could result in higher levels of signaling even at baseline levels of noxious aldehydes.

Examination of models of MS and PD provided insight into how acrolein contributes to the developing pathologies of neuroinflammation and neurodegeneration. Our study of post-TBI neuropathology provided initial evidence of acrolein modified α-synuclein after single mild bTBI. Furthermore, *in vitro* experimentation confirmed that acrolein is sufficient to induce α-synuclein oligomerization. Within our examination of EAE, we found that acrolein scavenging reduced levels of myeloperoxidase and that deficiency in ALDH2 causes the presence of MPO to increase. Regression analysis showed that these values are correlated. Together, these suggest that acrolein contributes to immune cell recruitment in EAE which is further compounded by oxidative burst from infiltrating immune cells and production of additional acrolein by MPO.

In summary, we have demonstrated that acrolein contributes to the pathology of neurotrauma, neuroinflammation, and neurodegeneration. Using acrolein scavengers, we have

demonstrated acrolein's involvement in inflicting functional loss and causing neuropathic pain related behaviors in animal models of MS, PD, and SCI. We have also produced initial evidence that TPRA1 upregulation may mediate the transition into chronic sensitivity to noxious stimuli such as acrolein and that acrolein scavenging can suppress TRPA1 overexpression after SCI. Finally, we found that acrolein can directly contribute the pathologies critical in development of MS and PD. Taken together, we suggest that acrolein a critical factor in the pathology of secondary neurotrauma, neuroinflammation, and neurodegeneration which contributes to observable symptoms through a variety of methods including protein adduction and recruitment of inflammatory immune cells.

REFERENCES

1. Zhelev Z, Bakalova R, Aoki I, Lazarova D, Saga T: **Imaging of superoxide generation in the dopaminergic area of the brain in Parkinson's disease, using mito-TEMPO**. *ACS Chem Neurosci* 2013, **4**(11):1439-1445.

2. Smith KJ, Kapoor R, Felts PA: **Demyelination: the role of reactive oxygen and nitrogen species**. *Brain Pathol* 1999, **9**(1):69-92.

3. Jana A, Pahan K: **Oxidative stress kills human primary oligodendrocytes via neutral sphingomyelinase: implications for multiple sclerosis**. *J Neuroimmune Pharmacol* 2007, **2**(2):184-193.

4. Bains M, Hall ED: **Antioxidant therapies in traumatic brain and spinal cord injury**. *Biochim Biophys Acta* 2012, **1822**(5):675-684.

5. Luo J, Uchida K, Shi R: **Accumulation of acrolein-protein adducts after traumatic spinal cord injury**. *Neurochem Res* 2005, **30**(3):291-295.

6. Gilgun-Sherki Y, Melamed E, Offen D: **The role of oxidative stress in the pathogenesis of multiple sclerosis: the need for effective antioxidant therapy**. *J Neurol* 2004, **251**(3):261-268.

7. DiSabato DJ, Quan N, Godbout JP: **Neuroinflammation: the devil is in the details**. *J Neurochem* 2016, **139 Suppl 2**:136-153.

8. Stevens JF, Maier CS: **Acrolein: Sources, metabolism, and biomolecular interactions relevant to human health and disease**. *Molecular Nutrition & Food Research* 2008, **52**(1):7-25.

9. Koch M, Mostert J, Arutjunyan AV, Stepanov M, Teelken A, Heersema D, De Keyser J: **Plasma lipid peroxidation and progression of disability in multiple sclerosis**. *Eur J Neurol* 2007, **14**(5):529-533.

10. Uchida K, Kanematsu M, Sakai K, Matsuda T, Hattori N, Mizuno Y, Suzuki D, Miyata T, Noguchi N, Niki E *et al*: **Protein-bound acrolein: potential markers for oxidative stress**. *Proc Natl Acad Sci U S A* 1998, **95**(9):4882-4887.

11. Wood PL, Khan MA, Kulow SR, Mahmood SA, Moskal JR: **Neurotoxicity of reactive aldehydes: the concept of "aldehyde load" as demonstrated by neuroprotection with hydroxylamines**. *Brain Res* 2006, **1095**(1):190-199.

12. Wood PL, Khan MA, Moskal JR, Todd KG, Tanay VA, Baker G: **Aldehyde load in ischemia-reperfusion brain injury: neuroprotection by neutralization of reactive aldehydes with phenelzine**. *Brain Res* 2006, **1122**(1):184-190.

13. Esterbauer H, Schaur RJ, Zollner H: **Chemistry and biochemistry of 4-hydroxynonenal, malonaldehyde and related aldehydes**. *Free Radic Biol Med* 1991, **11**(1):81-128.

14. Bizzozero OA: **Protein Carbonylation in Neurodegenerative and Demyelinating CNS Diseases**. In: *Handbook of Neurochemistry and Molecular Neurobiology: Brain and Spinal Cord Trauma*. edn. Edited by Lajtha A, Banik N, Ray SK. Boston, MA: Springer US; 2009: 543-562.

15. Singh IN, Gilmer LK, Miller DM, Cebak JE, Wang JA, Hall ED: **Phenelzine mitochondrial functional preservation and neuroprotection after traumatic brain injury related to scavenging of the lipid peroxidation-derived aldehyde 4-hydroxy-2-nonenal**. *J Cereb Blood Flow Metab* 2013, **33**(4):593-599.

16. Negre-Salvayre A, Coatrieux C, Ingueneau C, Salvayre R: **Advanced lipid peroxidation end products in oxidative damage to proteins. Potential role in diseases and therapeutic prospects for the inhibitors**. *Br J Pharmacol* 2008, **153**(1):6-20.

17. Moghe A, Ghare S, Lamoreau B, Mohammad M, Barve S, McClain C, Joshi-Barve S: **Molecular mechanisms of acrolein toxicity: relevance to human disease**. *Toxicol Sci* 2015, **143**(2):242-255.

18. Shi Y, Sun W, McBride JJ, Cheng JX, Shi R: **Acrolein induces myelin damage in mammalian spinal cord**. *J Neurochem* 2011, **117**(3):554-564.

19. Gianaris A, Liu NK, Wang XF, Oakes E, Brenia J, Gianaris T, Ruan Y, Deng LX, Goetz M, Vega-Alvarez S *et al*: **Unilateral microinjection of acrolein into thoracic spinal cord produces acute and chronic injury and functional deficits**. *Neuroscience* 2016, **326**:84-94.

20. Eckert E, Drexler H, Goen T: **Determination of six hydroxyalkyl mercapturic acids in human urine using hydrophilic interaction liquid chromatography with tandem mass spectrometry (HILIC-ESI-MS/MS)**. *J Chromatogr B Analyt Technol Biomed Life Sci* 2010, **878**(27):2506-2514.

21. Anderson MM, Hazen SL, Hsu FF, Heinecke JW: **Human neutrophils employ the myeloperoxidase-hydrogen peroxide-chloride system to convert hydroxy-amino acids into glycolaldehyde, 2-hydroxypropanal, and acrolein. A mechanism for the generation of highly reactive alpha-hydroxy and alpha,beta-unsaturated aldehydes by phagocytes at sites of inflammation**. *J Clin Invest* 1997, **99**(3):424-432.

22. Dong JZ, Moldoveanu SC: **Gas chromatography-mass spectrometry of carbonyl compounds in cigarette mainstream smoke after derivatization with 2,4-dinitrophenylhydrazine**. *J Chromatogr A* 2004, **1027**(1-2):25-35.

23. Alary J, Debrauwer L, Fernandez Y, Cravedi JP, Rao D, Bories G: **1,4-Dihydroxynonene mercapturic acid, the major end metabolite of exogenous 4-hydroxy-2-nonenal, is a physiological component of rat and human urine**. *Chem Res Toxicol* 1998, **11**(2):130-135.

24. Islam SMT, Won J, Kim J, Qiao F, Singh AK, Khan M, Singh I: **Detoxification of Reactive Aldehydes by Alda-1 Treatment Ameliorates Experimental Autoimmune Encephalomyelitis in Mice**. *Neuroscience* 2021, **458**:31-42.

25. Larson HN, Weiner H, Hurley TD: **Disruption of the coenzyme binding site and dimer interface revealed in the crystal structure of mitochondrial aldehyde dehydrogenase "Asian" variant**. *J Biol Chem* 2005, **280**(34):30550-30556.

26. Joshi AU, Van Wassenhove LD, Logas KR, Minhas PS, Andreasson KI, Weinberg KI, Chen CH, Mochly-Rosen D: **Aldehyde dehydrogenase 2 activity and aldehydic load contribute to neuroinflammation and Alzheimer's disease related pathology**. *Acta Neuropathol Commun* 2019, **7**(1):190.

27. Leung G, Sun W, Zheng L, Brookes S, Tully M, Shi R: **Anti-acrolein treatment improves behavioral outcome and alleviates myelin damage in experimental autoimmune encephalomyelitis mouse**. *Neuroscience* 2011, **173**:150-155.

28. Lin Y, Chen Z, Tang J, Cao P, Shi R: **Acrolein Contributes to the Neuropathic Pain and Neuron Damage after Ischemic-Reperfusion Spinal Cord Injury**. *Neuroscience* 2018, **384**:120-130.

29. Ambaw A, Zheng L, Tambe MA, Strathearn KE, Acosta G, Hubers SA, Liu F, Herr SA, Tang J, Truong A *et al*: **Acrolein-mediated neuronal cell death and alpha-synuclein aggregation: Implications for Parkinson's disease**. *Mol Cell Neurosci* 2018, **88**:70-82.

30. Miller E: **Multiple Sclerosis**. In: *Neurodegenerative Diseases.* edn. Edited by I AS; 2012: 222-238.

31. Osterberg A, Boivie J, Thuomas KA: **Central pain in multiple sclerosis--prevalence and clinical characteristics**. *Eur J Pain* 2005, **9**(5):531-542.

32. Compston A, Coles A: **Multiple sclerosis**. *Lancet* 2008, **372**(9648):1502-1517.

33. Disanto G, Morahan JM, Barnett MH, Giovannoni G, Ramagopalan SV: **The evidence for a role of B cells in multiple sclerosis**. *Neurology* 2012, **78**(11):823-832.

34. Gold R, Linington C, Lassmann H: **Understanding pathogenesis and therapy of multiple sclerosis via animal models: 70 years of merits and culprits in experimental autoimmune encephalomyelitis research**. *Brain* 2006, **129**(Pt 8):1953-1971.

35. Gonsette RE: **Oxidative stress and excitotoxicity: a therapeutic issue in multiple sclerosis?** *Mult Scler* 2008, **14**(1):22-34.

36. Dutta R, Trapp BD: **Pathogenesis of axonal and neuronal damage in multiple sclerosis**. *Neurology* 2007, **68**(22 Suppl 3):S22-31; discussion S43-54.

37. Frohman EM, Filippi M, Stuve O, Waxman SG, Corboy J, Phillips JT, Lucchinetti C, Wilken J, Karandikar N, Hemmer B *et al*: **Characterizing the mechanisms of progression in multiple sclerosis: evidence and new hypotheses for future directions**. *Arch Neurol* 2005, **62**(9):1345-1356.

38. Imitola J, Chitnis T, Khoury SJ: **Insights into the molecular pathogenesis of progression in multiple sclerosis: Potential implications for future therapies**. *Archives of Neurology* 2006, **63**(1):25-33.

39. Popescu BF, Lucchinetti CF: **Pathology of demyelinating diseases**. *Annu Rev Pathol* 2012, **7**:185-217.

40. Ferretti G, Bacchetti T, Principi F, Di Ludovico F, Viti B, Angeleri VA, Danni M, Provinciali L: **Increased levels of lipid hydroperoxides in plasma of patients with multiple sclerosis: a relationship with paraoxonase activity**. *Multiple Sclerosis* 2005, **11**(6):677-682.

41. Smith KJ, Lassmann H: **The role of nitric oxide in multiple sclerosis**. *The Lancet Neurology* 2002, **1**(4):232-241.

42. Tully M, Shi R: **New insights in the pathogenesis of multiple sclerosis--role of acrolein in neuronal and myelin damage**. *Int J Mol Sci* 2013, **14**(10):20037-20047.

43. Qi X, Lewin AS, Sun L, Hauswirth WW, Guy J: **Mitochondrial protein nitration primes neurodegeneration in experimental autoimmune encephalomyelitis**. *J Biol Chem* 2006, **281**(42):31950-31962.

44. Mirshafiey A, Mohsenzadegan M: **Antioxidant therapy in multiple sclerosis**. *Immunopharmacol Immunotoxicol* 2009, **31**(1):13-29.

45. Carlson NG, Rose JW: **Antioxidants in Multiple Sclerosis: Do They Have a Role in Therapy?** *CNS Drugs* 2006, **20**(6):433.

46. Karg E, Klivenyi P, Nemeth I, Bencsik K, Pinter S, Vecsei L: **Nonenzymatic antioxidants of blood in multiple sclerosis**. *J Neurol* 1999, **246**(7):533-539.

47. Tully M, Tang J, Zheng L, Acosta G, Tian R, Hayward L, Race N, Mattson D, Shi R: **Systemic Acrolein Elevations in Mice With Experimental Autoimmune Encephalomyelitis and Patients With Multiple Sclerosis**. *Front Neurol* 2018, **9**:420.

48. Bizzozero OA, DeJesus G, Callahan K, Pastuszyn A: **Elevated protein carbonylation in the brain white matter and gray matter of patients with multiple sclerosis**. *J Neurosci Res* 2005, **81**(5):687-695.

49. Wingerchuk DM: **Smoking: effects on multiple sclerosis susceptibility and disease progression**. *Ther Adv Neurol Disord* 2012, **5**(1):13-22.

50. Tully M, Zheng L, Acosta G, Tian R, Shi R: **Acute systemic accumulation of acrolein in mice by inhalation at a concentration similar to that in cigarette smoke**. *Neurosci Bull* 2014, **30**(6):1017-1024.

51. Dworkin RH, O'Connor AB, Backonja M, Farrar JT, Finnerup NB, Jensen TS, Kalso EA, Loeser JD, Miaskowski C, Nurmikko TJ *et al*: **Pharmacologic management of neuropathic pain: evidence-based recommendations**. *Pain* 2007, **132**(3):237-251.

52. Khan N, Smith MT: **Multiple sclerosis-induced neuropathic pain: pharmacological management and pathophysiological insights from rodent EAE models**. *Inflammopharmacology* 2014, **22**(1):1-22.

53. Khan N, Gordon R, Woodruff TM, Smith MT: **Antiallodynic effects of alpha lipoic acid in an optimized RR-EAE mouse model of MS-neuropathic pain are accompanied by attenuation of upregulated BDNF-TrkB-ERK signaling in the dorsal horn of the spinal cord**. *Pharmacol Res Perspect* 2015, **3**(3):e00137.

54. Arima Y, Kamimura D, Atsumi T, Harada M, Kawamoto T, Nishikawa N, Stofkova A, Ohki T, Higuchi K, Morimoto Y *et al*: **A pain-mediated neural signal induces relapse in murine autoimmune encephalomyelitis, a multiple sclerosis model**. *Elife* 2015, **4**.

55. Centers for Disease Control and Prevention (CDC): **Traumatic Brain Injury in the United States: Epidemiology and Rehabilitation**. In. Atlanta, GA: National Center for Injury Prevention and Control, Centers for Disease Control and Prevention; 2015.

56. Menon DK, Schwab K, Wright DW, Maas AI, Demographics, Clinical Assessment Working Group of the I, Interagency Initiative toward Common Data Elements for Research on Traumatic Brain I, Psychological H: **Position statement: definition of traumatic brain injury**. *Arch Phys Med Rehabil* 2010, **91**(11):1637-1640.

57. Faul M, Likang X, Marlena MW, Coronado V: **Traumatic brain injury in the United States: Emergency department visits, hospitalizations and deaths 2002-2006**. In.: National Center for Injury Prevention and Control, Centers for Disease Control and Prevention; 2010.

58. Corso P, Finkelstein E, Miller T, Fiebelkorn I, Zaloshnja E: **Incidence and lifetime costs of injuries in the United States**. *Inj Prev* 2006, **12**(4):212-218.

59. Marin JR, Weaver MD, Yealy DM, Mannix RC: **Trends in visits for traumatic brain injury to emergency departments in the United States**. *JAMA* 2014, **311**(18):1917-1919.

60. Summers CR, Ivins B, Schwab KA: **Traumatic brain injury in the United States: an epidemiologic overview**. *Mt Sinai J Med* 2009, **76**(2):105-110.

61. Malec JF, Brown AW, Leibson CL, Flaada JT, Mandrekar JN, Diehl NN, Perkins PK: **The mayo classification system for traumatic brain injury severity**. *J Neurotrauma* 2007, **24**(9):1417-1424.

62. Ponsford JL, Spitz G, McKenzie D: **Using Post-Traumatic Amnesia To Predict Outcome after Traumatic Brain Injury**. *J Neurotrauma* 2016, **33**(11):997-1004.

63. Stein SC: **Minor head injury: 13 is an unlucky number**. *Journal of Trauma-Injury Infection and Critical Care* 2001, **50**(4):759-760.

64. Teasdale G, Maas A, Lecky F, Manley G, Stocchetti N, Murray G: **The Glasgow Coma Scale at 40 years: standing the test of time**. *The Lancet Neurology* 2014, **13**(8):844-854.

65. Anstey KJ, Butterworth P, Jorm AF, Christensen H, Rodgers B, Windsor TD: **A population survey found an association between self-reports of traumatic brain injury and increased psychiatric symptoms**. *J Clin Epidemiol* 2004, **57**(11):1202-1209.

66. Chen Y, Huang W: **Non-impact, blast-induced mild TBI and PTSD: concepts and caveats**. *Brain Inj* 2011, **25**(7-8):641-650.

67. Riggio S, Wong M: **Neurobehavioral sequelae of traumatic brain injury**. *Mt Sinai J Med* 2009, **76**(2):163-172.

68. Masel BE, DeWitt DS: **Traumatic brain injury: a disease process, not an event**. *J Neurotrauma* 2010, **27**(8):1529-1540.

69. Jordan BD: **The clinical spectrum of sport-related traumatic brain injury**. *Nat Rev Neurol* 2013, **9**(4):222-230.

70. Bang SA, Song YS, Moon BS, Lee BC, Lee HY, Kim JM, Kim SE: **Neuropsychological, Metabolic, and GABAA Receptor Studies in Subjects with Repetitive Traumatic Brain Injury**. *J Neurotrauma* 2016, **33**(11):1005-1014.

71. Goldman SM, Tanner CM, Oakes D, Bhudhikanok GS, Gupta A, Langston JW: **Head injury and Parkinson's disease risk in twins**. *Ann Neurol* 2006, **60**(1):65-72.

72. Shaw NA: **The neurophysiology of concussion**. *Progress in Neurobiology* 2002, **67**(4):281-344.

73. Ommaya AK, Grubb RL, Jr., Naumann RA: **Coup and contre-coup injury: observations on the mechanics of visible brain injuries in the rhesus monkey**. *J Neurosurg* 1971, **35**(5):503-516.

74. Greve MW, Zink BJ: **Pathophysiology of traumatic brain injury**. *Mt Sinai J Med* 2009, **76**(2):97-104.

75. Harris JL, Yeh HW, Choi IY, Lee P, Berman NE, Swerdlow RH, Craciunas SC, Brooks WM: **Altered neurochemical profile after traumatic brain injury: (1)H-MRS biomarkers of pathological mechanisms**. *J Cereb Blood Flow Metab* 2012, **32**(12):2122-2134.

76. McKee AC, Daneshvar DH: **The neuropathology of traumatic brain injury**. *Handb Clin Neurol* 2015, **127**:45-66.

77. Bose R, Schnell CL, Pinsky C, Zitko V: **Effects of excitotoxins on free radical indices in mouse brain**. *Toxicology Letters* 1992, **60**(2):211-219.

78. Gilgun-Sherki Y, Rosenbaum Z, Melamed E, Offen D: **Antioxidant therapy in acute central nervous system injury: current state**. *Pharmacol Rev* 2002, **54**(2):271-284.

79. Murphy MP: **How mitochondria produce reactive oxygen species**. *Biochem J* 2009, **417**(1):1-13.

80. Lander HM: **An essential role for free radicals and derived species in signal transduction**. *FASEB J* 1997, **11**(2):118-124.

81. Kaminskas LM, Pyke SM, Burcham PC: **Strong protein adduct trapping accompanies abolition of acrolein-mediated hepatotoxicity by hydralazine in mice**. *J Pharmacol Exp Ther* 2004, **310**(3):1003-1010.

82. Walls MK, Race N, Zheng L, Vega-Alvarez SM, Acosta G, Park J, Shi R: **Structural and biochemical abnormalities in the absence of acute deficits in mild primary blast-induced head trauma**. *J Neurosurg* 2016, **124**(3):675-686.

83. Acosta G, Race N, Herr S, Fernandez J, Tang J, Rogers E, Shi R: **Acrolein-mediated alpha-synuclein pathology involvement in the early post-injury pathogenesis of mild blast-induced Parkinsonian neurodegeneration**. *Mol Cell Neurosci* 2019, **98**:140-154.

84. Shamoto-Nagai M, Maruyama W, Hashizume Y, Yoshida M, Osawa T, Riederer P, Naoi M: **In parkinsonian substantia nigra, alpha-synuclein is modified by acrolein, a lipid-peroxidation product, and accumulates in the dopamine neurons with inhibition of proteasome activity**. *J Neural Transm (Vienna)* 2007, **114**(12):1559-1567.

85. Plotegher N, Bubacco L: **Lysines, Achilles' heel in alpha-synuclein conversion to a deadly neuronal endotoxin**. *Ageing Res Rev* 2016, **26**:62-71.

86. Qin Z, Hu D, Han S, Reaney SH, Di Monte DA, Fink AL: **Effect of 4-hydroxy-2-nonenal modification on alpha-synuclein aggregation**. *J Biol Chem* 2007, **282**(8):5862-5870.

87. Atsmon-Raz Y, Miller Y: **Non-Amyloid-beta Component of Human alpha-Synuclein Oligomers Induces Formation of New Abeta Oligomers: Insight into the Mechanisms That Link Parkinson's and Alzheimer's Diseases**. *ACS Chem Neurosci* 2016, **7**(1):46-55.

88. Cernak I, Noble-Haeusslein LJ: **Traumatic brain injury: an overview of pathobiology with emphasis on military populations**. *J Cereb Blood Flow Metab* 2010, **30**(2):255-266.

89. Hausmann ON: **Post-traumatic inflammation following spinal cord injury**. *Spinal Cord* 2003, **41**(7):369-378.

90. Acosta SA, Tajiri N, Shinozuka K, Ishikawa H, Grimmig B, Diamond DM, Sanberg PR, Bickford PC, Kaneko Y, Borlongan CV: **Long-term upregulation of inflammation and suppression of cell proliferation in the brain of adult rats exposed to traumatic brain injury using the controlled cortical impact model**. *PLoS One* 2013, **8**(1):e53376.

91. Tian R, Shi R: **Dimercaprol is an acrolein scavenger that mitigates acrolein-mediated PC-12 cells toxicity and reduces acrolein in rat following spinal cord injury**. *J Neurochem* 2017, **141**(5):708-720.

92. Park J, Zheng L, Marquis A, Walls M, Duerstock B, Pond A, Vega-Alvarez S, Wang H, Ouyang Z, Shi R: **Neuroprotective role of hydralazine in rat spinal cord injury-attenuation of acrolein-mediated damage**. *J Neurochem* 2014, **129**(2):339-349.

93. Zheng L, Park J, Walls M, Tully M, Jannasch A, Cooper B, Shi R: **Determination of urine 3-HPMA, a stable acrolein metabolite in a rat model of spinal cord injury**. *J Neurotrauma* 2013, **30**(15):1334-1341.

94. Sangster AM, Zheng L, Bentley RT, Shi R, Packer RA: **Urinary 3-hydroxypropyl mercapturic acid (3-HPMA) concentrations in dogs with acute spinal cord injury due to intervertebral disc herniation**. *Vet J* 2017, **219**:12-14.

95. Due MR, Park J, Zheng L, Walls M, Allette YM, White FA, Shi R: **Acrolein involvement in sensory and behavioral hypersensitivity following spinal cord injury in the rat**. *J Neurochem* 2014, **128**(5):776-786.

96. Chen Z, Park J, Butler B, Acosta G, Vega-Alvarez S, Zheng L, Tang J, McCain R, Zhang W, Ouyang Z *et al*: **Mitigation of sensory and motor deficits by acrolein scavenger phenelzine in a rat model of spinal cord contusive injury**. *J Neurochem* 2016, **138**(2):328-338.

97. Macpherson LJ, Dubin AE, Evans MJ, Marr F, Schultz PG, Cravatt BF, Patapoutian A: **Noxious compounds activate TRPA1 ion channels through covalent modification of cysteines**. *Nature* 2007, **445**(7127):541-545.

98. McNamara CR, Mandel-Brehm J, Bautista DM, Siemens J, Deranian KL, Zhao M, Hayward NJ, Chong JA, Julius D, Moran MM *et al*: **TRPA1 mediates formalin-induced pain**. *Proc Natl Acad Sci U S A* 2007, **104**(33):13525-13530.

99. Bautista DM, Jordt SE, Nikai T, Tsuruda PR, Read AJ, Poblete J, Yamoah EN, Basbaum AI, Julius D: **TRPA1 mediates the inflammatory actions of environmental irritants and proalgesic agents**. *Cell* 2006, **124**(6):1269-1282.

100. Shi R, Sun W: **Potassium channel blockers as an effective treatment to restore impulse conduction in injured axons**. *Neurosci Bull* 2011, **27**(1):36-44.

101. Hazen SL, d'Avignon A, Anderson MM, Hsu FF, Heinecke JW: **Human neutrophils employ the myeloperoxidase-hydrogen peroxide-chloride system to oxidize alpha-amino acids to a family of reactive aldehydes. Mechanistic studies identifying labile intermediates along the reaction pathway**. *J Biol Chem* 1998, **273**(9):4997-5005.

102. Ciccarelli O, Barkhof F, Bodini B, Stefano ND, Golay X, Nicolay K, Pelletier D, Pouwels PJW, Smith SA, Wheeler-Kingshott CAM *et al*: **Pathogenesis of multiple sclerosis: insights from molecular and metabolic imaging**. *The Lancet Neurology* 2014, **13**(8):807-822.

103. Chen JW, Breckwoldt MO, Aikawa E, Chiang G, Weissleder R: **Myeloperoxidase-targeted imaging of active inflammatory lesions in murine experimental autoimmune encephalomyelitis**. *Brain* 2008, **131**(Pt 4):1123-1133.

104. Nagra RM, Becher B, Tourtellotte WW, Antel JP, Gold D, Paladino T, Smith RA, Nelson JR, Reynolds WF: **Immunohistochemical and genetic evidence of myeloperoxidase involvement in multiple sclerosis**. *Journal of Neuroimmunology* 1997, **78**(1-2):97-107.

105. Petrus M, Peier AM, Bandell M, Hwang SW, Huynh T, Olney N, Jegla T, Patapoutian A: **A role of TRPA1 in mechanical hyperalgesia is revealed by pharmacological inhibition**. *Mol Pain* 2007, **3**:40.

106. Chen J, Joshi SK, DiDomenico S, Perner RJ, Mikusa JP, Gauvin DM, Segreti JA, Han P, Zhang XF, Niforatos W *et al*: **Selective blockade of TRPA1 channel attenuates pathological pain without altering noxious cold sensation or body temperature regulation**. *Pain* 2011, **152**(5):1165-1172.

107. Sasaki A, Mizoguchi S, Kagaya K, Shiro M, Sakai A, Andoh T, Kino Y, Taniguchi H, Saito Y, Takahata H *et al*: **A mouse model of peripheral postischemic dysesthesia: involvement of reperfusion-induced oxidative stress and TRPA1 channel**. *J Pharmacol Exp Ther* 2014, **351**(3):568-575.

108. Schenkel LB, Olivieri PR, Boezio AA, Deak HL, Emkey R, Graceffa RF, Gunaydin H, Guzman-Perez A, Lee JH, Teffera Y *et al*: **Optimization of a Novel Quinazolinone-Based Series of Transient Receptor Potential A1 (TRPA1) Antagonists Demonstrating Potent in Vivo Activity**. *J Med Chem* 2016, **59**(6):2794-2809.

109. Klafke JZ, da Silva MA, Trevisan G, Rossato MF, da Silva CR, Guerra GP, Villarinho JG, Rigo FK, Dalmolin GD, Gomez MV *et al*: **Involvement of the glutamatergic system in the nociception induced intrathecally for a TRPA1 agonist in rats**. *Neuroscience* 2012, **222**:136-146.

110. Trevisan G, Benemei S, Materazzi S, De Logu F, De Siena G, Fusi C, Fortes Rossato M, Coppi E, Marone IM, Ferreira J *et al*: **TRPA1 mediates trigeminal neuropathic pain in mice downstream of monocytes/macrophages and oxidative stress**. *Brain* 2016, **139**(Pt 5):1361-1377.

111. Park J, Zheng L, Acosta G, Vega-Alvarez S, Chen Z, Muratori B, Cao P, Shi R: **Acrolein contributes to TRPA1 up-regulation in peripheral and central sensory hypersensitivity following spinal cord injury**. *J Neurochem* 2015, **135**(5):987-997.

112. Ritter C, Dalenogare DP, de Almeida AS, Pereira VL, Pereira GC, Fialho MFP, Luckemeyer DD, Antoniazzi CT, Kudsi SQ, Ferreira J *et al*: **Nociception in a Progressive Multiple Sclerosis Model in Mice Is Dependent on Spinal TRPA1 Channel Activation**. *Mol Neurobiol* 2020, **57**(5):2420-2435.

113. Dalenogare DP, Theisen MC, Peres DS, Fialho MFP, Luckemeyer DD, Antoniazzi CTD, Kudsi SQ, Ferreira MA, Ritter CDS, Ferreira J *et al*: **TRPA1 activation mediates nociception behaviors in a mouse model of relapsing-remitting experimental autoimmune encephalomyelitis**. *Exp Neurol* 2020, **328**:113241.

114. Zambelli VO, Gross ER, Chen CH, Gutierrez VP, Cury Y, Mochly-Rosen D: **Aldehyde dehydrogenase-2 regulates nociception in rodent models of acute inflammatory pain**. *Sci Transl Med* 2014, **6**(251):251ra118.

115. Fuhrich DG, Lessey BA, Savaris RF: **Comparison of HSCORE assessment of endometrial beta3 integrin subunit expression with digital HSCORE using computerized image analysis (ImageJ)**. *Anal Quant Cytopathol Histpathol* 2013, **35**(4):210-216.

116. Leung G, Tully M, Tang J, Wu S, Shi R: **Elevated axonal membrane permeability and its correlation with motor deficits in an animal model of multiple sclerosis**. *Transl Neurodegener* 2017, **6**:5.

117. Leung G, Sun W, Brookes S, Smith D, Shi R: **Potassium channel blocker, 4-aminopyridine-3-methanol, restores axonal conduction in spinal cord of an animal model of multiple sclerosis**. *Exp Neurol* 2011, **227**(1):232-235.

118. Kalia LV, Lang AE: **Parkinson's disease**. *The Lancet* 2015, **386**(9996):896-912.

119. Henchcliffe C, Beal MF: **Mitochondrial biology and oxidative stress in Parkinson disease pathogenesis**. *Nat Clin Pract Neurol* 2008, **4**(11):600-609.

120. Hirsch EC, Hunot S: **Neuroinflammation in Parkinson's disease: a target for neuroprotection?** *The Lancet Neurology* 2009, **8**(4):382-397.

121. Spiteller G: **Lipid peroxidation in aging and age-dependent diseases**. *Experimental Gerontology* 2001, **36**(9):1425-1457.

122. Stefanis L: **alpha-Synuclein in Parkinson's disease**. *Cold Spring Harb Perspect Med* 2012, **2**(2):a009399.

123. Crawford GD, Le WD, Smith RG, Xie WJ, Stefani E, Appel SH: **A novel N18TG2 x mesencephalon cell hybrid expresses properties that suggest a dopaminergic cell line of substantia nigra origin**. *The Journal of Neuroscience* 1992, **12**(9):3392-3398.

124. Jones BJ, Roberts DJ: **The quantitative measurement of motor inco-ordination in naive mice using an accelerating rotarod**. *Journal of Pharmacy and Pharmacology* 1968, **20**(4):302-304.

125. Chaplan SR, Bach FW, Pogrel JW, Chung JM, Yaksh TL: **Quantitative assessment of tactile allodynia in the rat paw**. *Journal of Neuroscience Methods* 1994, **53**(1):55-63.

126. Dixon WJ: **Efficient analysis of experimental observations**. *Annu Rev Pharmacol Toxicol* 1980, **20**:441-462.

127. Jafari S, Etminan M, Aminzadeh F, Samii A: **Head injury and risk of Parkinson disease: a systematic review and meta-analysis**. *Mov Disord* 2013, **28**(9):1222-1229.

128. Lee PC, Bordelon Y, Bronstein J, Ritz B: **Traumatic brain injury, paraquat exposure, and their relationship to Parkinson disease**. *Neurology* 2012, **79**(20):2061-2066.

129. Van Den Eeden SK, Tanner CM, Bernstein AL, Fross RD, Leimpeter A, Bloch DA, Nelson LM: **Incidence of Parkinson's disease: variation by age, gender, and race/ethnicity**. *Am J Epidemiol* 2003, **157**(11):1015-1022.

130. Defense Veterans Brain Injury Center (DVBIC): **DoD numbers for traumatic brain injury worldwide: Totals 2000-2015**. In.; 2016.

131. Galarneau MR, Woodruff SI, Dye JL, Mohrle CR, Wade AL: **Traumatic brain injury during Operation Iraqi Freedom: findings from the United States Navy-Marine Corps Combat Trauma Registry**. *J Neurosurg* 2008, **108**(5):950-957.

132. Elder GA, Cristian A: **Blast-related mild traumatic brain injury: mechanisms of injury and impact on clinical care**. *Mt Sinai J Med* 2009, **76**(2):111-118.

133. Hoge CW, McGurk D, Thomas JL, Cox AL, Engel CC, Castro CA: **Mild traumatic brain injury in U.S. Soldiers returning from Iraq**. *N Engl J Med* 2008, **358**(5):453-463.

134. Mario Schootman LJF: **Ambulatory care for traumatic brain injuries in the US, 1995-1997**. *Brain Injury* 2009, **14**(4):373-381.

135. Cebak JE, Singh IN, Hill RL, Wang JA, Hall ED: **Phenelzine Protects Brain Mitochondrial Function In Vitro and In Vivo following Traumatic Brain Injury by Scavenging the Reactive Carbonyls 4-Hydroxynonenal and Acrolein Leading to Cortical Histological Neuroprotection**. *J Neurotrauma* 2017, **34**(7):1302-1317.

136. Mackay GM, Forrest CM, Stoy N, Christofides J, Egerton M, Stone TW, Darlington LG: **Tryptophan metabolism and oxidative stress in patients with chronic brain injury**. *Eur J Neurol* 2006, **13**(1):30-42.

137. Cruz-Haces M, Tang J, Acosta G, Fernandez J, Shi R: **Pathological correlations between traumatic brain injury and chronic neurodegenerative diseases**. *Transl Neurodegener* 2017, **6**:20.

138. Ransohoff RM: **How neuroinflammation contributes to neurodegeneration**. *Science* 2016, **353**(6301):777-783.

139. Acosta SA, Tajiri N, de la Pena I, Bastawrous M, Sanberg PR, Kaneko Y, Borlongan CV: **Alpha-synuclein as a pathological link between chronic traumatic brain injury and Parkinson's disease**. *J Cell Physiol* 2015, **230**(5):1024-1032.

140. Paxinos G, Watson C: **The Rat Brain in Stereotaxic Coordinates**. In., 3rd edn. San Diego, CA: Academic Press, Inc; 1997.

141. Maikos JT, Qian Z, Metaxas D, Shreiber DI: **Finite element analysis of spinal cord injury in the rat**. *J Neurotrauma* 2008, **25**(7):795-816.

142. Hamann K, Nehrt G, Ouyang H, Duerstock B, Shi R: **Hydralazine inhibits compression and acrolein-mediated injuries in ex vivo spinal cord**. *J Neurochem* 2008, **104**(3):708-718.

143. Nozawa K, Kawabata-Shoda E, Doihara H, Kojima R, Okada H, Mochizuki S, Sano Y, Inamura K, Matsushime H, Koizumi T *et al*: **TRPA1 regulates gastrointestinal motility through serotonin release from enterochromaffin cells**. *Proc Natl Acad Sci U S A* 2009, **106**(9):3408-3413.

144. Pfizer Inc: **Nardil**. In. New York, NY: Pfizer Inc; 2009.

145. Ludden TM, Shepherd AM, McNay JL, Lin MS: **Hydralazine kinetics in hypertensive patients after intravenous administration**. *Clin Pharmacol Ther* 1980, **28**(6):736-742.

146. Shepherd AM, Ludden TM, McNay JL, Lin MS: **Hydralazine kinetics after single and repeated oral doses**. *Clin Pharmacol Ther* 1980, **28**(6):804-811.

147. Reece PA, Cozamanis I, Zacest R: **Kinetics of hydralazine and its main metabolites in slow and fast acetylators**. *Clin Pharmacol Ther* 1980, **28**(6):769-778.

148. Reece PA: **Hydralazine and related compounds: chemistry, metabolism, and mode of action**. *Med Res Rev* 1981, **1**(1):73-96.

149. Caddy B, Stead AH, Johnstone EC: **The urinary excretion of phenelzine**. *Br J Clin Pharmacol* 1978, **6**(2):185-188.

150. Robinson DS, Cooper TB, Jindal SP, Corcella J, Lutz T: **Metabolism and pharmacokinetics of phenelzine: lack of evidence for acetylation pathway in humans**. *J Clin Psychopharmacol* 1985, **5**(6):333-337.

151. Sharma V, McNeill JH: **To scale or not to scale: the principles of dose extrapolation**. *Br J Pharmacol* 2009, **157**(6):907-921.

152. White CR, Seymour RS: **Allometric scaling of mammalian metabolism**. *J Exp Biol* 2005, **208**(Pt 9):1611-1619.

153. Mahmood I: **Prediction of clearance, volume of distribution and half-life by allometric scaling and by use of plasma concentrations predicted from pharmacokinetic constants: a comparative study**. *J Pharm Pharmacol* 1999, **51**(8):905-910.

154. Cao Q, Yu J, Connell D: **New allometric scaling relationships and applications for dose and toxicity extrapolation**. *Int J Toxicol* 2014, **33**(6):482-489.

155. Reece PA, Stanley PE, Zacest R: **Interference in assays for hydralazine in humans by a major plasma metabolite, hydralazine pyruvic acid hydrazone**. *J Pharm Sci* 1978, **67**(8):1150-1153.

PUBLICATIONS

* Denotes equal contribution.

1. Shi L, Lin Y, Jiao Y, Herr SA, **Tang J**, Rogers E, Chen Z, Shi R: Acrolein scavenger dimercaprol offers neuroprotection in an animal model of Parkinson's disease: implication of acrolein and TRPA1. *Transl Neurodegener* 2021, 10(1):13.

2. Vike N*, **Tang J***, Talavage T, Shi R, Rispoli J: Determination of acrolein-associated T1 and T2 relaxation times and noninvasive detection using nuclear magnetic resonance and magnetic resonance spectroscopy. *Appl Magn Reson* 2019, 50(11):1291-1303.

3. Acosta G, Race N, Herr S, Fernandez J, **Tang J**, Rogers E, Shi R: Acrolein-mediated alpha-synuclein pathology involvement in the early post-injury pathogenesis of mild blast-induced Parkinsonian neurodegeneration. *Mol Cell Neurosci* 2019, 98:140-154.

4. Garcia-Gonzalez D, Race NS, Voets NL, Jenkins DR, Sotiropoulos SN, Acosta G, Cruz-Haces M, **Tang J**, Shi R, Jerusalem A: Cognition based bTBI mechanistic criteria; a tool for preventive and therapeutic innovations. *Sci Rep* 2018, 8(1):10273.

5. Tully M*, **Tang J***, Zheng L, Acosta G, Tian R, Hayward L, Race N, Mattson D, Shi R: Systemic Acrolein Elevations in Mice With Experimental Autoimmune Encephalomyelitis and Patients With Multiple Sclerosis. *Front Neurol* 2018, 9:420.

6. Lin Y, Chen Z, **Tang J**, Cao P, Shi R: Acrolein Contributes to the Neuropathic Pain and Neuron Damage after Ischemic-Reperfusion Spinal Cord Injury. *Neuroscience* 2018, 384:120-130.

7. Ambaw A, Zheng L, Tambe MA, Strathearn KE, Acosta G, Hubers SA, Liu F, Herr SA, **Tang J**, Truong A, Walls E, Pond A, Rochet JC, Shi R: Acrolein-mediated neuronal cell death and alpha-synuclein aggregation: Implications for Parkinson's disease. *Mol Cell Neurosci* 2018, 88:70-82.

8. Cruz-Haces M*, **Tang J***, Acosta G, Fernandez J, Shi R: Pathological correlations between traumatic brain injury and chronic neurodegenerative diseases. *Transl Neurodegener* 2017, 6:20.

9. Leung G, Tully M, **Tang J**, Wu S, Shi R: Elevated axonal membrane permeability and its correlation with motor deficits in an animal model of multiple sclerosis. *Transl Neurodegener* 2017, 6:5.

10. Chen Z, Park J, Butler B, Acosta G, Vega-Alvarez S, Zheng L, **Tang J**, McCain R, Zhang W, Ouyang Z, Cao P, Shi R: Mitigation of sensory and motor deficits by acrolein scavenger phenelzine in a rat model of spinal cord contusive injury. *J Neurochem* 2016, 138(2):328-338.